Identification, Expression and Characterization of Archaeal-Type Opsins of *Chlamydomonas reinhardtii*

vorgelegt von
Suneel Kateriya
aus Indian
2004

Identification, Expression and Characterization of Archaeal-Type Opsins of *Chlamydomonas reinhardtii*

Dissertation
zur Erlangung des Doktorgrades
der Naturwissenschaften (Dr. rer.nat.)
der Naturwissenschaftlichen Fakultät III
-Biologie und Vorklinische Medizin-
der Universität Regensburg

vorgelegt von
Suneel Kateriya
aus Indian
2004

Promotionsgesuch eingereicht am: 29.11.04

Die Arbeit wurde angeleitet von : Prof. Dr. P. Hegemann

Prüfungsausschuß:

Vorsitzender: Prof. Dr. S. Schneuwly

Erster Gutachter: Prof. Dr. P. Hegemann

Zweiter Gutachter: Prof. Dr. G. Hauska

Dritter Gutachter: Prof. Dr. Ch. Förster

This research work was carried out during the period October 2000 to October 2004 under the supervision of Prof. Dr. Peter Hegemann at the Institute for Biochemistry-I in the University of Regensburg, Germany. The financial support for this research project was obtained from the Graduate College (GRK 640) "Sensory photoreceptors in natural and artificial systems", funded by DFG.

The list of publication and presentation from this research work:

Publications:

Kateriya, S., Nagel, G., Bamberg, E., and Hegemann, P. (2004). "Vision" in single-celled algae. News Physiol Sci *19*, 133-137.

Nagel, G., Szellas, T., Huhn, W., **Kateriya, S**., Adeishvili, N., Berthold, P., Ollig, D., Hegemann, P., and Bamberg, E. (2003). Channelrhodopsin-2, a directly light-gated cation-selective membrane channel. Proc Natl Acad Sci U S A *100*, 13940-13945.

Fuhrmann, M., Deininger, W., **Kateriya, S**., and Hegemann, P. (2003). Rhodopsin-related proteins, Cop1, Cop2 and Chop1, in Chlamydomonas reinhardtii. (Cambridge, UK, Royal Society of Chemistry).

Nagel, G., Ollig, D., Fuhrmann, M., **Kateriya, S**., Musti, A. M., Bamberg, E., and Hegemann, P. (2002). Channelrhodopsin-1: a light-gated proton channel in green algae. Science *296*, 2395-2398.

Hegemann, P., Fuhrmann, M., and **Kateriya, S** (2001). Algal sensory photoreceptors. J Phycol *37*,, 668-676.

Poster Presentation:

Chlamyrhodopsin-3 (Cop-3) is an archaeal type photoreceptor with intrinsic H^+-conductance in *Chlamydomonas reinhardtii*. Dissecting G-Protein-Coupled Receptors (GPCR): Structure, Function and Ligand Interaction, Germany. Jan. 24-26, 2002.

Chlamyopsin-3 (COP-3) is an algal photoreceptor with intrinsic light-regulated proton conductance. The 10^{th} International Conference on the Cell and Molecular Biology of *Chlamydomonas***,** Vancouver, Canada - June 11-16, 2002**.**

Opsin coupled tow-component system in *Chlamydomonas reinhardtii*. 11^{th} International Conference on Retinal Proteins- (11th ICRP). June 20-24, 2004, Germany.

Acknowledgements

I express my heartfelt gratitude to my supervisor, Prof. Dr. Peter Hegemann. Thank you very much for your encouragement and support without, which I would not have been able to carry out this work.

I thank the speaker of the graduate college, Prof. Dr. B. Dick and the previous speaker Prof. Dr. P. Hegemann and all my teachers and colleagues at the graduate college of "Sensory photoreceptors in natural and artificial systems" and Institute für Biochemie-I of university of Regensburg, Germany.

I thank DFG and SFB for providing me fellowship for four years.

I thank all my lab members, M. Fuhrmann, M. Heitzer, C. Griesbeck, A. Stahlberg, S. Ehlenbeck, P. Berthold, T. Schiereis, and Jerry, B. Zorin, S. Dulev, without their co-operation and support I could not have managed this endeavour. It is my great pleasure to acknowledge Prof. Dr. Kaup and his group members at Research Centre Julich. My special thanks to Timo. I thank Dr.G Nagel for all his help. I thank Stephan for all his help and support.

I am very thankful to Nic for her kind help at all time. My special friends Bindu, Shobi and other present and previous Indian fellows at University of Regensburg, Germany, they encouraged me at difficult time.

I am very thankful to my family for their encouragement, affection and unconditional support throughout.

My parent in-law and Sini provided me support and love all the time.

And finally yet importantly I am thankful to my wonderful wife, she has provided me encouragement, emotional support and inspiration. I could not have managed this task without her help and support.

Dedicated to my Family

Contents 1
Abbreviations 5
1. Summary 8
2. Introduction 11
2.1. Retinylidene Protein 11
2.2. Rhodopsins in Vertebrates and Phototransduction 12
2.2.1. Rhodopsins in Invertebrates and Phototransduction 13
2.3. Archaeal-Type Rhodopsins in *H.salinarium* 13
2.4. Two-Component System and Phototaxis in *H. salinarium* 14
2.5. Distribution of Archaeal Rhodopsins in Nature 15
2.6. The Eyespot of *C. reinhardtii* 15
2.6.1. Rhodopsin Based Photoreceptors for Photobehavior in *C. reinhardtii* 17
3. Results 21
3.1. Channelopsin-1 21
3.1.1. Identification and Bioinformatic Analysis of Channelopsin-1 21
3.1.1.1. Identification of Channelopsin-1 21
3.1.1.2. Homology between Channelopsin-1 and Other Archaeal Type Opsins 21
3.1.1.3. Prediction of Secondary Structure and Modular Domain of Channelopsin-1 23
3.1.1.4. Prediction of Signal Peptide in Chop-1 protein Sequence 24
3.1.1.5. Homology Based 3D Modeling of Channelopsin-1 24
3.1.1.6. Homology Based Prediction of Proton Pathway of Channelopsin-1 25
3.1.2. Heterologous Expression of *chop-1* Gene in *E.coli* 26
3.1.2.1. Expression of *chop-1* Native Gene in *E. coli* 26
3.1.2.2. Expression of Chop-1S and Chop-1-SS in *E. coli* 27
3.1.3. Heterologous Expression of Chop-1-SS in *P. pastoris* 31
3.1.3.1. The *P. pastoris* Expression System 31
3.1.3.2. Expression of Chop-1SS in *P. pastoris* 31
3.1.4. Expression and Characterization of Chop-1 in *X. laevis* Oocytes 32
3.1.4.1. The Expression System 32
3.1.4.2. Vector for Expression in *X. laevis* Oocytes 33
3.1.4.3. Expression of Chop-1 in *X. laevis* Oocytes 33
3.2. Channelopsin-2 36
3.2.1. Identification and Bioinformatic Analysis of Channelopsin-2 36
3.2.1.1. Homology between Channelopsin-2 and Other Archaeal Type Opsins 36
3.2.1.2. Secondary Structure Prediction of Channelopsin-2 36
3.2.1.3. Phylogenetic Analysis of Channelopsin-2 38
3.2.2. Expression and Characterization of Channelopsin-2 39
3.2.2.1. Heterologous Expression of the *chop-2* Gene in *E. coli* 39
3.2.3. Expression and Characterization of Chop-2 in *X. laevis* Oocytes 41

3.2.4. Specificity Test of Chop-1 and Chop-2 Antibodies 43
3.2.4.1. Expression of the C-terminus of Chop-1 and Chop-2 in *E.coli* 43
3.2.5. Light Dependent Expression of ChR1 and ChR2 in *C. reinhardtii* 44
3.2.5.1. Expression Profile of ChR1 and ChR2 during Life Cycle of *C. reinhardtii* 45
3.3. Opsin Coupled Two-Component System 47
3.3.1. Opsin-Related Proteins in *C. reinhardtii* 47
3.3.2. Isolation of *chlamyopsin-5* Gene 48
3.3.2.1. Screening of cDNA library for Isolation of *cop-5* Gene 49
3.3.2.2. Isolation of *cop-5* Gene by RT-PCR and Genomic-PCR Method 49
3.3.2.3. Mining and Screening of a BAC Library for Isolation of the *cop-5* gene .. 49
3.3.3. Bioinformatic Characterization of Cop-5 50
3.3.3.1. Predicted Gene Structure and Primary Sequence of Chlamyopsin-5 50
3.3.3.2. Identification of Modular Domains of Chlamyopsin-5 50
3.3.3.3. Prediction of Leader Peptide Sequence and Secondary Structure 51
3.3.3.4. Homology Relation of Cop-5 Modular Domains with Known Prototype Proteins 51
3.3.4. Comparative Molecular Modeling of Modular Domains of Cop-5 53
3.3.4.1. General Procedure for Comparative Molecular Modeling 53
3.3.4.2. The 3D Models of Modular Domains of Cop-5 53
3.3.4.3. Proposed Model for Functional Activity of Cop-5 Protein 54
3.3.5. Heterologous Expression of Cop-5 in *E. coli* 55
3.3.5.1. Cloning and Expression of *cop-5* Full Length Gene in *E. coli* 55
3.3.5.2. Heterologous Expression of Cop-5 Opsin Domain in *E. coli* 55
3.3.5.3. Expression of Cop-5 HK, RR and CYCc Domains in *E. coli* 57
3.3.6. Transient Expression of Cop-5 in HEK-293 58
3.3.6.1. Expression Constructs for HEK-293 Cells 58
3.3.6.2. Transfection and Expression of Cop-5 in HEK-293 cells 59
3.3.6.3. Calcium Imaging of Cop-5 Expressing HEK-293 Cells 60
4. Discussion 61
4.1. Channelopsin-1 is an archaeal type opsin of *C. reinhardtii* functioning as a light-gated ion channel 61
4.2. A second archaeal-type opsin, Channelopsin-2, of *C.reinhardtii* also functions as a light-gated cation channel 65
4.3. Opsin coupled two-component system in *C. reinhardtii* 70
5. Future Prospective 74
6. Materials and Methods 77
6.1. Methods 77
6.1.1.1. Culturing of *C. reinhardtii* in Liquid Medium 77

6.1.1.2. Synchronization of *C. reinhardtii* cw 806 Culture 77
6.1.1.3. *C.reinhardtii* Gametogenesis 77
6.1.2. *E. coli* Culture 77
6.1.2.1. Preparation of *E. coli* Competent (DH5 α) or (BL-21) Cells 78
6.1.2.2. Transformation of *E. coli* competent cells 78
6.1.2.3. Storage of *E. coli* cells 78
6.1.3. *P. pastoris* Culture 78
6.1.3.1. Preparation of *P. pastoris* competent cells 79
6.1.3.2. Transformation and expression Chop-1SS in *P. pastoris* (GS115) 79
6.1.3.3. Storage of the *P. pastoris* cells 79
6.1.4. Isolation and Purification of Nucleic Acids 80
6.1.4.1. Isolation of Genomic DNA from *C. reinhardtii* 80
6.1.4.2. Isolation of RNA from *C. reinhardtii* 80
6.1.4.3. Screening of cDNA Libraries 80
6.1.4.4. Screening of BAC clone Libraries 80
6.1.4.5. Isolation of Plasmid-DNA from *E. coli* 80
6.1.4.6. Agarose gel Electrophoresis of DNA 81
6.1.4.7. Isolation and Purification of DNA from Agrose gel 81
6.1.4.8. Synthesis of Codon Adapted Opsin Domain of Chop-1 and Cop-5 Genes 81
6.1.4.9. Sequencing of DNA 81
6.1.4.10. Digestion of DNA by Restriction Enzymes 81
6.1.4.11. Dephosphorylation of the Vector DNA 82
6.1.4.12. Ligation of DNA-Fragment into Vector DNA 82
6.1.4.13. Polymerase Chain Reaction 82
6.1.4.14. Colony-PCR for Screening of Positive Clones 83
6.1.5. Protein Chemistry Methods 83
6.1.5.1. Heterologous Expression of Proteins in *E.coli* 83
6.1.5.2. Expression of Cop-5 in *E.coli* using BL-21 (C41) Expression strain 83
6.1.5.3. Preparation of Membrane Fraction of *E. coli* 84
6.1.6. Gene Constructs for Expression of Chlamyopsins 84
6.1.6.1. Expression of Chlamyopsins in *E.coli* 85
6.1.6.2. Protein Estimation by BCA Method 86
6.1.6.3. Precipitation of Proteins by TCA 86
6.1.6.4. Sodium Dodecyl Sulphate-Poly-Acrylamide Gel Electrophoresis (SDS-PAGE) 86
6.1.6.5. Staining of Protein Gel 86
6.1.6.6. Western Blotting for Protein Detection 86
6.1.7. Detection of Channelopsin Proteins from *C. reinhardtii* 87

6.1.8. Transient Expression of Cop-5 in HEK-293 87
6.1.9. Flow Chart for Bioinformatic Analysis of the Chlamyopsins 88
6.2. Materials 89
6.2.1. Cell Strains 89
6.2.2. Vectors 89
6.2.3. EST and BAC clones 90
6.2.4. Computer Programs used for the Analysis of Chlamyopsins 90
6.2.5. Chemicals, Enzymes and Kits 91
6.2.5.1. Chemicals 91
6.2.5.2. Enzymes and Proteins 92
6.2.5.3. Kits 92
6.2.6. Instruments 92
6.2.7. Antibodies 93
6.2.7.1. Primary Antibody 93
6.2.7.2. Secondary Antibodies 93
6.2.8. Solutions and Buffers 94
6.2.9. Oligonucleotides 96
7. Appendix 97
7.1. Bioinformatic Analysis of Channelopsin-1 97
7.1.1. Prediction of Putative TMH for Chop-1 Protein Sequence 97
7.1.2. Prediction of Leader Peptide Sequence in Chop-1 98
7.1.3. Prediction of Putative Phosphorylation Sites in Chop-1 99
7.1.4. Homology of Acetabularia Opsin (Aop) to Channelopsins 99
7.2. Bioinformatic Analysis of Channelopsin-2 100
7.2.1. Prediction of Putative TMH for Chop-2 Protein Sequence 100
7.2.2. Prediction of Leader Peptide Sequence in Chop-2 101
7.2.3. CDART Analysis of Chop-2 for Identification of Domain 102
7.2.4. Identification of Putative Phosphorylation Sites for Chop-2 102
7.2.5. Homology between Channelopsins and Putative Vop-2 103
7.3. Bioinformatic Analysis of Chlamyopsin-5 104
7.3.1. Prediction of Putative TMH for Cop-5 Protein Sequence 104
7.3.2. Prediction of Leader Peptide Sequence in Putative Cop-5 105
7.3.2.1. Homology between pSRII and Opsin Domain of Cop-5 106
7.3.2.2. Homology between Cop-5 HK Domain and HK Domain of *E.coli* 107
7.3.2.3. Homology between Cop-5 RR Domain and *E.coli* RR Domain 107
7.3.2.4. Homology between Cop-5 Cyclase and Cyclase of *T. brucei* 108
7.3.2.5. Homology between Opsin Domain of Cop-5 and Putative Vop-3 108
8. References 109
Bio-Data 120

Abbreviations

aa	Amino Acids
Ac	Acetate
AMP	Adenosine Monophosphate
Amp	Ampicillin
Aop	Acetabularia opsin
ATP (ADP, AMP)	Adenosine-5´-tri (Di, Mono-) Phosphate
BAC	Bacterial Artificial Chromosomes
bp	Base Pair
BCA	Bicinchoninic acid
BCIP	5-Bromo-4-Chlor-3-Indolyl-Phospahte
BLAST	Basic Local Alignment Search Tool
Bop	Bacterio-opsin
BR	Bacteriorhodopsin
BSA	Bovine Serum Albumin
cAMP	Cyclic AMP
cDNA	Complimentary DNA
cGMP	Cyclic Guanosine Monophosphate
CDART	Conserved Domain Architecture Retrieval Tool
Cop	Chlamyopisn
Chop	Channelopsin
Chop-1-S	Synthetic Chop-1 (1-317 a.a) gene
Chop-1-SS	Chop-1-Semi-Synthetic (Chop-1-S+318-388 aa Native gene)
Chop-1-C	Chop-1-C terminus (310-712 aa)
Chop-2	Channelopsin-2
Chop-2-C	Channelopsin-2-C-terminus (273-723 aa)
ChR	Channelrhodopsin (Chop+ all-*trans* retinal)
CIAP	Calf Intestine Alkaline Phosphatase
cw	Cell Wall Deficient
DEPC	Diethylpyrocarbonate
DMSO	Dimethylsulphoxide
DNA	Deoxyribonucleic acid
dNTP	Deoxy-Nucleotriphosphate

DTT	Dithiothreitol
ECFP	Enhanced Cyan Fluorescence Protein
EDTA	Ethylenediaminetetraacetate
EST	Expressed Sequence Tag
EtBr	Ethidium bromide
g	Gram
HEK	Human Embryo Kidney Cells
HK	Histidine Kinase
Hop	Halo-opsin
HR	Halorhodopsin
hrs	Hours
HSA	High Salt Acetate-Medium
Hz	Hertz
IPTG	Isopropyl-β-D-Thioglucoside
M	Molar
MCS	Multiple Cloning Site
Min	Minute
ml	Milliliter
mM	Milli Molar
NBT	4-Nitroblue-Tetrazoliumchloride
NC	Nitro Cellulose membrane
OD	Optical Density
OLP	Over-Lapping-PCR
ORF	Open Reading Frame
PAGE	Polyacrylamide Gel Electrophoresis
PCR	Polymerase Chain Reaction
pH_o	pH outside
pH_i	pH inside
PR	Proteorhodopsin
PRC	Photoreceptors Current
RNA	Ribonucleic acid
RR	Response Regulator
RT	Room Temperature
RT-PCR	Reverse Transcriptase PCR

SDS	Sodium Dodecylsulphate
SF	Soluble Fractions
Sop	Sensory Opsin
SR	Sensory Rhodopsin
t	Time
TCA	Trichloroacetic acid
TCS	Two-Component System
TEMED	N, N, N´, N´ Tetramethylethylenediamine
TEVC	Two Electrode Voltage Clamp
TMF	Total Membrane Fractions
TMH	Trans Membrane Helices
Tris	Tris (hydroxymethy) amino methane
U	Unit
UTR	Un-translated Region
V	Volt
Vop-2	Volvoxopsin-2
Vop-3	Volvoxopsin-3

1. Summary

Phototaxis and photophobic responses of green algae are mediated by rhodopsin-based photoreceptors that use microbial-type chromophores (all-*trans* retinal). Light absorption of algal rhodopsin triggers photoreceptor currents that have been studied intensively with a suction pipette technique. Analysis of stimuli-response curves of the *C. reinhardtii* photoreceptor current led to the suggestion that they are based on two photosystems, one of which is more active at low flash intensities, whereas the other dominates at high flash energies.

Thus, this research work was intended to identify the opsin-based photoreceptor responsible for photobehavioural responses of *C. reinhardtii*. Two cDNA sequences were identified in the EST database of the *C.reinhardtii* that encoded microbial-type opsins, which were named Chlamyopsin-3 and 4 (Cop-3 and Cop-4) respectively, based on their homology to the known microbial-type opsins. The seven-transmembrane helices at the N-terminus of these opsins showed homology to the light-activated proton pump, bacteriorhodopsin (BR). However, after functional expression in the oocytes of *X. laevis* these opsins were renamed as Channelopsin-1 and 2 (Chop-1 and Chop-2) based on their ion channel activity.

The amino acids that form the H^+-conducting network in BR are conserved in Chop-1 and Chop-2, whereas the rest of their sequences are different. The predicted secondary structure (7TMH) and hypothetical retinal-binding site (conserved lysine residue) of the Channelopsins led to the suggestion that these proteins are members of the archaeal-type family. Furthermore, bioinformatic analysis suggested that new rhodopsins might be functioning as ion transporters in active or passive mode upon functional expression. Heterologoulsy expressed Channelopsins (Chop-1 and 2) in *E.coli* formed inclusion bodies, and thus recombinant proteins were not functional. Moreover, the expression of Channelopsins (Chop-1 and 2) was toxic for the *E.coli*. Expression of Chop-1 in *P. pastoris* led to the production of non-functional protein, since it did not bind all-*trans* retinal.

Functional expression of *Chop-1 mRNA* in the oocytes of *X. laevis* (Chop-1 + all-*trans* retinal =ChR1) showed a light-gated ion channel conductance, which was studied in detail using a two-electrode voltage clamp technique (Nagel et al., 2002). The observed transport

activity was purely passive and directly dependent on the membrane potential and the proton concentration gradient in bath solution. Outward photocurrents could be observed at high exracellular pH or low intracellular pH. The conductance was highly selective for protons, and other monovalent or divalent ions were not found to be permeating. The amplitude of the current was graded with the light intensity, and the currents only saturated when all rhodopsin was activated (> 10^{20} photons.m-^{2}.S-^{2}). The action spectra obtained was rhodopsin shaped, with a maximum in the green at 500 nm. It was also observed by mutational analysis that the H^{173} residue of Chop-1 does not function as a proton donor of a deprotonated Schiff base. Therefore, it was suggested that in ChR1 the retinal Schiff base is not de-protonated during the photocycle. These experiments left no doubt that the oocytes had expressed an ion channel with an intrinsic sensor. It is likely that such light sensitive ion channels are widely distributed in other phototactic microalgae, as well as in gametes and zoospores of the macroalgae. This claim is corroborated by the observation that Volvoxopsin-2 (Vop-2) a partial opsin like sequence was identified in the *V. carteri* genome project, which showed 75% identical amino acid residues to Channelopsins in the helices 5-7 of the opsin domain.

Heterologous expression of Chop-2 was also carried out in *E.coli* to produce functional recombinant protein. It was observed that the expression characteristic of Chop-2 were similar to that of Chop-1. Therefore, Chop-2 was directly expressed in *Xenopus* oocytes, in the presence of all-trans retinal to produce functional Channelrhodopsin-2 (ChR2) (Nagel et al., 2003). Photocurrents were recorded from these oocytes using two-electrode voltage clamp method. However, the cells not only became conductive for protons but also, most surprisingly, for monvalent and divalent cations like Na^{+} K^{+} and Ca^{++}. It was demonstrated by using the giant patch-clamped method, (i.e., under cell free condition) that the channel activity of ChR-2 was independent of any soluble factor or endogenous protein of the oocytes. It was concluded that ChR-2 functions as a cation-selective channel. Surprisingly, and in contrast to ChR1, the light-gated conductance of ChR-2 inactivates in continuous light to a smaller steady-state level. Both channelrhodopsins are most active at low pH and high negative membrane potential. Western blotting analysis with membrane fractions of *C. reinhardtii* using anti-Chop1 and Chop2 antibodies revealed that both proteins were abundant, when cells were grown in low light conditions, both are degraded under high light conditions and that ChR2 was degraded more rapidly than ChR1. In conclusion, it is likely that both channelrhodopsins control photophobic responses and only indirectly influence phototaxis.

Very recently, three more protein sequences were found in *C. reinhardtii* genome database, which showed homology to the sensory opsin. Most amino acids that interact with retinal were conserved in the newly identified opsin like protein sequences. Surprisingly, all three sequences were coupled to a transducer like protein (HtrI and II). We have provisionally named these sequences Cop5, Cop6 and Cop7. Isolation, sequencing and bioinformatic analysis of Cop-5 protein sequence revealed that it is a unique putative opsin, which has four modular domains (Opsin, HK, RR and CYCc) in one protein. The functional expression of Cop-5 in heterologous expression systems (*E.coli* and HEK-293 cells) could still not be achieved. The assumption that one of these new rhodopsins could be responsible for phototaxis movement in *C. reinhardtii* seems to be justified. Nevertheless, other functions like control of retinal biosynthesis or developmental processes should also be taken into account.

2. Introduction

Sunlight is the primary source of energy for all living beings (except for autolithotrophic and a few deep vent organisms). Plants and microorganisms use light to orient themselves spatially and to guide their movements and/or growth. Photosynthetic organisms are the most important component of food chain. Only photoautotrophic organisms are capable of fixing light energy into chemical energy. This fixed chemical energy (food) is available to all consumers (herbivores and carnivorous) in the food chain. Higher animals utilize light for visual signal transduction and in this manner image their surroundings. Rhodopsin is the primary photoreceptor in the visual system of all animals, both invertebrates and vertebrates. The first step in the transduction of light signal to a neural signal is the light-induced isomerization of a chromophore, specifically a vitamin A derivative (retinal). This chromophore is bound to a membrane protein called an opsin, retinal bound opsin is known as rhodopsin. Almost all animals (including human beings) and plants also use light to set their internal clocks (circadian rhythm). This circadian rhythm is accomplished by the flavin and/ or rhodopsin based sensory photoreceptors.

2.1. Retinylidene Protein

Retinylidenes are photochemically reactive proteins that use retinal as their chromophore. Retinylidenes have been found in both prokaryotic and eukaryotic domains of life. Rhodopsins are members of the seven transmembrane receptor family, which are able to sense light and propagate a signal transduction cascade (Ruiz-Gonzalez and Marin, 2004). The seven transmembrane helices of rhodopsin are involved in forming an internal pocket, which binds with retinal via a Schiff-base linkage (Lanyi, 2004)). The primary sequence alignment classifies retinylidene proteins into two families. First family, archaeal-type (Type-1) rhodopsin, was found in the archaeon *H. salinarium*, halophilic prokaryotes and was also recently reported to be found in eukaryotes (Spudich et al., 2000). The archaeal (Type-1) rhodopsins functions as light driven ion pump (bacteriorhodopsin and halorhodopsin), phototaxis receptors (sensory rhodopsin I and II) and the function of the fungal opsin (Nop-1) is elusive. The second family, animal (Type-2) rhodopsins, consists of photosensitive receptor proteins of animal eyes, including human rod and cone visual pigments, receptor proteins in the pineal gland, hypothalamus, and other tissues of lower

vertebrates (Spudich et al., 2000). The best characterized Type-2 rhodopsins are the animal visual rhodopsins (Yokoyama, 2000). The presence of rhodopsin is independent of the structural and functional complexity of the optical apparatus and neural network of a particular animal (Hegemann et al., 2001).

2.2. Rhodopsins in Vertebrates and Phototransduction

Vision is one of the most important senses for vertebrates; light triggers an enzymatic cascade, called the phototransduction cascade, which leads to the hyperpolarization of photoreceptor cells (Hisatomi and Tokunaga, 2002). Visual signal transduction begins with absorption of the photon by rhodopsin. Rhodopsins are localized in the outer segment of the rod and cone cells. It is connected to the inner segment of the rod/cone cells that bears synaptic terminal contacting bipolar and horizontal cells (Baylor, 1996). Rod cells are able to detect even single photons. This ultimate sensitivity is achieved because of the high probability of absorption and efficient photochemical reactions. Rhodopsins are members of the G protein-coupled receptor family that also includes many hormone receptors, odorant receptors, and metabotropic synaptic receptors. Rhodopsin is an unusual case among the G protein-coupled receptors, in that it is bound in darkness to a chromophore (Burns and Baylor, 2001). The 11-*cis*-retinal is covalently bound via a Schiff base linkage to the terminal (ε) amino group of a lysine residue, and this Schiff base is in the protonated state (Rao and Oprian, 1996). The absorption of a photon by the 11-*cis*-retinal chromophore leads to its photoisomerization to all-*trans*-retinal (Fain et al., 2001), resulting in a subtle change in the conformation of rhodopsin, converting it into an active rhodopsin (metarhodopsin). This metarhodopsin activates a G protein (transducin) and a subsequent phosphodiesterase (PDE), resulting in the hydrolysis of cGMP and closure of the cGMP-regulated cation channels. The Na^{+}/Ca^{2+} influx into the photoreceptor cell (rods or cones) is abolished, which leads to the hyper-polarization of the plasma membrane (Burns and Baylor, 2001). This membrane potential will be sensed by a particular neural network and processed to complete transduction of the vision signal.

2.2.1. Rhodopsins in Invertebrates and Phototransduction

The invertebrate phototransduction process also utilizes rhodopsin as the primary photoreceptor to receive light signals. A detailed structure of invertebrate rhodopsins has recently been performed by Gärtner (Gärtner, 2000). The current knowledge of invertebrate rhodopsin was primarily determined from studies of rhodopsin-related events during the phototransduction cascade in *Drosophila* (Zuker, 1996). Invertebrate rhodopsins are also members of the rhodopsin super family of proteins within the phylogenetically related hyperfamily of G-protein coupled receptors (Sakmar, 1998). Photoreceptor cells of *Drosophila* express a variety of rhodopsin isoforms (Rh1-6). The secondary structure of invertebrate rhodopsin is remarkably similar (possess seven trans-membrane helices) to rhodopsins from other domains of life. In particular, there is a positional conservation of a lysine residue of the seventh transmembrane helix in the retinal binding motif of Rh1 of *Drosophila* (Montell, 1999). This binding site of Drosophila rhodopsin is characterized by a protonated Schiff base chromophore stabilized via a single negatively charged counterion (Vought et al., 2000). Absorption of a photon leads to the isomerization of retinal from 11-*cis* to the all-*trans* configuration and activation of rhodopsin (metarhodopsin). These metarhodopsins can activate G proteins, which induces activation of phospholipase-C. Phospholipase-C releases diacylglycerol, which in turn activates the TRP/TRPL (Transient Receptor Potential/Transient Receptor Potential Like) channels (Hardie and Raghu, 2001). The opening of these channels can enhance Na^{+}/Ca^{2+} influx and in this manner plasma membrane depolarization is achieved (Hardie, 2001). The depolarized receptor potential can be sensed by photoreceptor neurons for completion of the visual signal transduction in *Drosophila*. In addition to excitation, photoreceptor neurons have evolved sophisticated mechanisms to control termination of the light response (deactivation) and light and dark adaptation (Baylor, 1996).

2.3. Archaeal-Type Rhodopsins in *H.salinarium*

Certain archaea like (*H. salinarium*) have four classes of archaeal type rhodopsins. Two of them are transporter rhodopsins called bacteriorhodopsin (BR), which functions as a proton-extruding pump (Luecke et al., 1998), and halorhodopsin (HR), which functions as a chloride uptake pump (Kolbe et al., 2000). The other two are the sensory rhodopsins SRI and SRII, which mediate the phototaxis response by coupling to specific transducer

proteins (halobacterial transducers HtrI and HtrII; Valentin et al., 2002). As in *E. coli* chemotaxis, analogous transducers (Histidine Kinase) activate a response regulator (RR) that in turn switches rotation of the flagella motor (target response). This type of non-electrical signal transmission between sensor and effector organ is known as a two-component system (Oprian, 2003).

The BR, HR and SRII display close similarity at the secondary structure level within the transmembrane helices 3-7 (Landau et al., 2003). This structural conservation also leads to their functional similarity. Upon light absorption, all four microbial rhodopsins undergo a cyclic reaction (Photocycle). During the photocycle of these opsins, the physiological response, either vectorial ion transport or initiation of the signal transduction chain is achieved (Spudich et al., 2000). The reversible molecular events associated with the photocycle includes the isomerization of the retinal chromophore from all-*trans* to 13-*cis* (Feng Gai et al., 1998), the deprotonation of the Schiff base (HR is an exception), and conformational changes of the protein backbone. All of these light-triggered thermal reactions have to be reversible because once a cycle is completed the protein has to regain its dark state (Schafer et al., 1999).

The photocycle of BR has been studied in detail compared to the other three rhodopsins. The general picture that has emerged from these investigations can be summarized as follows: the intermediates of the BR photocycle are named in alphabetical order, starting with J for onset of the reaction product. The J intermediate is followed by five other intermediates, K, L, M, N, and O. These letters were chosen by analogy to the photocycle reaction sequence observed in visual pigments, with Lumi and Meta, identified as physiologically important states (Stoeckenius and Lozier, 1974).

2.4. Two-Component System and Phototaxis in *H. salinarium*

A typical two-component system comprises a histidine kinase (HK) protein that receives stimuli and transmits it to a partner response regulator (RR) protein. The two-component signal transduction cascade has been investigated in detail for the chemosensory system of *E.coli* and some enteric bacteria (Stock et al., 1990). The signal is transmitted between the HK and the RR via a phosphorelay system. In the recent years, a similar signaling system has been reported in *H. salinarium* to elucidate the mechanism of phototaxis. It has been found that the histidine kinase (CheA) is required for phototaxis and chemotaxis in *H. salinarium* (Oprian, 2003; Rudolph and Oesterhelt, 1995). Genome analysis of

H. salinarium species NRC-1 revealed the presence of the complete set of *B. subtilis che* gene homologues, with the exception of CheZ indicating that chemotaxis signal transduction of *H. salinarium* is similar to that of enteric bacteria (Ng et al., 2000).

2.5. Distribution of Archaeal Rhodopsins in Nature

In recent years, evidence has emerged that the archaeal type rhodopsins have spread beyond the borders of archaea taxa in nature (Gartner and Losi, 2003; Spudich et al., 2000). Following their discovery in archaea, genes with clear sequence similarities to archaeal rhodopsins were characterized in other lineages. The first one was found in the fungus *Neurospora* (Bieszke et al., 1999). However, despite being very similar in sequence, some other opsin-like fungal proteins were unable to act as photosensors, because they lack a critical lysine motif, which is involved in retinal binding. These type of proteins are called opsin-related proteins (Spudich et al., 2000). Typical archaeal type rhodopsin genes were later found in some non-cultivated proteobacteria that encoded a protein called proteorhodopsin, a transport rhodopsin that functions as a light-driven proton pump (Beja et al., 2000).

Recently, archaeal-type rhodopsins (Chlamyopsin-3 and 4; Cop-3 and 4) have been found in the green alga *C. reinhardtii* (Hegemann et al., 2001), which is described in greater detail in this research work. We have found that Cop-3 and 4 function as light-gated proton and non-selective cation channel respectively, when heterologously expressed in *Xenopus laevis* Oocytes (Nagel et al., 2002; Nagel et al., 2003). The detailed characterization of Cop-3 and 4 is summarized in this thesis work. Type-I rhodopsin was also found in the cyanobacteria (*Nostoc*), where it possess features of a typical sensory rhodopsin (Jung, 2003).

2.6. The Eyespot of *C. reinhardtii*

C. reinhardtii has been used as the most prominent model system for research to answer many fundamental questions of photobiology, cell and molecular biology. The alga is only 8 to 10 µm in size, possesses a cell wall, chloroplast, an eyespot (stigma) that perceives light, and two anterior flagella (Fig.1). The eyespot takes up approximately one percent of the cell surface and is about 1µm in diameter. The eyespot allows the cell to perform

phototaxis, in order to locate optimal light for growth and to avoid photodamage (Dieckmann, 2003). In *C. reinhardtii* the eyespot is located in equatorial position of the cell body, with slight variation during the cell cycle (Hegemann, 1997). An electron microscopic study revealed that the eyespot is a multilayered membrane sandwich, in which the plasma membrane is closely apposed to the chloroplast envelope membrane (Melkonian and Robenek, 1980). The eyespot of *C. reinhardtii* may have up to eight layers of membranous structure. These peculiar structures enable the organism to perceive maximum incident light when the eyespot is facing towards the light source. The plasma membrane of the eyespot has been described as an ideal location of the photoreceptor. Such location of the photoreceptor provides a credible means for communication with the flagella, since the plasma membrane is in continuum with the flagellar membrane. Therefore, pigmented eyespot functions as an optical device (quarter wave stack) in conjunction with the photoreceptors (Foster and Smyth, 1980).

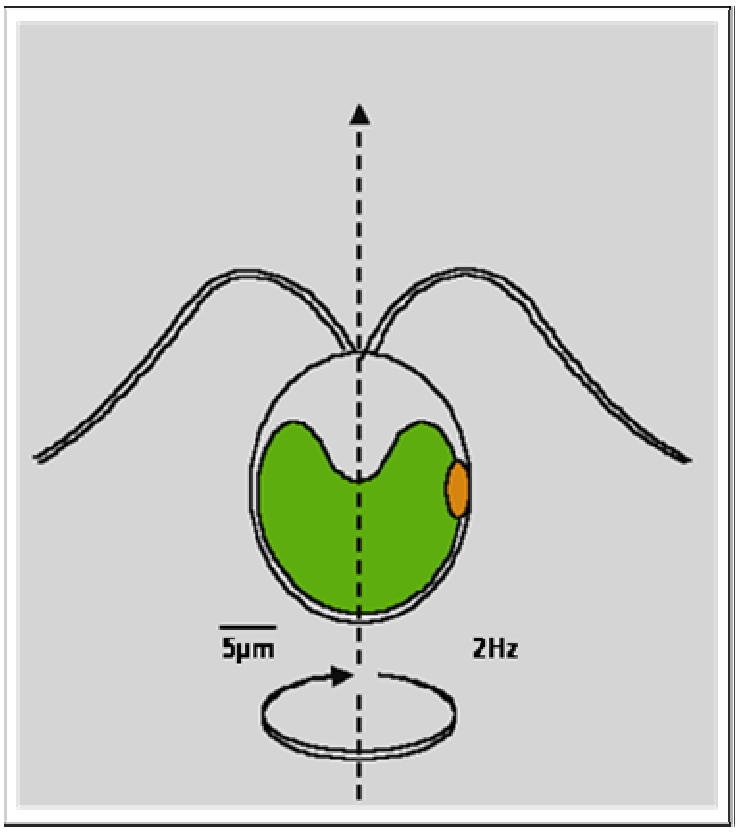

Figure 1. A *Chlamydomonas* cell. The cell is about 5µm in size, has two anterior flagella, a large chloroplast (green) and an eyespot (yellow/orange). The flagella beat with a frequency of 2Hz. This figure has been taken from a published paper (Kateriya et. al., 2004).

The function of these eyes is based on certain physical principles such as reflection, interference and polarization (Hegemann and Harz, 1998). It should be noted that absolute light sensitivity of the visual system is achieved by the number of photoreceptor molecules, whereas the spatial resolution is solely depended on its optics.

2.6.1. Rhodopsin Based Photoreceptors for Photobehavior in *C. reinhardtii*

C. reinhardtii cells are capable of responding to light stimuli by changes in their behavior, which leads to their accumulation under optimal light conditions (Phototaxis). Cells are able to adjust their movement path according to the direction of incident light in phototaxis. The phototaxis action spectra recorded from the vegetative or gamete cells of unicellular algae (including *C.reinhardtii*) were typically rhodopsin shaped. This type of action spectra led to the suggestion that most flagellate algae use rhodopsin as the photoreceptor for phototaxis (Foster et al., 1984). In a key experiment, Foster et al. restored phototaxis in "Blind" *C.reinhardtii* cells by addition of retinal, thus showing for the first time that the photoreceptor is rhodopsin. Later, it has been established by *in vivo* experiments with the isomer and analogue of retinal that photophobic and phototaxis responses each require a chromophore with an all-*trans* conformation, and the ability to isomerize only around the retinal C13-C14 double bond (Takahashi et al., 1991; Zacks et al., 1993). Finally, all-*trans* retinal was extracted from wild type cells and analyzed by HPLC (Beckmann and Hegemann, 1991). Thus, *C. reinhardtii* was the first eukaryote that showed the presence of an archaeal-type rhodopsin. The photoreceptor current is the earliest so far detectable process in the cascade of photobehavioural responses of green algae. The first detailed analysis of rhodopsin-mediated photocurrent became possible by employing a suction pipette technique. This technique was first used for *Haematococcus* (Litvin et al., 1978) and then on *C. reinhardtii* cells, which lacked a cell wall (Harz and Hegemann, 1991). The flash induced photoreceptor currents in the colonial green alga *V. carteri* showed strong dependence on pH and are mainly carried by H^+ (Braun and Hegemann, 1999). However, in the single-celled *C. reinhardtii,* flash induced H^+ current is hidden by a secondary Ca^{++}-current that rises almost with the same kinetics before it rapidly decays after few milliseconds (Braun and Hegemann, 1999). Under physiological conditions, only the fast Ca^{++}-carried photoreceptor current is able to trigger voltage-sensitive channels in the flagellar membrane, which in turn causes massive Ca^{++} influx into

the flagella. This sudden Ca^{++}-influx induces a switch of flagellar motion from breaststroke swimming to symmetrical flagellar undulation that is seen under the microscope as a photophobic response. Analysis of a stimulus-response curve of the *C. reinhardtii* photoreceptor currents led to the suggestion that they are based on two photosystems, one of which is more active at low flash intensities, whereas the other dominates at high flash energies (Ehlenbeck et al., 2002).

At low flash intensities (< 1% rhodopsin bleaching); the photoreceptor current is delayed by several milliseconds, suggesting that the low intensity photoreceptor system involves a signal amplification system that activates an eyespot channel indirectly. These proteins are yet to be characterized (Braun and Hegemann, 1999; Ehlenbeck et al., 2002). It was also envisaged from electrophysiological data that algal opsins form a complex with the ion channel protein constituting the high light-saturating ion conductance responsible for the photophobic responses (Holland et al., 1996). The presence of a light-dependent delay and the sensitivity of the current amplitude to the physiological state of the cell indicate the likely involvement of biochemical mechanisms in the generation of the late photoreceptor current.

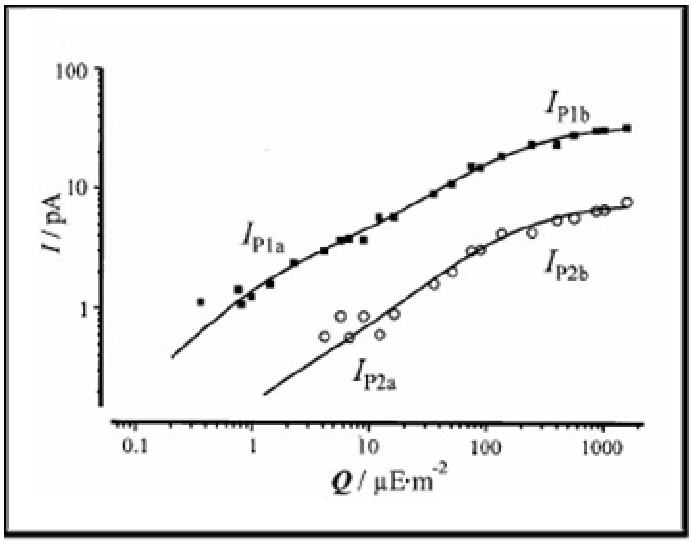

Figure 2. Dependency of amplitude of I_{P1} and I_{P2} on photon exposure, Q of the light flashes. Peak amplitudes of $I_{P1}$and I_{P2} plotted vs. the flash photon exposure Q. The data grouped for the fit for photocurrents at acidic conditions are $Q_{1/2\ a}$ =1.52 and $Q_{1/2\ b}$ = 136.24 µE m^{-2}. The resulting amplitude values are I_{P1a} = 3.03 pA; I_{P1b} = 31.32 pA; I_{P2a} = 0.31 pA; and I_{P1b} = 7.58 pA. This figure has been taken from a published paper (Ehlenbeck et al., 2002).

At neutral pH, all eyespot restricted photocurrents appearing in *C. reinhardtii* after a flash or upon step-up stimulation are sufficiently explained by two light induced conductances (Ehlenbeck et al., 2002). The major photoreceptor current was proposed to result from a conductance that is closely coupled to rhodopsin (Harz and Hegemann, 1991). The high light saturating component of I_{P1}, I_{P1b}, has been known to be carried by Ca^{2+} (Holland et al., 1997). A large body of evidence has accumulated showing that the I_{P1b}-induced depolarization triggers the flagellar currents, that in turn, cause a switch from forward to backward swimming (Holland et al., 1997). The other component of I_{P1}, I_{P1a}, saturating at low light has not been studied in detail because of its small amplitude. These biophysical studies have propounded the presence of at least two rhodopsin photoreceptors in *C. reinhardtii* (Ehlenbeck et al., 2002).

Supplementation of white retinal-deficient cells with ^{3}H-retinal or exchanging the endogenous retinal in purified eyespot membranes against ^{3}H-retinal identifies only one retinal binding protein, which has been purified and sequenced (Beckmann and Hegemann, 1991). Based on its sequence homology to invertebrate opsins (Type 2), it was named Chlamyopsin (Cop-1). It is a mixture of two splice variants of one gene, which translated to two almost equal size proteins (Cop-1 and Cop-2) but have different hypothetical retinal binding sites (Fuhrmann, 2003). These Chlamyopsins (Cop1 and 2) as well as its homolog from *V. carteri*, volvoxopsin (Ebnet et al., 1999) are highly charged and the overall sequences are unlikely to be composed of a 7-transmembrane helices. In addition, these sequences were hardly comparable to the Type-1 rhodopsin chromophore, which was characterized *in vivo* (Hegemann et al., 2001). Several enzymes characteristic for visual transduction cascades in animals have been detected in isolated eyespot preparations of green flagellate algae (Calenberg, 1998), although their possible role in phototaxis signaling is yet to be elucidated. Recently, it was shown on the bases of biophysical studies on antisense transformants of *C.reinhardtii* with reduced Cop1 and Cop2 content, that both are not the photoreceptors for phototaxis and photophobic responses (Fuhrmann et al., 2001). Therefore it was important to identify new opsin-based photoreceptor(s) for photobehavioural responses of *C.reinhardtii*. The only alga in which a second retinal protein has been identified is *D. salina* (Hegemann et al., 2001). It was not surprising because phototaxis and photophobic responses of *D. salina* exhibit rhodopsin action spectra with different maxima (Wayne et al., 1991). More specifically, labeling of eyespot membranes with ^{3}H-retinal identified a 28 kDa retinal-binding protein, probably the homologue of Chlamyopsin and Volvoxopsin. In addition, a larger retinal protein of 45kDa

(Fig.4) was also identified in this alga suggesting that a second class of rhodopsin might exist in green algae (Hegemann et al., 2001).

The aim of this project was to identify new opsin gene(s) using bioinformatics and molecular biology tools. Heterologously express and characterize the newly identified gene(s) product(s).

3. Results

3.1. Channelopsin-1

3.1.1. Identification and Bioinformatic Analysis of Channelopsin-1

3.1.1.1. Identification of Channelopsin-1

With the completion of the *C. reinhardtii* genome project, many web resources are maintaining a wealth of information like the Expressed Sequence Tag (EST) and Bacterial Artificial Chromosome (BAC) clone sequences of *C. reinhardtii*. *C. reinhardtii* genome database was mined with Basic Local Alignment Search Tool (BLAST) to fetch out unidentified opsin homologue sequences. *C. reinhardtii* EST database search showed the existence of overlapping cDNA sequences which encodes 712 amino acids (aa) of an opsin-related protein (Gene Bank accession no. AF385748). Initially it was named Chlamyopsin-3 (Hegemann et al., 2001); however, based on its function as a light-gated ion channel activity in *Xenopus* oocytes, it was later renamed as Channelopsin-1, described below in detail (Nagel et al., 2002).

3.1.1.2. Homology between Channelopsin-1 and Other Archaeal Type Opsins

The deduced protein sequence of Chop-1 was compared to the known archaeal type opsins (Fig.3). Chop-1 protein shows <21% homology to sensory rhodopsins from the archaea and <14 % to the opsin protein from *Neurospora* (Nop-1). The retinal binding K in Type-1 rhodopsin is embedded in a conserved retinal binding region LDXXXKXXF/W^{299}, suggesting that K^{296} of Chop-1 is a retinal-binding amino acid (Nagel et al., 2002). In archaeal type opsins, twenty-two amino acids are in direct contact with the retinal binding pocket. In Chop-1, nine of these amino acids are identical and four additional underwent conservative exchange (Fig.3).

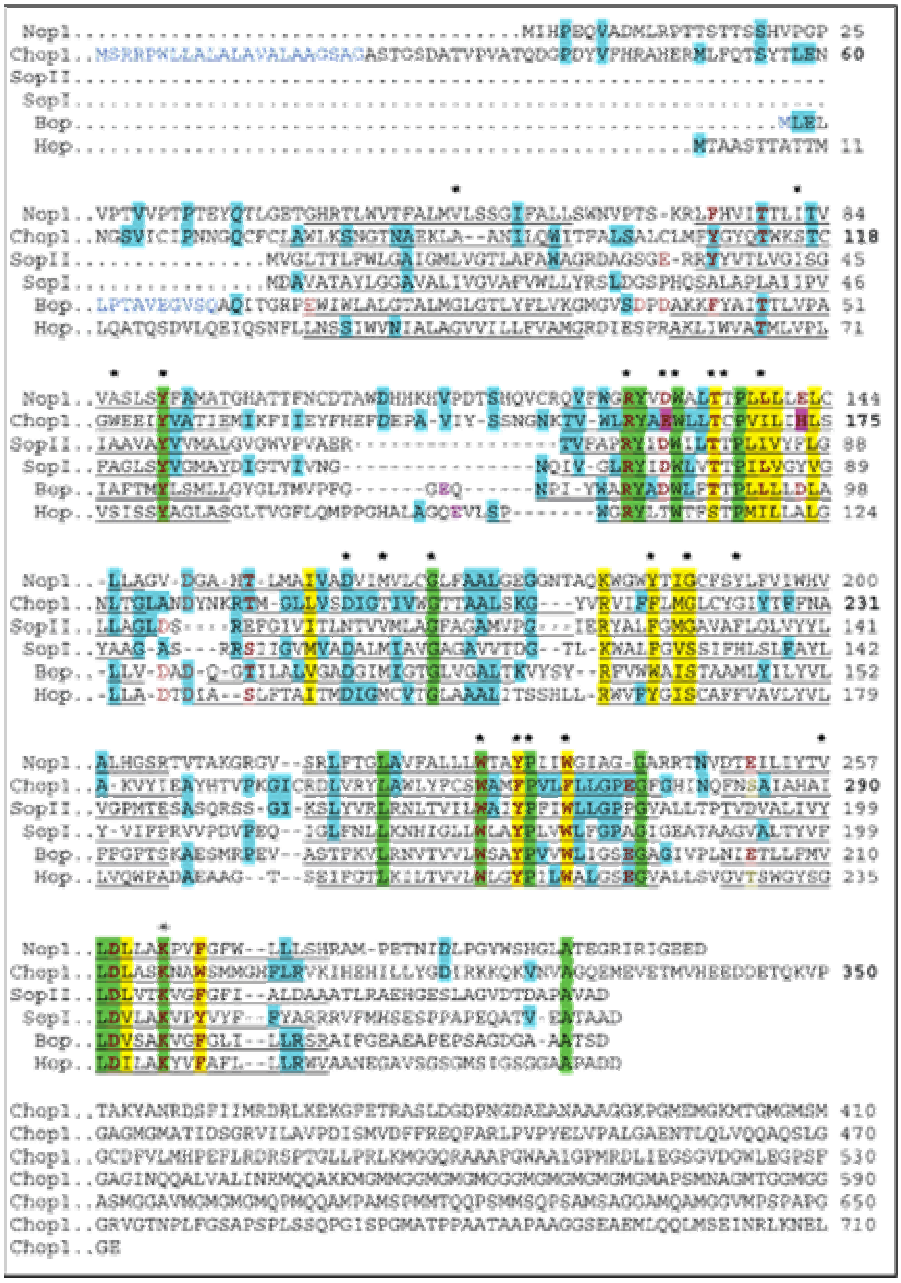

Figure 3. Multiple sequence alignment of microbial type opsins. Amino acids that are known from the bacterio-opsin (Bop) and Sensory Opsin (SopII) structure to interact directly with the retinal (Kimura et al., 1997; Luecke et al., 1998; Luecke et al., 2001) are indicated by *. Amino acids that are identical in all opsins are labeled in green, those that are functionally homologous in all sequences are labeled in yellow and those that are identical in Chop1 and only some of the other opsins are labeled in blue. Amino acids that contribute to the H^+-conducting network in bacteriorhodopsin, BR (Kimura et al., 1997; Luecke et al., 1998) and identities in the other opsins are shown in red. Residues that are part of the transmembrane H^+-network are printed in bold. The key replacements, D^{85} and D^{96} in BR to E^{162} and H^{173} in Chop1 are labeled in red background. Underlined amino acids indicate the seven transmembrane helices region of opsins. This figure has been taken from a published paper (Nagel et al., 2002).

This homology study also suggests relative position of 7TMH in the N-terminus region (Fig.3), in which the residues surrounding the chromophore in haloarchaeal opsins are conserved. It could be concluded that Chop-1 is a member of the classical archaeal rhodopsin (Type-1 rhodopsins) type of protein. Moreover, these studies also showed that Chop-1 is closer to BR than to SRI and II. Therefore, it could be speculated that Chop-1 might be functioning as a light activated transporter in an active/ or passive mode.

3.1.1.3. Prediction of Secondary Structure and Modular Domain of Channelopsin-1

Hydropathy plot analysis has predicted 8TMH in Chop-1 protein sequence (*Appendix*.A1.1); seven of them from the N-terminus (76-309 aa) showed 21% homology to archaeal type opsins and only one 1THM have been predicted at the C-terminus.

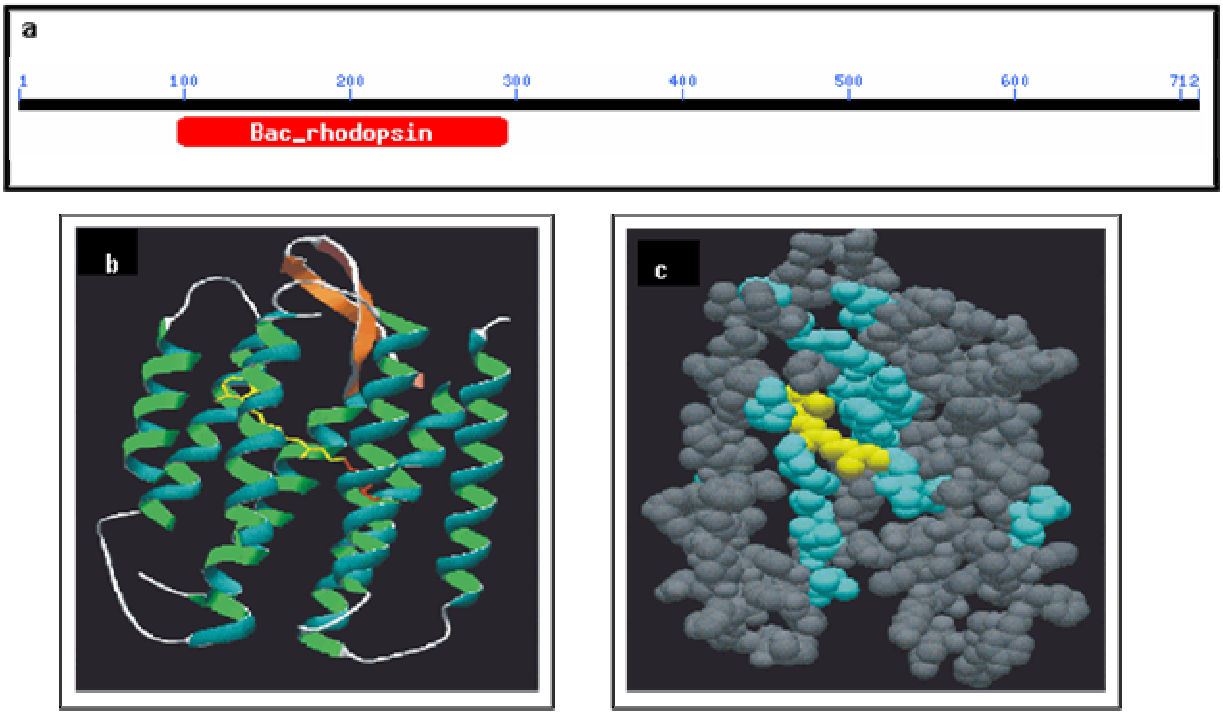

Figure 4. (a) The CDART analysis has demonstrated the presence of a bacteriorhodopsin domain in Chop-1 protein sequence. (b) 3D-backbone model of the hypothetical Type-1 rhodopsin *C. reinhardtii* encoded by the cDNA: AccNo AF 385748. The deduced amino acid sequence was aligned and modeled to the BR-structure 1FBB (Subramaniam and Henderson, 2000) from PDB (Berman et al., 2000), as a template using SWISS-MODEL and Swiss PDB-viewer 3.7b2 available from http://www.expasy.ch/swissmod/SWISS-MODEL.html with default parameters (Hegemann, 2001). Note that the loop structure, the end of helix 4, and the extended N and C termini are not completely represented. (c) A section through a space filling model of the same protein showing the retinal in yellow and amino acids identical to the reference bacteriorhodopsin from *H. salinarium* in cyan (Hegemann et al., 2001).

It is interesting to note that Sineshchekov *et al* have reported two TMH in the C-terminus of Chop-1 (Sineshchekov et al., 2002). The presence of second TMH at the C-terminus of Chop-1 seems to be controversial, which need further validation and prediction.

The Chop-1 protein sequence was then analyzed using the Conserved Domain Architecture Retrieval Tool. The CDART performs similarity searches of the NCBI Entrez Protein Database based on domain architecture, defined as the sequential order of conserved domains in proteins. The algorithm finds protein similarities across significant evolutionary distances using sensitive protein domain profiles rather than by direct sequence similarity. The analysis of Chop-1 protein sequence with CDART identified a bacteriorhodopsin like domain in the protein sequence (Fig. 4a). This analysis also found more than 100 opsin related sequences from different organisms, which are homologous to Chop-1. These results strongly suggest that Chop-1 of *C. reinhardtii* might be the first microbial-type opsin identified in plants.

3.1.1.4. Prediction of Signal Peptide in Chop-1 protein Sequence

Signal peptides control the entry of virtually all proteins to the secretory pathway, both in eukaryotes and prokaryotes (Gierasch, 1989). They comprise the N-terminal part of the amino acid chain and are cleaved off while the protein is translocated through the membrane. The common structure of signal peptides from various proteins is commonly described as a positively charged n-region, followed by a hydrophobic h-region and a neutral but polar c-region. Chop-1 protein contains a soluble N-terminus with 77 aa, of which the 22 amino acid leader peptide is likely to be cleaved off during posttranslational modification (*Appendix*; A1.2).

3.1.1.5. Homology Based 3D Modeling of Channelopsin-1

The 3-D structure of a protein can be experimentally determined by X-ray crystallography or by Nuclear Magnetic Resonance (NMR) spectroscopy. When no experimental structure is available, homology modeling provides a starting point for the biologist involved in structure and function relationship study. Comparative molecular modeling of putative opsin domain of Chop-1 was performed using the web resource SWISS-MODEL program. Predicted 3-D structure was visualized with a web free resource (http://www.umass.edu/microbio/rasmol/) Rasmol program. Predicted 3D model of the opsin domain of Chop-1 shows the presence of 7TMH topology (Fig.4b) and hypothetical retinal binding site (Fig.4b and c).

3.1.1.6. Homology Based Prediction of Proton Pathway of Channelopsin-1

The conserved amino acids of opsin domain in Chop-1 are located in helices 3, 4, 6 and 7 and found near the polar Schiff base side (Fig.3). More specifically, the 9-methyl and 13-methyl groups in BR are 3.6 to 3.7Å from the closest heavy atom of W^{182} and L^{93}, respectively, which is consistent with the evidences that these residues are essential for thermal re-isomerization from 13-*cis* to all-*trans* at the end of the photocycle (Lanyi, 2004). These residues are W^{262} and I^{170} in Chop-1. During the BR photocycle, the proton is released to D^{85}, which is E^{162} in Chop-1. In BR, the H^+ is released to the surface via E^{204} and E^{194}, the equivalent of which in Chop-1 are E^{244} and S^{154}.

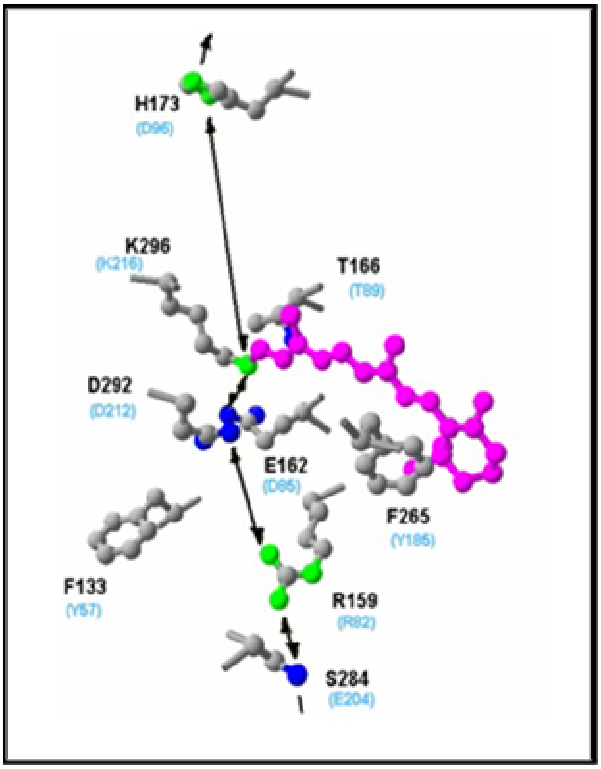

Figure 5. Scheme of the proposed H^+- transport pathway in Chop-1. The scheme includes those amino acids of Chop-1 (black) that are at positions that are most critical for the proton transporting hydrogen bonding network in BR (light blue) . The all-trans retinal is shown in red, nitrogen atoms are in green and oxygen atom in dark blue. Black arrow represents the proposed proton pathway. This figure has been taken from a published paper (Fuhrmann et al., 2003).

The release of proton in BR from D^{85} is accompanied by a new bond between D^{85} and R^{82}. The equivalent bonding is expected to occur in Chop-1 between E^{162} and R^{159} after proton

release from E^{162}. This results in the proposed extracellular H^+-transport pathway for Chop-1 depicted in Figure.5. The cytoplasmic region of BR with D^{96} as the proton donor of the unprotonated Schiff base is flanked by F^{42} and F^{219}. In archaeal sensory rhodopsins, this D is replaced by Y and the reprotonation process is slowed down. In Chop-1, it is H^{173}, which can be reversibly protonated and deprotonated at acidic pH and is expected to be in contact with Y^{109} and W^{269} (Fuhrmann et al., 2003).

3.1.2. Heterologous Expression of *chop-1* Gene in *E.coli*

The bacterium *E. coli* remains the most versatile host for the production of heterologous proteins (Baneyx, 1999). Recent progress in the field of heterologous expression of functional archaeal rhodopsin protein in *E. coli* has provided the basis for heterologous production of Chop-1 (Hohenfeld et al., 1999; Schmies et al., 2000; Shimono et al., 1997). The heterologous expression of functional opsins in *E. coli* was known (Chen and Gouaux, 1996; Shimono et al., 1997). An attempt to increase expression of the synthetic opsin gene by introducing codons that were preferred in *E. coli*, have been shown to improve BR expression (Nassal et al., 1987). A striking increase in expression of the *bop* gene in *E. coli* occurred when the codons for several of the N-terminal amino acids were changed to increase the A=T content (Karnik et al., 1987). High-yield production of bacteriorhodopsin via expression of a synthetic gene in *E. coli* has also been achieved by Pompejus and colleagues (Pompejus et al., 1993). The yield was in the range of 30-50 mg pure protein/liter culture medium, depending on the individual preparations. This material could be used for reconstitution of fully functional bacteriorhodopsin. These findings were taken into account to obtain functional expression of *chop-1* gene in *E. coli*.

3.1.2.1. Expression of *chop-1* Native Gene in *E. coli*

The pMAL-c2 uses the strong `tac´ promoter and the malE translation initiation signal to give high-level expression of the cloned gene (Amann, 1985). Therefore, pMALc2 expression vector was used for the expression of Channelopsin-1 in *E. coli*.

Table-1. Expression optimization for Chop-1 native gene in *E. coli*

E.coli strains	Growth Temperature and Induction Period	Amount of Inducer	Outcome
BL21 (DE3 λ)	37°C (2.5hrs), 30°C (3hrs) and 18°C (16hrs)	1.0 mM	Expression not observed
BL21 (DE3 λ)	37°C (2.5hrs), 30°C (3hrs) and 18°C (16hrs)	0.6 mM	Expression not observed
BL21 (DE3 λ)	37°C (2.5hrs), 30°C (3hrs) and 18°C (16hrs)	0.3 mM	Expression not observed
BL21CodonPlus-RIL	37°C (2.5hrs), 30°C (3hrs) and 18°C (16hrs)	1.0 mM	Expression not observed
BL21CodonPlus-RP	37°C (2.5hrs), 30°C (3hrs) and 18°C (16hrs)	1.0 mM	Expression not observed

Chop-1 native gene was tried to be expressed in *E. coli* by using *chop-1*-pMALc2 construct under various experimental conditions as described in Table-1. Nonetheless, expression could not be observed under any of the experimental conditions.

3.1.2.2. Expression of Chop-1S and Chop-1-SS in *E. coli*

It is known that synonymous codon usage differs among genome (Xia, 1996), among different genes within the same genome (Sharp et al., 1988) and even different segments of the same gene (Akashi, 1994). Earlier studies have suggested that clusters of AAG/AGA, CUA, AUA, CGA or CCC codons can reduce both quality and quantity of the synthesized protein. In addition, it is likely that an excess of any of these codons, even without cluster, could create translational problem (Kane, 1995) because, optimization of the translational machinery in cells requires the mutual adaptation of codon usage and tRNA concentration, and the adaptation of tRNA concentration to amino acid usage (Xia, 1998).

Since codon usage influences expression of foreign gene in *E. coli*, Chop-1 DNA sequence was analyzed for codon bias in *E. coli*. It was observed that Chop-1 DNA sequence contained ~21% codons that are rarely used by *E. coli* (very little tRNA is made for rare codons). Therefore, the codons of *chop-1* gene were changed and optimized for *E. coli* by using a free web resource program from www.entelechon.de/eng/backtranslation.html, and this codon -adapted gene sequence was sent for synthesis to Entelechon, Germany. It must

be noted that only 1-317aa encoding portion of the *chop-1* gene, which shows homology to the opsin domain of the archaeal type opsin was synthesized. It must also be noted that this region of the protein was shown to be sufficient for the functionality of the protein in all other archaeal type opsins. Channelopsin-1-Synthetic gene (Chop-1-S; 951bp) was cloned under the control of ´tac´ promoter in pMALc2 plasmid. *Bam*H1 and *Hind*III restriction sites were introduced upstream and downstream of the *chop-1-S* gene by PCR and the *Bam*H1 and *Hind*III containing gene fragment was cloned into the pMALc2 vector, which allows addition of a histidine tag at the N-terminus (Fig.6a). The pMALc2-Chop-1S construct was transformed into various *E. coli* expression strains (Table1) for the production of recombinant Chop1 protein (for details refer Materials and Methods section). Expression was induced using various experimental parameters as mentioned in Table1. However, few other conditions were also used as described below to obtained better expression and solubility of the expressed protein.

The expression of a foreign gene in *E. coli* sometimes diminishes the growth of the cells. Therefore, evaluation of the toxicity of Chop-1S expression in *E. coli* was performed. pMALc2-Chop-1S construct was transformed into expression strains (BL21-DE3pLys and BL-21 λ DE3) and plated on to two set of LB-Amp plates, one with 0.6mM IPTG and another without the inducer. Very few colonies were observed on the IPTG containing plate compared to the one without IPTG. Moreover, size of the clones was smaller in the presence of IPTG, and the colonies took 24 hrs to appear at 37°C (BL21-DE3pLys was less affected by the expression of Chop-1). Further experiments were carried out to confirm the toxicity of Chop-1S expression in *E.coli*. Chop-1S transformant culture was grown at 37°C and OD_{578} nm of the culture was measured before and after induction with 1.0mM IPTG. It was observed that the cell density of the culture decreases drastically after induction (Table-2).

Table-2. Toxicity of Chop-1 Expression *in E.coli*

Expression Construct	OD_{578} nm before induction	OD_{578} nm after 2hrs of induction
Control (pMALc2 plasmid)	0.53	1.1
pMALc2-Chop-1S	0.55	0.275

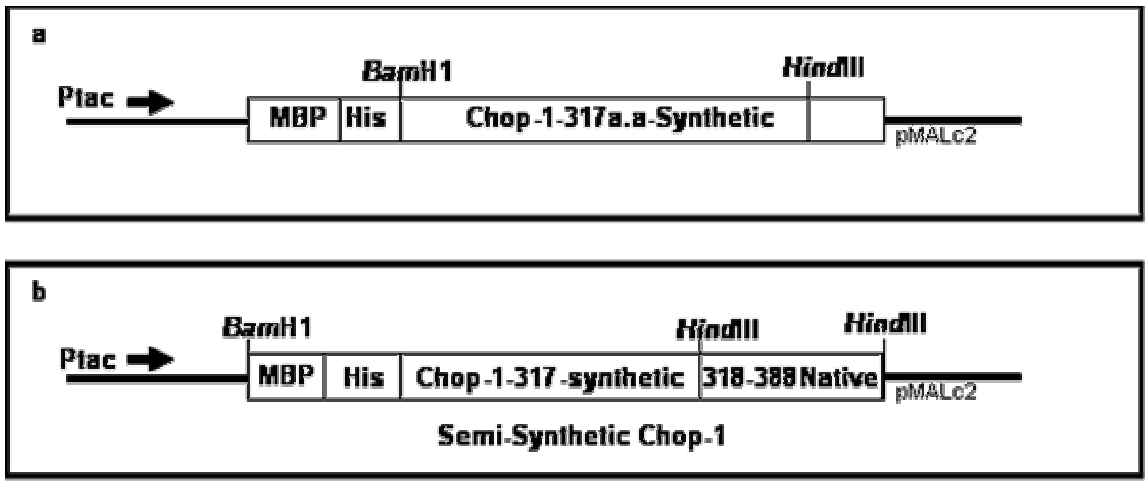

Figure 6. Channelopsin-1 Synthetic (Chop-1S) and Channelopsin-1-Semi-Synthetic (Chop-1-SS) genes were cloned in pMALc2 vector for expression in *E.coli.* (a) Chop-1-S gene was cloned in the *Bam*H1 and *Hind*III restriction sites under the control of ´tac´ promoter to produce an MBP-Chop-1S fusion protein with an extended His-tag at the N-terminus. (b) Native part of *chop-1* gene (318-388 aa) was PCR amplified from the cDNA clone and cloned in the *Hind*III restriction site of pMALc2-Chop-1S construct.

It was also observed that BL-21DE3*pLys* was less affected by the toxicity of Chop-1 expression (BL-21DE3*pLys* has tight control over the leaky expression of protein). Therefore, all further experiments were carried out with this strain. A temperature downshift from 37 to 30°C for the tac promoter containing expression vector in *E.coli* produces better yields of β-glactosidase enzyme (Vasina and Baneyx, 1997). Therefore, the expression of Chop-1S was checked at 37°C and 30°C with various concentrations of IPTG. It was observed that a better yield was obtained when induction was carried out with 0.3mM IPTG at 30°C for 3hrs (Fig.7a). All retinal binding studies with expressed Chop-1S-MBP fusion were performed as described by Chen and colleagues (Chen and Gouaux, 1996). Despite getting the expression of Chop-1S, retinal binding could not still be achieved. However, retinal binding could be obtained with expressed Proteorhodopsin (PR) under similar experimental condition (Data not shown). In an effort to get functional expression of the Chop-1S with pMALc2 in *E. coli*, it was observed that the yield of the protein was very low, which ruled out the possibility of doing refolding studies of the expressed protein.

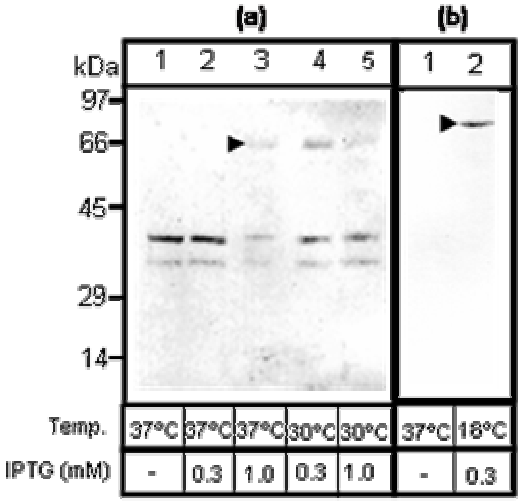

Figure 7. Expression of synthetic and semi-synthetic Channelopsin-1 (Chop-1-S; Chop-1SS*)* in *E. coli.* (a) pMALc2-Chop-1S transformant culture was induced with different concentrations of IPTG and incubated at different temperatures for 2.5 hrs. 25µg of total cell lysate was resolved on 12% SDS-PAGE, electro blotted to nitrocellulose membrane and immunoblotting was carried out using anti-His-tag antibody. (b) pMALc2-Chop-1SS transformant culture was induced with 0.3mM IPTG and incubated at 18°C for 16 hrs and immunoblotting was carried out as described in (a). The expressed protein bands are indicated by arrowheads.

Since the Chop-1S gene that was constructed encoded only 317 aa (7TMH), whereas the full-length gene had an extended C-terminus end with a stretch of hydrophilic aminoacids, it was speculated that this hydrophilic region of the protein might have role in the functionality of the recombinant protein. Therefore, a Semi-synthetic-Channelopsin-1 (Chop-1SS) construct was made for expression in *E. coli*. A region of the gene, downstream of the above mentioned 317aa coding gene was PCR amplified using an EST clone (AV396596) as a template. *Hin*dIII restriction sites were introduced upstream and downstream of the PCR product. The PCR product was digested and cloned into Chop-1S-pMALc2 vector at the *Hin*dIII site (Fig. 6b). Induction of Chop-1SS was carried out in BL21-DE3pLys cells with 0.3mM IPTG at 30ºC for 3hrs. Western blot analysis with an anti His-tag antibody revealed the presence of His-tagged Chop-1SS in the total cell lysate of induced transformant culture of *E.coli* (Fig.7b; lane 2). However, *all-trans* retinal binding could not be observed with expressed Chop-1SS protein.

As functional expression of Chop-1 could not be achieved in *E. coli*, an alternative expression system *P.pastoris* was employed to obtain functional expression of Chop-1 protein heterologously.

3.1.3. Heterologous Expression of Chop-1-SS in *P. pastoris*

3.1.3.1. The *P. pastoris* Expression System

In the past decades, the methylotrophic yeast *P. pastoris* has been developed as a host for the heterologous production of proteins (Reilander and Weiss, 1998). Compared to other expression systems, *P. pastoris* offers many advantages, since the produced proteins are correctly folded and secreted into the medium. Thus, fermentation of genetically engineered *P. pastoris* provides an excellent alternative to the *E. coli* expression systems. Moreover, since *P. pastoris* has been used for the functional expression of Nop-1 gene (Brown et al., 2001), Chop-1SS was tried to be expressed in *P. pastoris*.

3.1.3.2. Expression of Chop-1SS in *P. pastoris*

The pPIC9K expression vector uses AOX promoter, which is able to drive over-expression of the foreign gene in *P. pastoris*. Chop-1SS was cloned into pPIC9K vector under ´AOX´ promoter. *Eco*R1 and *Avr*II restriction sites were introduced upstream and downstream of the *chop-1-SS* gene by PCR and the *Eco*R1 and *Avr*II containing gene fragment was cloned into the respective sites of the pPIC9K vector (Fig.8a). Expression of Chop-1SS was induced with the addition of methanol (0.5% V/V) every 24 hrs and incubated for 48 hrs at 30ºC, and 10 µM *all trans*-retinal was added at the time of induction for regeneration of opsin (Brown et al., 2001). Induction of protein was not visible on SDS-PAGE; therefore, expression profile was checked by western blotting using protein specific anti-Chop-1 antibody. It was observed that Chop-1SS protein expression appeared after 24hrs of induction (Fig.8b). Even though expression of Chop-1SS protein was obtained in *P. pastoris*, retinal binding could still not be observed. It was therefore clear that *E.coli* and *P. pastoris* expression systems were not suitable for functional expression of Chop-1. Therefore, focused was shifted on yet other expression system, oocytes of *X. laevis* for functional expression and characterization of Chop-1.

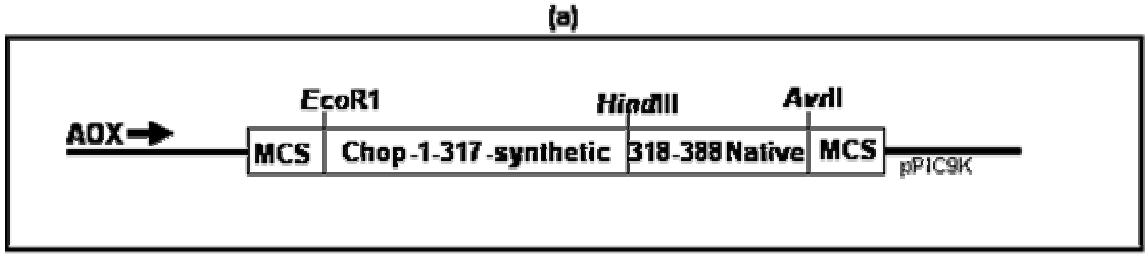

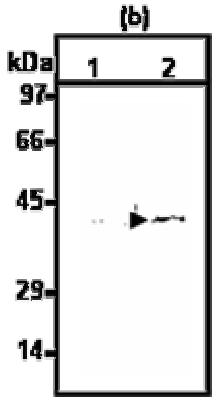

Figure 8. Chop-SS expression construct and its expression in *P.pastoris.* (a) Semi-synthetic Chop-1 gene was cloned into pPIC9K vector in *Ec*oR1 and *Avr*II restriction sites in the multiple cloning site (MCS), for expression of Chop-1. (b) pPIC9K-Chop-1SS transformant culture was induced with methanol (0.5% V/V) at 30ºC for 24hrs. 25µg of total cell lysate of uninduced (lane 1) and induced (lane 2) cultures were resolved on 12% SDS-PAGE, electro blotted to nitrocellulose membrane and immunoblotting was carried out using anti-Chop-1 antibody. The expressed protein band is shown by arrowhead.

3.1.4. Expression and Characterization of Chop-1 in *X. laevis* Oocytes

3.1.4.1. The Expression System

Xenopus oocyte as a heterologous expression system has gained tremendous popularity in recent years. It is a reliable expression system for membrane-bound proteins, in particular for ion channel and transport system. The large size of *Xenopus* oocytes (Ø=1.2 mm), allows easy injection of nucleic acids, chemicals and even the insertion of pipettes containing a patch, which is a clear advantage of using this as an expression system. Since, the first demonstration by Miledi that ion channel and neural receptors can be functionally expressed in *Xenopus* oocytes (Miledi, 1982) this system has become a standard for demonstrating that a specific cloned cDNA encodes a functional channel or receptor. Many different ion channel and receptors have been expressed in oocytes for functional analysis (Snutch, 1988), and oocytes have been used for functional cloning of receptors/channels. RNA for injection into oocytes can be isolated from the appropriate tissue sample or cell line or it can be synthesized *in vitro* from a cDNA clone.

3.1.4.2. Vector for Expression in *X. laevis* Oocytes

The only essential element of a vector for RNA transcription and expression in oocytes is a promoter for a DNA-dependent RNA polymerase, such as one of the polymerase isolated from phage T7, T3 or SP6. However, it is important to obtain high level expression of a particular channel, such as for the detection by immunofluroscence, immunoprecipitation and the measurement of gating current in many cases. The *X. laevis* β-globin gene is one of the most stably expressed mRNA transcripts. It has also been shown that adding the 5´ and 3´ untranslated region from the β-globin gene greatly increases the expression of exogenous protein in oocytes. The pGEM-HE vector (Liman and Buck, 1994; Liman et al., 1992) was used for expression of Channelopsins, which was able to fulfill all above described criteria for high level of expression of foreign gene in *Xenopus* oocytes as previously shown by expression of bacteriorhodopsin in oocytes (Nagel et al., 1995). This vector contains a T7 promoter followed by the 5´UTR of β-globin gene, a multiple cloning site (MCS) region for subcloning of exogenous DNA, the 3´ UTR of β-globin gene and a poly (A) tail. There is a polylinker following the poly (A) tail so that the construct can be linerized before transcribing RNA. Additional manipulations can be performed to increase the level of expression, such as altering the 5´ UTR of the cDNA insert.

3.1.4.3. Expression of Chop-1 in *X. laevis* Oocytes

The expression of bacterial retinal proteins and insertion into the plasma membrane of *Xenopus* oocytes has opened the opportunity to study the transport activity of the sensory rhodopsins and the interaction of these proteins with their corresponding transducers using two electrode voltage clamp (TEVC) methods (Nagel et al., 1998; Nagel et al., 1995; Schmies et al., 2001). It has been shown that the two photoreceptors SRI and pSRII as well as the functional signaling complexes with their corresponding transducers HtrI and pHtrII can also be expressed into the plasma membrane of *Xenopus* oocytes (Nagel et al., 1998; Schmies et al., 2001). The electrophysiological studies with *C.reinhardtii* have shown that it might uses a proton conducting channel for photobehavioural responses (Ehlenbeck et al., 2002). It was speculated from the homology of Chop-1 to other known microbial type opsins that it might function as a transporter in active/passive mode upon functional expression followed by illumination with green/blue light. Chop-1 cDNA variants were cloned in pGEM-HE vector to check the proposed activity of the protein upon functional expression. These constructs were prepared and expressed in *X. laevis* oocytes by Georg

Nagel and co-workers to measure the proposed function of the protein. It must be noted that all electrophysiological experiments of Chop-1in oocytes were done by G. Nagel.

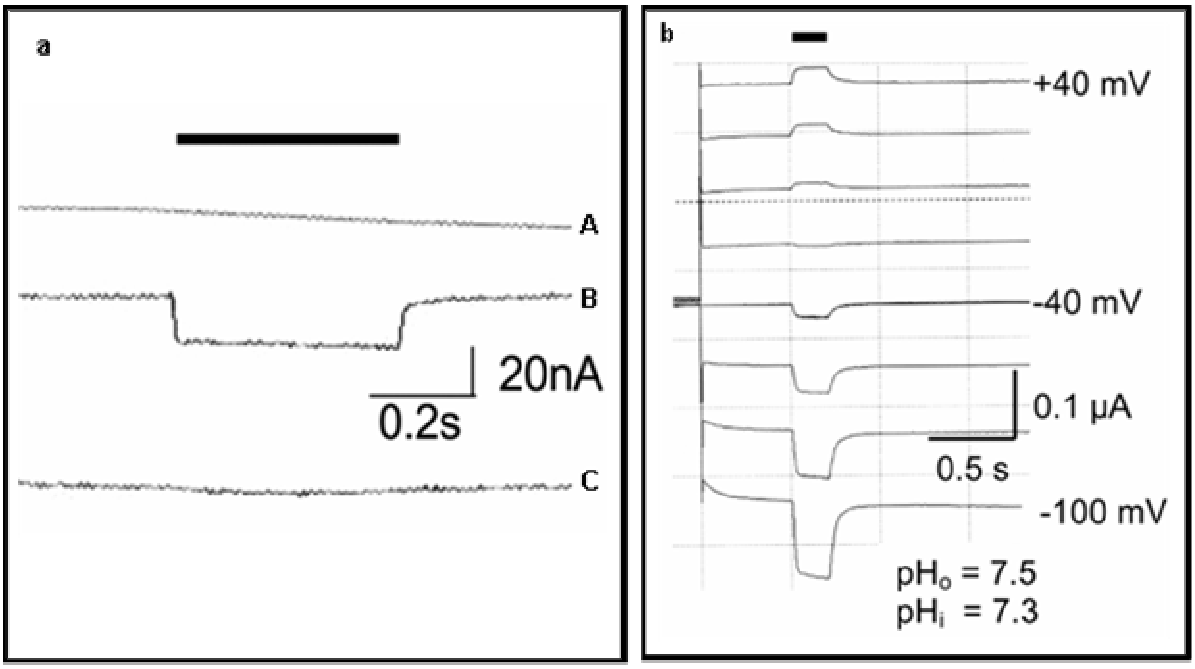

Figure 9. Light and voltage dependence of photocurrents at pH = 7.5. (a) Photocurrents recorded during illumination of *oocytes* with green or red light (500 ± 25 nm or 700 ± 25 nm, respectively; 10^{22} photons m^{-2} s^{-1}). Membrane potential (*V*) = -100 mV; the light pulse is indicated by a bar. Bath solution: 96 mM NaCl, 5 mM KCl, 2 mM $CaCl_2$, 1 mM $MgCl_2$, 5 mM MOPS (pH = 7.5). Trace A: A noninjected oocyte, green light. Trace B: A Chop1 oocyte, green light. Trace C: The same Chop1 oocyte as in trace B, irradiated with red light. (b) Current responses of a Chop1 oocyte to voltage steps from -100 mV to +40 mV (in 20-mV steps; holding potential V_h = -40 mV), followed by green light pulses of 200-ms duration. Bath solution: 96 mM NaCl, 5 mM KCl, 2 mM $CaCl_2$, 1 mM $MgCl_2$, 5 mM MOPS (pH = 7.5). This figure has been taken from a published paper (Nagel et al., 2002).

Expression of all three *chop-1* gene constructs in oocytes led to light-gated H^+-conductance. Illumination of *Chop-1-cRNA* injected oocytes using green light, but not red light, induced inward currents in Chop1 RNA-injected oocytes at a membrane potential of -100 mV (Fig. 9a). Similar results were obtained with truncated *Chop1* RNAs encoding only amino acids 1 to 346 or 1 to 517. At an external pH (pH_o) of 7.5, the inward current induced by green light reversed at a voltage near -15 mV (Fig. 9b) with clearly visible outward photocurrents at positive membrane potentials. Reversal potential of -15 mV is close to the Nernst potential for Cl^- (-20 mV). It was deduced by expressing CFTR (cystic

fibrosis transmembrane conductance regulator) Cl^- channels in oocytes (Nagel et al., 2001) or H^+ [-12 mV, at an intracellular pH (pH_i) of 7.3, as measured with microelectrodes by Nagel and others (Stewart et al., 2001)], but far from Nernst potentials for Na^+, K^+, or Ca^{2+}. To investigate the ionic specificity of the light-induced permeability of Chop-1, Nagel *et al* have systematically changed the composition of the bath solution (Nagel et al., 2002).

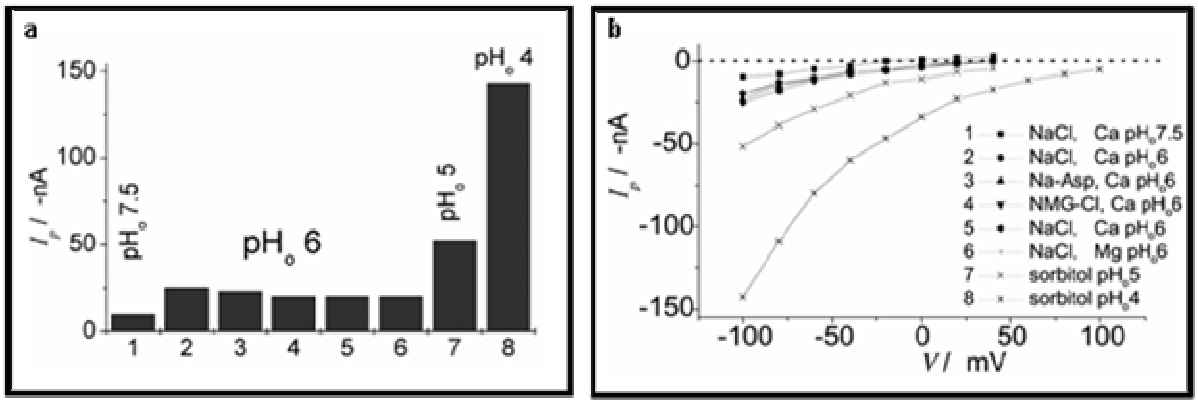

Figure 10. Dependence of photocurrent (I_P) on ionic condition and pH_o. (a) Results from one (out of five) characteristic Chop1 oocyte, plotted in the order of measurement (~150-s interval); V = -100 mV, green light as in Fig. 11a. Solutions were buffered with 5 mM MOPS (pH = 7.5), MES (pH = 6), or citrate (pH = 5 and 4). Concentration (mM): bar 1: 100 NaCl, 2 $CaCl_2$ (pH = 7.5); bar 2: 100 NaCl, 2 $CaCl_2$ (pH = 6.0) (reference condition); bar 3: 100 Na-aspartate, 2 $CaCl_2$ (pH = 6.0); bar 4: 100 NMG-Cl, 2 $CaCl_2$ (pH = 6.0); bar 5: same as bar 2; bar 6: 100 NaCl, 2 EGTA, 2 $MgCl_2$ (pH = 6.0); bar 7: 200 sorbitol, 5 EGTA (pH = 5.0); bar 8: 200 sorbitol, 5 EGTA (pH = 4.0). (b) Voltage dependence of photocurrents (I_p) from (a) concentrations as in (a). Figure has been taken from a published paper (Nagel et al., 2002).

Lowering the pH_o to 6.0 increased inward photocurrents and shifted the reversal potential to > + 40 mV (Fig. 12a and b). Replacing Cl^- by aspartate (pH_o = 6) had no discernible effect on the photocurrent amplitude or its current-voltage (*I-V*) relation (Fig. 10a and b), thus excluding Cl^- as the conducted ion. Similarly, Na^+ and Ca^{2+} were excluded: Photocurrents were not changed by replacing Na^+ by *N*-methyl-D-glucamine (NMG) or by replacing Ca^{2+} with Mg^{2+} (Fig. 10a and b).

3.2. Channelopsin-2

3.2.1. Identification and Bioinformatic Analysis of Channelopsin-2

C. reinhardtii genome database was mined using BLAST program to search for homologues of Chop-1. This search revealed the existence of few more overlapping EST clones. One such EST clone (AV643095) showed the presence of an ORF, which encoded a different protein sequence than that of Chop-1. This particular EST clone (AV643095) was obtained, complete sequencing of the clone was done, and the corresponding protein sequence was deduced. The protein sequence thus obtained was named Chop-2 based on its homology to Chop-1. This sequence information was submitted to NCBI, AccNo: AF461397.

3.2.1.1. Homology between Channelopsin-2 and Other Archaeal Type Opsins

Chop-2 protein sequence was aligned with the other known Type-1 opsins (Including Chop1; Fig.11). The seven transmembrane helices region (1-310 aa from N-terminus) of Chop-2 protein shows <22% homology to sensory rhodopsins from the archaea and <14% to the opsin protein from *Neurospora* (Nop-1). The retinal binding residue K in Type-1 opsin is present in a conserved retinal binding motif LDXXXKXXF/W^{259}, suggesting that K^{257} of Chop-2 is the retinal-binding amino acid (Nagel et al., 2003). Chop-2 full-length protein showed very high homology ~75% to the known Chop-1 protein. It could therefore be concluded that Chop-2 is a member of the classical archaeal rhodopsin (Type I rhodopsins) superfamily.

3.2.1.2. Secondary Structure Prediction of Channelopsin-2

The hydropathy plot analysis has predicted 11-transmembrane helices in Chop-2 protein sequence (*Appendix*A2.1), seven of them from N-terminus showed homology to the known archaeal type opsins (Including Chop-1; Fig.11). It must be noted that Sineshchekov *et al* claimed from hydropathy plot analysis of the C-terminus of Chop-2 protein that it have no sign for the presence of TMH. However, they have also observed that the 400-residue of C-terminal domains of both Chop-1 and Chop-2 were membrane associated when expressed in *E.coli* (Sineshchekov et al., 2002). Therefore, it seems that our predictions for TMH of Channelopsins are matching with experiments.

It was observed using SignalP program that Chop-2 showed the presence of a leader peptide sequence (*Appendix*.A2.2) at the N-terminus, which cleaves off during posttranslational modification.

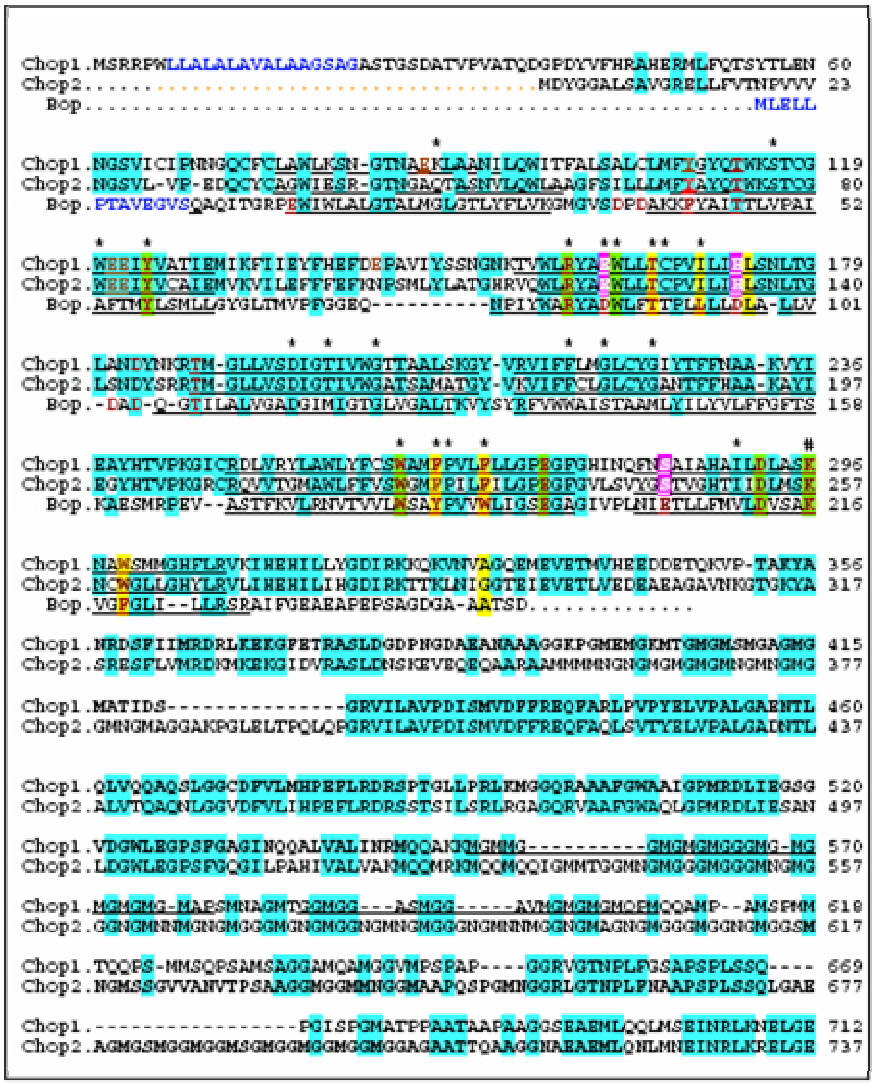

Figure 11. Comparison of amino acid sequences of Channelopsin-1 (Chop1; AF385748), Channelopisn-2 (Chop2; AF461397) and Bacteriorhodopsin from *H. halobium*. Amino acids that are known from the bacteriorhodopsin structure to interact directly with retinal are indicated with an asterisk (*). Amino acids that are conserved in most microbial opsins are highlighted in green; those that are functionally homologous in microbial opsin sequences are in yellow, other identities are shown in blue. Amino acids that contribute to the H^+- conducting network in BR are shown in red. Residues that are part of the transmembrane H^+-network are in bold type. The key substitutions, D^{85}, D^{96} and E^{204} in BR to E^{162}, H^{173} and S^{284} in Chop1 and E^{123}, H^{134}, S^{245} in Chop2 are seen as white letters on red background. Underlined regions indicate identified or hypothetical transmembrane regions. Amino acid sequences indicated in bold were used for expression in *E. coli* and antibody preparation. This figure has been taken from a published paper (Nagel et al. 2003).

Bioinformatic analysis of Chop-2 using Conserved Domain Architecture Retrieval Tool (CDART) identified a bacteriorhodopsin like domain in the protein sequence (*Appendix*.A2.3). The CDART analysis has also recognized more than 110 opsin related sequences from different organisms, which were homologous to Chop-2. These results strongly suggest that Chop-2 could be the second microbial-type opsin of *C. reinhardtii*. In general, *in silico* predictions of Chop-2 were similar to the ones for Chop-1. Therefore, it was suggested that Chop-2 might be functionally similar to Chop-1 protein. Chop-2 protein sequence was also analyzed for presence of putative phosphorylation sites in protein sequence. It was observed that C-terminus region of Chop-2 protein contains several serine residues(S), which are predicted to be potential phosphorylation sites (*Appendix* A2.4). This predicted phosphorylation patter of the protein might have significant physiological implications *in-vivo.*

3.2.1.3. Phylogenetic Analysis of Channelopsin-2

A dendogram of archaeal type opsins was constructed based on homology among different opsins (Fig.12). It was observed that Channelopsins (Chop-1 and 2) were closer to haloarchaeal and eubacterial opsins than to fungal opsins, which had previously been known as the only archaeal-type opsin subfamily in eukaryotes.

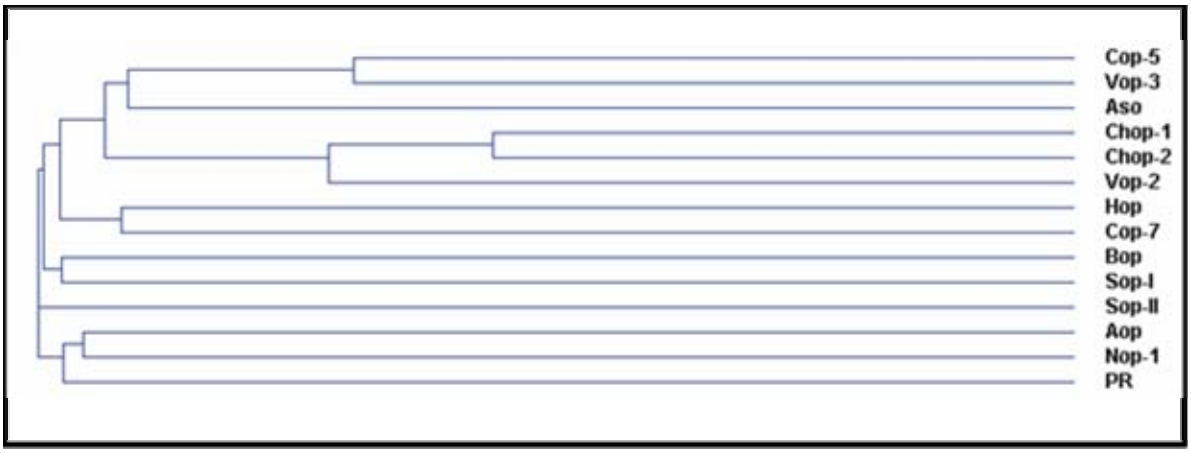

Figure 12. Phylogenetic relationship of opsin domain (helices 3-7) of a variety of archaeal type opsins is represented as a dendogram. Abbreviations mentioned above are as follows: Cop-5 (Putative Chlamyopsin-5), Vop-3 (Putative Volvox Opsin-3), Aso (Anabena Sensory Opsin), Chop-1 (Channelopsin-1), Chop-2 (Channelopsin-2), Vop-2 (Putative Volvox Opsin-2), Hop (Halo-opsin) Cop-7 (Putative Chlamyopsin-7), Bop (Bacterio-opsin), Sop-I (Sensory Opsin-1), Sop-II (Sensory Opsin-II), Aop (Putative Acetabularia Opsin), Nop-1 (Neurospora opsin) PR (Proteorhodopsin). Putative sequences were fetched from the genome database of the particular organisms, respectively.

Interestingly, putative Volvoxopsins (Vop-2 and Vop-3) were found to be closer to Channelopsins and Chlamyopsin-5 respectively, suggesting a possible functional similarity.

3.2.2. Expression and Characterization of Channelopsin-2

Previous results have shown that expression of Chop1 in oocytes of *X. laevis* produces a light-gated conductance that is highly selective for protons, and Nagel *et al* have suggested that Channelrhodopsin-1 (ChR1 = Chop1 + all-*trans* retinal) is the photoreceptor system that mediates the H^+-carried photoreceptor current (Nagel et al., 2002). Sineshchekov and colleagues have generated transformants in which the ratio of Chop1 and its homolog Chop2 was changed by an antisense approach (Sineshchekov et al., 2002). In an electrical cell population assay that monitors the differential response of cells facing the light versus cells facing away from the light, the authors demonstrated that both ChR1 and ChR2 contribute to the photoreceptor currents (Sineshchekov et al., 2002). It was observed that in ChR1-deprived cells, photocurrents at high flash intensities were reduced, whereas in ChR2-deprived cells photocurrents at low flash energies were reduced. The authors have concluded that ChR1 mediates the high-intensity response, whereas ChR2 is responsible for low-intensity photocurrents (Sineshchekov et al., 2002). The mechanism for how ChR1 and ChR2 contribute to the photocurrents and to what extent to photophobic responses and phototaxis could not be resolved. Takahashi and colleagues (Suzuki et al., 2003) generated antibodies against Chop1 and Chop2. They were not able to localize the Channelrhodopsin proteins within the total membrane fraction but detected Chop1 as a 66-kDa protein in enriched eyespot membranes. Untill now, heterologous expression of Chop-2 has not been reported, and its primary mode of action remains obscure. Therefore, our aim was to express the *chop-2* gene heterologously and carry out further characterizations.

3.2.2.1. Heterologous Expression of the *chop-2* Gene in *E. coli*

Since *E. coli* is the first choice for heterologous expression of any foreign gene, heterologous expression of *chop-2* was tried in *E. coli* to produce protein for characterization. A truncated *chop-2* (981bp) gene was cloned into the pET21a+ expression vector under ´T7´ promoter control. *Eco*R1 and *Hind*III restriction sites were introduced upstream and downstream of the *chop-2* gene by PCR, respectively. The *Eco*R1 and *Hind*III containing gene fragment was cloned into the respective enzyme sites in

pET21a+ vector, which allows addition of a five-histidine amino acid tag at the C-terminus (Fig.13a) of *chop-2* gene.

It was observed that BL-21DE3*pLys* expression strain could overcome the toxicity of Chop-2 expression (BL-21DE3*pLys* had tight control over the leaky expression of protein). Therefore, this strain was taken for all further experiments. As it was previously observed that a temperature downshift from 37 to 30 °C had positive influence on expression of Chop-1, the expression of Chop-2 was checked only at 30°C with various concentrations of IPTG. Chop-2 expression was obtained when induction was carried out with 0.6 mM IPTG at 30°C for 3hrs (Fig.13b).

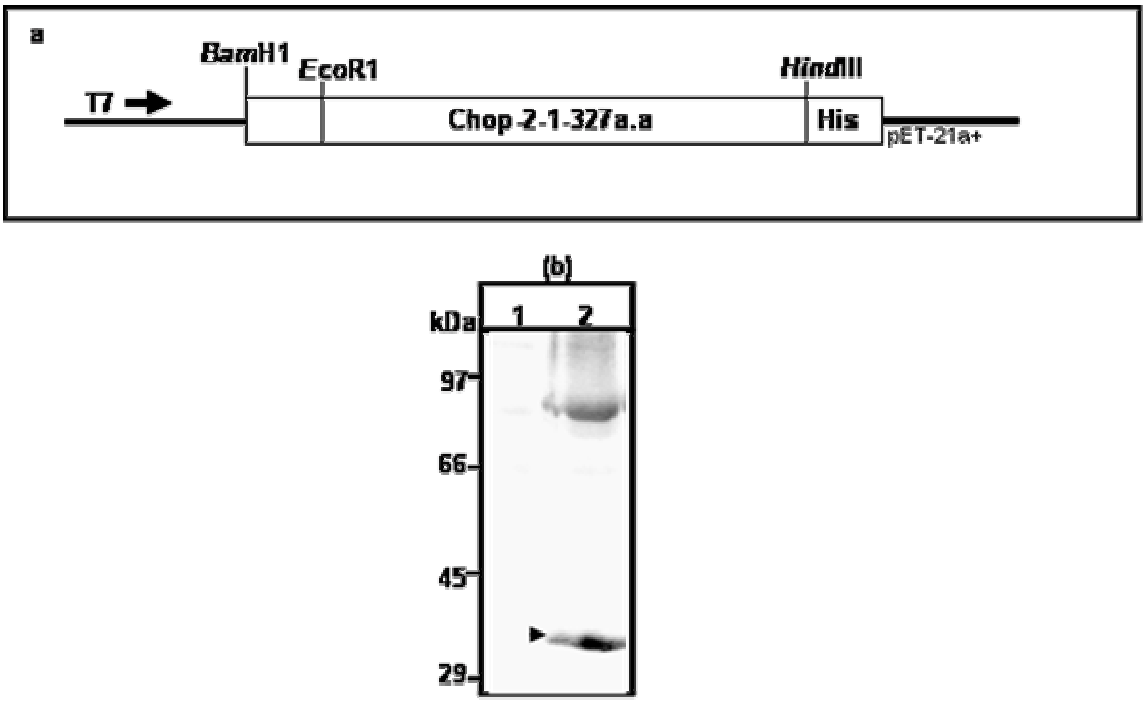

Figure 13. Cloning and expression of truncated Channelopsin-2 (Chop-2) in *E. coli*. (a) Chop-2 gene fragment (1-327aa) was cloned into pET21a+ expression vector in *Eco*R1 and *Hind*III restriction sites. (b) pET21a+-Chop-2 transformant culture was induced with 0.6 mM IPTG at 30ºC for 3 hrs. 25µg of total cell lysate of uninduced (lane 1) and induced (lane 2) cultures were resolved on 12% SDS-PAGE, electro blotted to nitrocellulose membrane and immunoblotting was carried out using anti-His-tag antibody. The expressed protein band is shown by arrowhead.

All retinal binding studies with expressed Chop-2 protein were performed as described by Chen and colleagues (Chen and Gouaux, 1996). Better expression of Chop-2 was obtained when cultures were grown in terrific broth medium (TB) and induction was carried out

with 0.6 mM IPTG. Even though, Chop-2 could be heterologously expressed in *E. coli* retinal binding could not be achieved. Since, it was observed that expression characteristic of Chop-2 in *E. coli* was very similar to that of Chop-1, and that functional expression of Chop-1 could be obtained only in *X. laevis* oocytes it was speculated that Chop-2 might be functionally expressed in the *Xenopus* oocytes. Therefore, focus was directly shifted to *Xenopus* oocytes expression system.

3.2.3. Expression and Characterization of Chop-2 in *X. laevis* Oocytes

A full length and C-terminally truncated Chop-2 gene fragment were generated from a full-length cDNA clone (AV643095) by PCR and cloned into pGEM-HE vector. It must be noted that all electrophysiological recording with ChR2 expressing oocytes were done by George Nagel. *Chop2-mRNA* was expressed in oocytes of *X. laevis*, in the presence of *all-trans* retinal, to test whether a functional rhodopsin (with covalently linked retinal: ChR2) could be obtained. Oocytes were examined by using two electrode voltage-clamp techniques (Nagel et al., 1998; Nagel et al., 1995). A full-length ChR2 or a ChR2 gene fragment comprising only amino acids 1–315 were tested (Fig. 14a).

Large light-activated currents were observed with both constructs, in standard oocyte Ringer's solution (Fig. 16b). These photocurrents were completely absent in non-injected oocytes, as reported in previous studies on other rhodopsins, expressed in oocytes under similar conditions (Nagel et al., 1998; Nagel et al., 1995; Schmies et al., 2001). In continuous light, the photocurrent decays to a steady-state level, i.e., desensitizes (Fig. 14b). The amplitude and direction of the photocurrent varied with the membrane potential, indicating that light triggers a passive ion conductance of ChR2. The cation conductance of ChR2 is confined to the hypothetical 7-TM helices, as identical photocurrents and very similar current–voltage relationships were obtained with ChR2–737 or ChR2–315, allowing the conclusion that those amino acids (316–737aa) do not contribute to the ion conductance.

In contrast to the proton-selective ion channel ChR1, ChR2 photocurrents greatly varied in solutions containing different cations (Fig.14c), suggesting that several cations may permeate ChR2, that anions were not contributing to photocurrents was proved by replacing extracellular chloride for aspartate, which changed neither the magnitude nor the reversal potential of photocurrents (data not shown). The dependence of photocurrents on different salt solutions shows a strong inverse relationship with the atomic radius of the

cation (Fig.14c). The small inward photocurrent in presence of the large monovalent cation *N*-methyl-D-glucamine (NMG^+) at pH 7.6 might indicate that ChR2 is permeable for NMG^+. However, since the inward photocurrent completely vanishes at pH 9 in NMG-Cl, whereas it remains for LiCl at pH 9, we conclude that the inward photocurrent in the presence of NMG-Cl is a proton flux, which becomes highly obvious at pH 5 (Fig.14d).

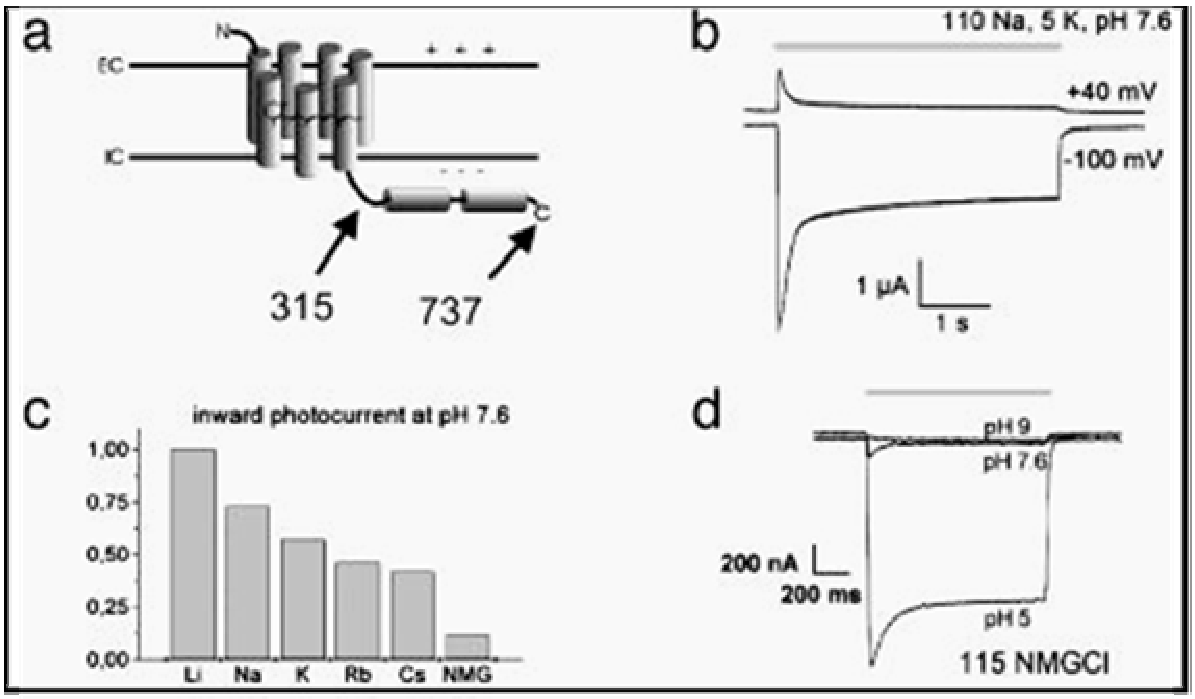

Figure 14. Ion dependence of light-activated conductance mediated by ChR2–315: Photocurrents of full-length ChR2–737 were indistinguishable. (*a*) Scheme of full-length ChR2-1–737 aa and truncated part of the protein ChR2-1–315. (*b*) Two-electrode voltage-clamp records from oocytes, expressing ChR2–315, in Ringer's solution (110 mM NaCl, 5 mM KCl, 2 mM $CaCl_2$, 1 mM $MgCl_2$, pH 7.6). Illumination with blue (450 ± 25 nm) light is indicated by the gray bar. Currents are typical of those in (Nagel et al. 2002) other experiments. (*c*) Normalized inward photocurrents at –100 mV, pH 7.6, for 115 mM salt solutions of: LiCl, NaCl, KCl, RbCl, CsCl, and NMG-Cl, measured in the same oocyte. (*d*) Photocurrents at –100 m, from the same oocyte, in 115 mM NMG-Cl, at pH 9, pH 7.6, or pH 5, this figure has been taken from a published paper (Nagel et al., 2003).

3.2.4. Specificity Test of Chop-1 and Chop-2 Antibodies

The polyclonal antibodies (Chop-1 and Chop-2) used in this were kindly provided by Peter Berthold. These antibodies were generated against the C- terminal part of Chop-1 (310-547 aa) and Chop-2 (617-723 aa). Since, MBP-Channelopsin (MBP-Chop-1 and 2) fusion proteins were used as antigen to generate these antibodies, it was required that the specificity of the antibodies for Channelopsins (Chop-1 and 2) be checked.

3.2.4.1. Expression of the C-terminus of Chop-1 and Chop-2 in *E.coli*

The C- terminus of Chop-1 (310-712 aa) and Chop-2 (273-723 aa) were cloned in pMALc2 and pET 21a+ vectors in order to express C-terminal domain of Channelopsins with and without MBP fusion, respectively.

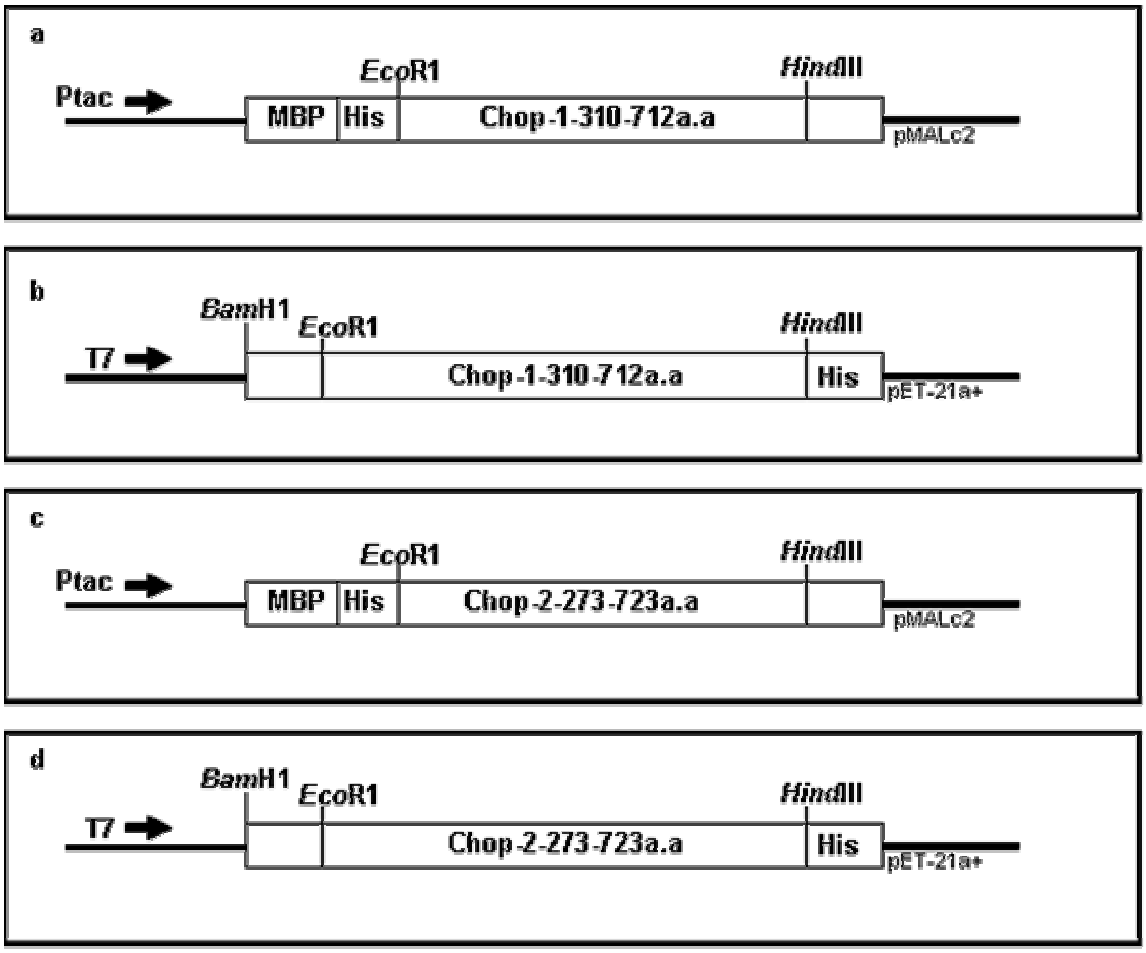

Figure 15. Cloning of C-terminus regions of Chop-1-C and Chop-2-C. (a-d) Chop-1(310-712 aa) and Chop-2 (272-723 aa) gene fragments were cloned in to the *Eco*RI and *Hind*III restriction sites of pMALc2 and pET21a vectors respectively.

The C- terminus of Chop-1 and Chop-2 were cloned in to the *Eco*RI and *Hind*III restriction sites of pMALc2 and pET21a vectors under 'tac' and T7 promoters, respectively (Fig.15 a-d). It was observed from western blotting experiments that the anti-Chop-1 and anti-Chop-2 antibodies could recognize expressed Chop-1-C and Chop-2-C proteins with and without the MBP- fusion (Fig.16 a-b) respectively.

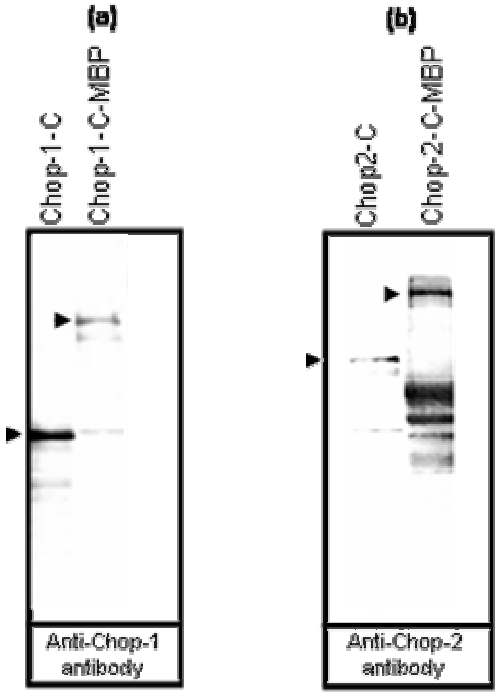

Figure 16. Immunoblotting of Chop-1-C and Chop-2-C expressed in *E.coli*. (a) Westen blotting of Chop-1-C and Chop-1-C-MBP was performed using anti Chop-1-antibody (1:1000 dilution). (b) Western blotting of Chop-2-C and Chop-2-C-MBP was performed using anti-Chop-2-antibody (1:1000 dilution). The corresponding protein bands are shown by arrowheads.

3.2.5. Light Dependent Expression of ChR1 and ChR2 in *C. reinhardtii*

The mining of *C. reinhardtii* EST sequence database (*C. reinhardtii* Genetic Centre) using BLAST search revealed that Chop-1 was present in a cDNA library of light grown cells whereas Chop-2 was present in a cDNA library of dark grown cells. Therefore, the expression profile of Chop-1 and Chop-2 were checked under different light conditions using Chop-1 and Chop-2 specific antibodies. *C. reinhardtii* cells (806 strain) were grown under different light conditions (high light, low light and darkness) and western blot

analysis was performed with the membrane fractions prepared from these cell cultures. It was observed that ChR2 appeared as a 70-kDa protein band, whereas ChR1 was seen as a triplet with molecular masses between 60 and 66 kDa. These molecular masses were smaller than the calculated molecular weight (from the predicted protein sequence) of 76 kDa for Chop-1 and 77 kDa for Chop-2. This could probably be due to post-translational modifications (i.e. phosphorylation) or a net negative charge at neutral pH. It was also observed that both proteins were most abundant, when the cells were grown under low-light conditions or in darkness. Both the proteins were degraded under high light conditions (Fig. 17a and b) and almost completely disappeared when the cell culture approached the stationary phase. The degradation of ChR2 was noted to be more rapid.

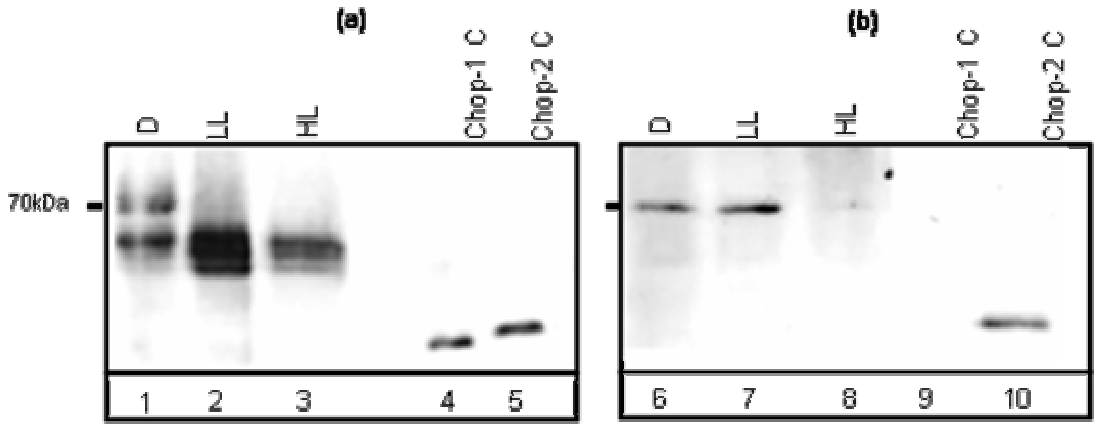

Figure 17. Expression profile of Chop-1 and 2 in *C. reinhardtii* membrane fractions under different light conditions.(D) cells grown in darkness, (LL) low light conditions (0.5W.m^{-2}), (HL) high light conditions (10 W.m^{-2}). (a) Membrane fractions were collected at different light conditions and immunoblotting was performed using anti-Chop-$1_{310-547}$ antibody (1:1000 dilution). (b) Membrane fractions were collected at different light conditions and immunoblotting was performed using anti-Chop-$2_{617-723}$ antibody (1:1000 dilution). Lanes 4, 5, 9 and 10 contains Chop-1 and Chop-2 fragments expressed in *E.coli* for specificity comparison. The anti-Chop-1 antibody recognized both Chop-1 and Chop-2 whereas; anti-Chop-2 antibody was specific to Chop-2.

3.2.5.1. Expression Profile of ChR1 and ChR2 during Life Cycle of *C. reinhardtii*

The expression profile of Channelopsin proteins studied under different light conditions revealed that the expression of Channelopsins in *806* cell strain is regulated in a light dependent manner (Fig.17). It was therefore, interesting to study the light dependent temporal expression of these proteins in *C. reinhardtii*. In order to check the expression profile of ChR1 and ChR2 during the life cycle of *C. reinhardtii*, cell strains CC-124^{+} and

125^{-} were grown under different light conditions. Samples were collected at intermittent intervals, the vegetative cells, gametes and zygotes were separated to observe expression of ChR1 and ChR2 during different phases of the *C. reinhardtii* life cycle under low light conditions (0.5W.m^{-2}). Expression pattern of ChR1 and ChR2 were checked by western blot using protein specific antibody (anti-Chop-1). In consistence with the previous results (Fig.17), cell strain CC-124^{+} showed light dependent expression of ChR1 and ChR-2 (Fig. 18; lane 1-3). It was observed that gametes of the strain CC-124^{+} expressed very low level of Chop-1, no Chop-2 (Fig.18; lane 4). The expression of Chop-1 was dominant in the pre-gamete and log phase grown vegetative cells of CC-124^{+} strain (Fig.18; lane 5 and 10). Similar expression pattern was found when the cell strain CC-125^{-} was used (Fig. 18; lane 8 and 9). Expression of Chop-1 was very low in the zygotic cells and Chop-2 expression was not observed in (Fig.18; lane 6 and 7). Cells in the mid log phase of growth showed equal expression of both proteins (Fig.18; lane 10 and 11). These experiments led to the conclusion that both channelopsin proteins were predominantly expressed in the pre-gamete stage and their expression was diminished in the subsequent growth phases.

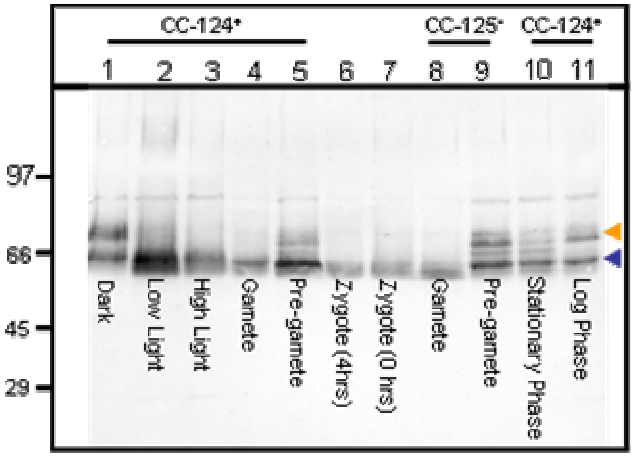

Figure 18. Expression profile of Channelrhodopsins during the life cycle of *C. reinhardtii.* Membrane fractions from cells at different stages of the life cycle were isolated and western blotting was performed using anti-Chop-1 antibody (1:1000 dilution). Blue arrowhead represents ChR1 protein and orange arrowhead represents ChR2 protein.

3.3. Opsin Coupled Two-Component System

Even though evidence strongly suggests that ChR1 and ChR2 are both responsible for photophobic responses, several mysteries remains to be solved. Firstly, since it has been shown that in *C. reinhardtii* the fast photoreceptor current is a Ca^{2+} current, which is quite insensitive to the extra-cellular pH (Ehlenbeck et al., 2002), it is obvious that it must be carried by a secondary conductance and not by ChR1 or ChR2. The protein responsible for this secondary conductance awaits molecular identification. Secondly, if ChR1 and ChR2 are responsible for photophobic responses with different spectral sensitivity, then the question, which arises is, which rhodopsin might be triggering phototaxis? In a recent publication, (Sineshchekov et al., 2002) the authors argued that ChR2 as the phototaxis receptor might couple to a transducer protein like the archaeal *Halobacterium* transducers (HTRs), which are activated by their sensory rhodopsins, SRI or SRII. Even if the conductance of ChR1/2 measured in *Xenopus* oocytes does not depend on the large COOH-terminal extension (Nagel et al., 2002; Nagel et al., 2003), this C-terminal extension of channelopsin might serve as a hinge to a secondary protein which awaits identification. Therefore, in order to identify this transducer like protein, the genome database of *C. reinhardtii* was mined using HtrI and II sequences as query sequence.

3.3.1. Opsin-Related Proteins in *C. reinhardtii*

The *C. reinhardtii* genome database was searched to identify transducer sequences from EST and BAC clone sequences. *H. salinarium* transducer protein (HtrI and II) and sensory opsin protein sequences were used as query sequences to identify its homologue in the *C. reinhardtii* genome database. Blast searches revealed the existence of three sequences that showed homology to prokaryotic transducer proteins. Furthermore, these sequences were found to be coupled to rhodopsin like sequences. Moreover, these three novel opsin sequences showed higher homology to the SRI and SRII from halobacteria than to ChR1 and ChR2. We provisionally named these sequences Cop5, Cop6, and Cop7 (Fig.19).

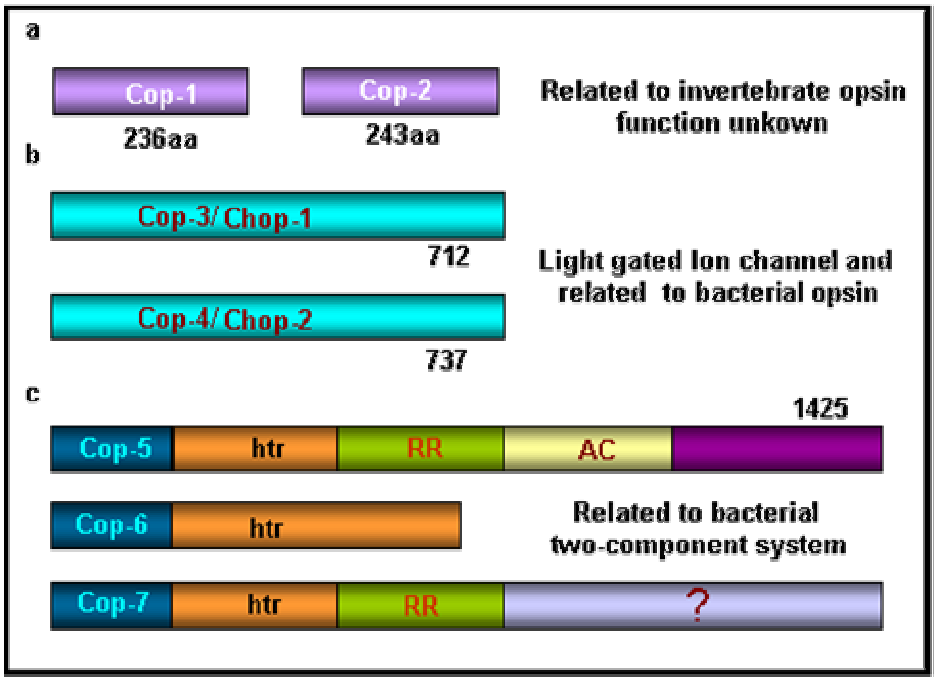

Figure 19.The diversity of opsin like proteins of *C. reinhardtii.* (a) Opsin related protein (Cop1) (S60158) and Cop2 (AAG02503). (b) The channelrhodopsins Cop3/Chop1 (channelopsin 1, AF385748) and Cop4/Chop2 (channelopsin 2, AF461397). (c) The hypothetical signal transducing rhodopsins Cop5 (AY272055), Cop6, and Cop7. Abbreviations: htr, transducer; RR, response regulator; AC/GC, adenylate or guanylate Cyclase. This figure has been taken from a published paper (Kateriya et al., 2004).

3.3.2. Isolation of *chlamyopsin-5* Gene

After having identified novel opsin like sequences from *C. reinhardtii* with the help of bioinformatics tools, the next objective was to isolate the corresponding gene and cDNAs. Initially, the BLAST search had revealed only a partial protein sequence of 121 amino acids, which showed homology to the third helix of the sensory rhodopsin. Therefore, an *in silico* cloning strategy was carried out to isolate full-length opsin encoding gene sequence from the database. The partial protein sequence obtained was used as a query sequence to locate the upstream and downstream overlapping gene sequences of new the opsin from the genome database. *In silico,* gene sequence walking was performed until the 5´ and 3´ UTR sequences were obtained for the new opsin sequences. The full-length sequence obtained was used for the prediction of gene structure and conceptual translation for obtaining the protein sequence. The *C. reinhardtii* Expressed Sequence Tag

(http://www.kazusa.or.jp/en/plant/chlamy/EST/) database was searched to obtain EST clones of *cop5*. BLAST search revealed the existence of only one cDNA clone (AV394119) in the database. The cDNA clone was obtained and sequenced. However, complete sequencing of the EST clone revealed that it was a partial cDNA clone containing region encoding exon 8 to exon 13.

Therefore, in order to isolate the full length gene three different strategies were adopted:

1. Isolation of full length *cop-5* cDNA by screening *C. reinhardtii* cDNA libraries
2. Screening of bacterial artificial chromosomes (BAC library)
3. PCR based methods (Genomic and/or RT-PCR).

3.3.2.1. Screening of cDNA library for Isolation of *cop-5* Gene

Four different λ ZAPII *C. reinhardtii* cDNA libraries generated under different growth conditions were obtained from *Chlamydomonas* genome project, USA. These cDNA libraries were screened by PCR with a *cop-5* gene fragment specific primers. However, *cop-5* cDNA could not be isolated from this cDNA library.

3.3.2.2. Isolation of *cop-5* Gene by RT-PCR and Genomic-PCR Method

RNA was isolated from culture grown under different light conditions (high, low and dark) and RT-PCR was carried out using Cop-5-opsin domain specific gene primers. Cop-5-opsin domain encoding gene could not be isolated by RT-PCR method.

Genomic PCR was performed for the isolation of Cop-5-opsin domain by using gene specific primers. Cop-5-opsin domain encoding fragment was isolated by genomic PCR, which was cloned and sequenced. The completion of the sequencing and prediction of gene structure confirmed to the sequence of *cop-5* gene in genome database.

3.3.2.3. Mining and Screening of a BAC Library for Isolation of the *cop-5* gene

The BAC clone sequences of *C. reinhardtii* are available from Clemson University Genome Institute (https://www.genome.clemson.edu/orders/). Mining of the BAC clones sequence database using BLAST search with 3´and/or 5´untranslated region (UTR) of *cop-5* gene revealed the presence of three BAC clones (026I2, 024P13 and 08F6), which showed identical DNA sequence to query sequences. All three BAC clones were purchased from the Genome Institute, Clemson University. The screening of BAC clones enabled us to isolate *cop-5* gene fragment, which contained gene information of the missing N-terminus fragment until the eighth exon of the *cop-5* gene. Moreover, full length genomic

DNA of *cop-5* gene was also obtained from the 024P13 BAC clone by PCR. The sequence of the full length genomic DNA obtained from the BAC clone was identical to that of *cop-5* gene available in the genome database.

3.3.3. Bioinformatic Characterization of Cop-5

After obtaining the full length genomic DNA of *cop-5* gene, the resultant gene sequence was used for further *in silico* characterizations. The gene structure, protein sequence, modular domain arrangement and homology based 3D structure were predicted. Bioinformatic characterizations were performed using web free resources and prediction programs available online.

3.3.3.1. Predicted Gene Structure and Primary Sequence of Chlamyopsin-5

The genomic DNA sequence of the putative opsin (*cop-5*) was used for the prediction of gene structure using web free resource GeneScan http://genes.mit.edu/GENSCAN.html program. It was revealed that *cop-5* gene consisted of 13 exons in the genomic sequence (Data not shown). The corresponding protein sequence was obtained and was predicted to encode1425 amino acids. The predicted gene structure and protein sequence information was submitted to the NCBI (AY272055.2) genome database, which is available online.

3.3.3.2. Identification of Modular Domains of Chlamyopsin-5

Simple Modular Architecture Research Tool (SMART), is a web-based resource used for the annotation of protein domains and the analysis of domain architectures, with particular emphasis on mobile eukaryotic domains (Letunic et al., 2002). Extensive annotation for each domain family is available, providing information related to function, sub-cellular localization, phylogenetic distribution and tertiary structure. User interfaces to this database allow searches for proteins containing specific combinations of domains in defined protein sequence (Schultz et al., 2000). The Chlamyopsin-5 (AY272055) protein sequence was analyzed using SMART available at http://smart.embl-heidelberg.de. The Cop-5 protein sequence had five modular domains (Fig.20). It also identified the presence of seven TMH at the N-terminus of the protein.

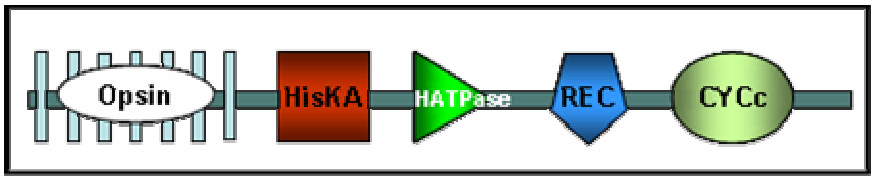

Figure 20.Putative arrangement of modular domains of Cop-5 within the protein sequence. Opsin (7TMH), Histidine Kinase (HisKA), ATPase (HATPase), Response Regulator (Rec) and Cyclase (CYCc) domains. These modular domains were identified using web free resource SMART.

3.3.3.3. Prediction of Leader Peptide Sequence and Secondary Structure

The *in silico* analysis further showed that the protein sequence of cop-5 predicted from the genome database lacked a leader peptide sequence; this led to the speculation that the predicted methionine was not the real start codon. Therefore, the upstream region of the *cop-5* gene was scanned to find another possible start codon in the same ORF. This search revealed an extended N-terminus of 70 amino acids with another methionine within the same ORF. Secondary structure topology of Cop-5 was predicted and it was found that Cop-5 protein sequence contains 15 putative TMH (*Appendix*; A3.1). This protein sequence was then analyzed for the presence of leader peptide sequence using SignalP, which then identified the presence of a leader peptide sequence at the N-terminus (*Appendix*; A3.2).

3.3.3.4. Homology Relation of Cop-5 Modular Domains with Known Prototype Proteins

The Chlamyopsin-5 sequence was aligned to sensory rhodopsin-II (SR-II) and putative Cop-7. It was observed that the homology between Cop5 and Cop7 is ~30% from helix 3 to 7, and the homology between Cop5 and the SR-II including Nop-1 from *N. pharaonis* is ~25% (Fig.21). Moreover, most amino acids that interact with retinal are conserved (Kateriya et al., 2004). These results suggested that Cop-5 might be a member of the classical type I opsin proteins.

The Cop-6 sequence was excluded in the multiple alignments because full-length gene sequence was not available in the genome database. Moreover, available partial sequence did not possess the conserved seventh helix that is an important characteristic of opsin proteins. Overall conservation of the transducer (HK) is higher, and the catalytically most prominent boxes H, X, D, G, and N can be easily identified (Table 3). This was quite surprising since such microbial-type transducers have not yet been identified in any plant.

Prokaryotic transducers couple to the so-called response regulators (RRs), constituting the heart of the two-component signaling system.

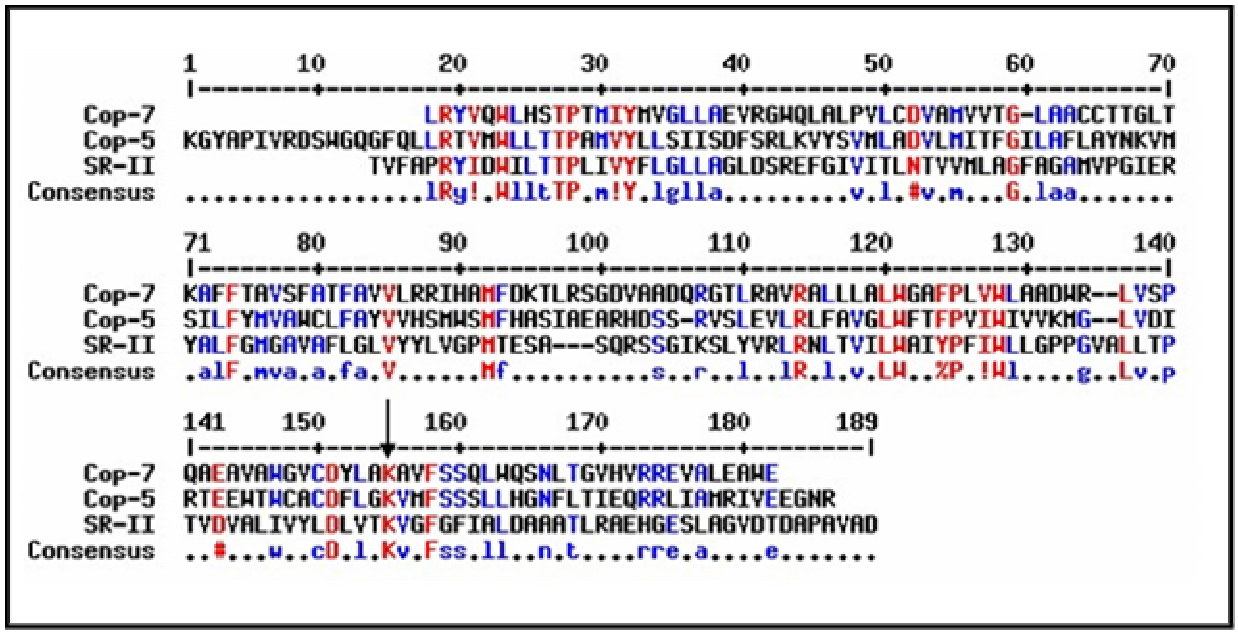

Figure 21. Multiple sequence alignment of transmembrane helix 3-7 of the Chalymopsins-5 and 7 with known sensory rhodopsin-II (SR-II). Identical and homologous amino acids in all three opsin sequences are marked by red letters and blue letters represent identical amino acids in any of the two-opsin sequences. A black arrow indicates conserved K residue in the 7th helix of all three opsins, which is supposed to bind with retinal via a Schiff base linkage.

Table-3: Homology between Modular Domains of Cop-5 and Prototype Sequences

Prototype Protein Sequence	Chlamyopsin-5 (AY2772055)	Conserved Domain in Cop-5
Sensory Rhodopsin (1H68A)	25%Identical (56-303a.a)	Helix 3 to 7 are Conserved
Histidine Kinase (1ID0A) Or HiskA	40%Identical (390-550a.a)	H,X,D,G and N Boxes
Response Regulator(1EAYA) Or Rec	35%Identical (705-820a.a)	Phosphate Acceptor Motif
Adenylate Cyclase (1FX2A) Or Guanylate Cyclase (CYC)	20%Identical (860-1055a.a)	Catalytic Unit (Highly Conserved)

In Cop5, a unique case was observed where all four modular domains: opsin domain, transducer, response regulator, and effector (AC/GC), are encoded by one open reading frame that is possibly translated into one large protein upon expression. However, there is no indication yet under which conditions these rhodopsins with potential linked enzymatic

activity (enzymerhodopsins) are expressed. The only hint of such expression is the availability of one partial Cop5 EST clone (AV394119) that appears in the *C. reinhardtii* expressed sequence tag (EST) database.

3.3.4. Comparative Molecular Modeling of Modular Domains of Cop-5

3.3.4.1. General Procedure for Comparative Molecular Modeling

The web server (Geno3D) that is available from the web link (http://geno3d-pbil.ibcp.fr) uses distance geometry, simulated annealing and energy minimization algorithms to build 3D models of the submitted query. In homology modeling, restrain co-ordinates derived from a structural 3D template are used to fold the query sequence in the distance geometry step. Comparative molecular modeling of Cop-5 modular domains was performed. Server performed the homology modeling of the protein sequence in six successive steps. I: identify homologous proteins with known 3D structures by using PSI-BLAST. II: provide the user all potential templates through a very convenient user interface for target selection. III: perform the alignment of both query and subject sequences. IV: extract geometrical restraints (dihedral angles and distances) for corresponding atoms between the query and the template. V: perform the 3D construction of the protein by using a distance geometry approach. VI: finally send the results by e-mail to the user (Christophe, 2001). The resultant PDB format files were visualized for 3-D structure with a web free Rasmol program.

3.3.4.2. The 3D Models of Modular Domains of Cop-5

The above-mentioned general procedure for molecular modeling was repeated for each modular domain of the Chlamyopsins-5, respectively. A homology-based approach was used for the prediction of boundaries of the modular domains of Cop-5.

The query sequence of each modular domain was used to fetch homologous proteins from PDB with known 3D structures using Geno 3 program. Possible 3D models of each domain were predicted based on the known structure of the prototype protein. The structure thus obtained was visualized using Rasmol (Fig.22). Using homology based protein modeling; it was demonstrated that all modular domains of Chlamyopsin-5 have conserved secondary structure and active site fold like their prototype proteins for each of the domains (Fig.22 a-d).

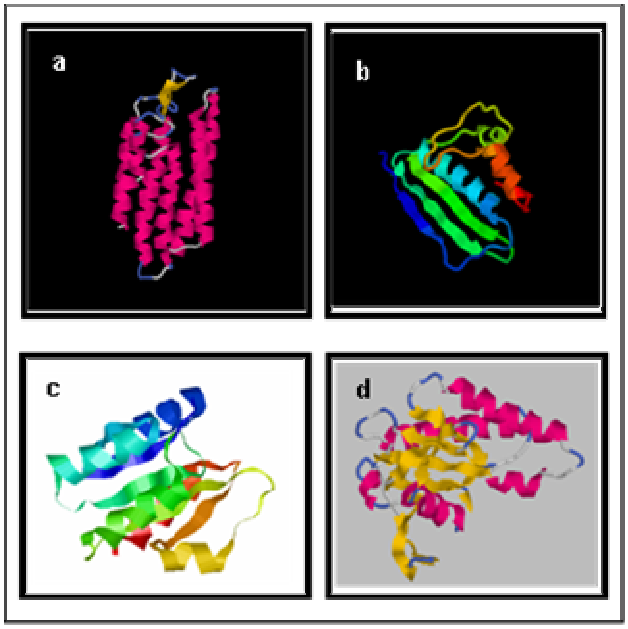

Figure 22.The predicted 3-D structure of putative modular domains of Cop-5. (a) Opsin domain. (b) Histidine Kinase. (c) Response Regulator. (d) Cyclase domain.

3.3.4.3. Proposed Model for Functional Activity of Cop-5 Protein

It was proposed based on homology of the Cop-5 domains that Cop-5 might show light regulated adenylate/guanylate cyclase activity upon functional expression. Therefore, a model was proposed to explain the possible activity of this novel opsin: Upon expression and illumination with light Cop-5 opsin domain might activate the transducer (HK) domain via conformational changes, which could lead to the phosphorylation of a conserved histidine residue in the H-box of the HK domain. The phosphorylated HK domain can switch the activation of the response regulator (RR) by transferring a phosphate group from a histidine residue of HK domain and it would then phosphorylate an aspartic amino acid residue of the acceptor motif in the RR domain like in two-component signaling, and finally regulate the activity of the cyclase domain. If the proposition holds true, the activity of Cop-5 will be able to hydrolyze cAMP/cGMP second messenger of the signal transduction pathway. It would then activate cAMP/cGMP gated ion channel in the cell and/or cAMP/cGMP could lead to the phosphorylation of cAMP/cGMP dependent protein kinases. These steps of the signal transduction could influence phototaxis activity directly/indirectly in *C. reinhardtii.*

It was therefore decided to express Cop-5 heterologously to characterize its functional activity.

3.3.5. Heterologous Expression of Cop-5 in *E. coli*

In order to study in detail the structure and functional characteristics of any protein it is desirable that a sizeable amount of the protein is available. High-level heterologous expression of the protein is therefore a useful tool for its characterization. As the first step to characterize, *Cop-5* full-length gene and its modular domains were separately tried to be heterologously expressed in *E. coli.*

3.3.5.1. Cloning and Expression of *cop-5* Full Length Gene in *E. coli*

Chlamyopsin-5 full-length gene was assembled by putting together different regions (exon 1-5 from the opsin domain of Synthetic Cop-5 gene, exon 6-8 from genomic DNA and exon 9-14 from the EST clone AV394119) using the overlapping PCR (OLP) method. The gene thus assembled was subsequently cloned into *Eco*R1 and *Hind*III restriction sites of the *E.coli* expression vector pET21a+ (Fig.23a). Cop-5-pET21a+ construct was transformed into different strains of *E.coli* namely; Origami, BL-21 λDE3, and Rosetta cells. Origami 2 host strains are K-12 derivatives that have mutations in both the thioredoxin reductase (*trxB*) and glutathione reductase (*gor*) genes, which greatly enhance disulfide bond formation in the cytoplasm. Rosetta host strains are BL21 derivatives designed to enhance the expression of eukaryotic proteins that contain codons rarely used in *E. coli*. These strains supply tRNA genes for AGG, AGA, AUA, CUA, CCC, and GGA on a Col-E1 compatible chloramphenicol resistant plasmid. Thus, the Rosetta strains allows for "universal" translation, which is otherwise limited by the codon usage of *E. coli*. Maximum expression of Cop-5 was obtained with Origami cells and no expression was observed with BL-21 λDE3 cell (Fig.24a). It was concluded that the size of the protein is too large (150 kDa) to be expressed functionally in *E.coli*; therefore, it was aimed to express each domain of the protein separately.

3.3.5.2. Heterologous Expression of Cop-5 Opsin Domain in *E. coli*

It was speculated that the opsin domain (1-303aa from the N-terminus) of Cop-5 protein might regulate the functional activity of the novel photoreceptor. Therefore, in order to understand the underlying phenomenon it was required that a large amount of functional protein be produced for further biochemical and biophysical characterizations. Codon compatibility of opsin domain was analyzed for expression in *E.coli*. A codon-adapted *cop-5-S* (*cop-5-synthetic*) gene was synthesized commercially by the KFZ department of

Biopark, Regensburg, Germany. *Eco*R1 and *Hind*III restriction sites were introduced upstream and downstream of the *chop-5-S* gene, respectively by PCR. The *Eco*R1 and *Hind*III containing gene fragment was ligated into the pET21a+ vector, which allows addition of five-histidine amino acids tag at the C-terminus of the Cop-5 protein (Fig.23b).

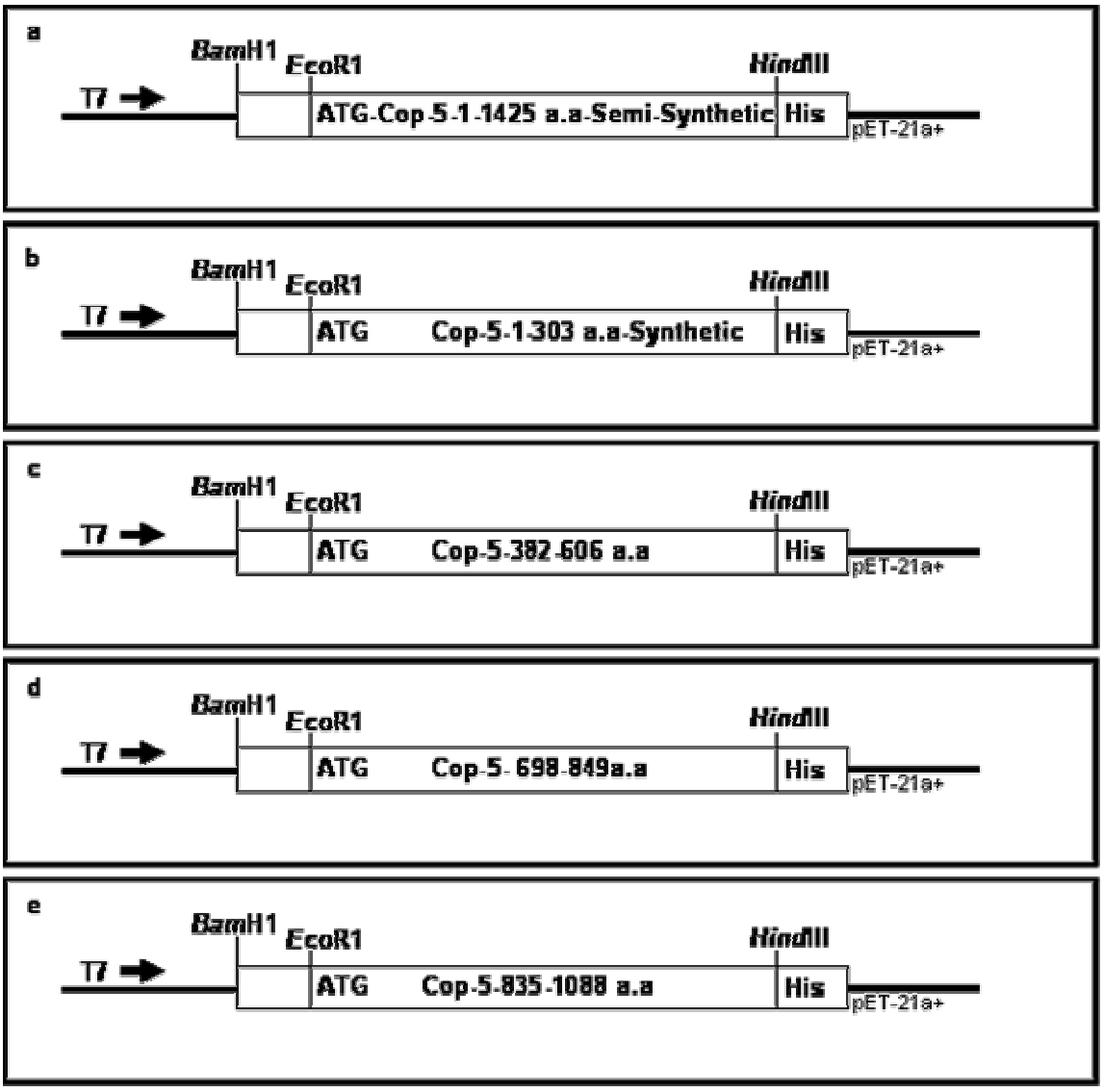

Figure 23. Chlamyopsin-5 (*cop-5*) gene constructs for heterologously expression in *E.coli*. Full length as well as different modular domains of *cop-5* gene was cloned into pET21a+ vector in *Eco*R1 and *Hind*III restriction sites under ´T7´ promoter to produce proteins with an extended His-tag at the C-terminus. (a) Full-length *cop-5* gene. (b) Opsin domain. (c) Histidine Kinase. (d) Response Regulator. (e) Cyclase Domain.

In collaboration with Martin Engelhardt at the Max-Planck Institute, Dortmund, Germany, *cop-5-S* was expressed and solubilization studies were carried out as described in Materials and Methods. Solubilization studies showed that the expressed protein in *E.coli* formed

inclusion bodies and it could not be solubilized even upon using Dodocyelmaltose (Fig.24b).

3.3.5.3. Expression of Cop-5 HK, RR and CYCc Domains in *E. coli*

Fragments of Cop-5 gene encoding the HK, RR and CYCc domains were cloned into *Eco*R1 and *Hind*III restriction sites in the multiple cloning site of pET21a+ vector (Fig.23c-e).

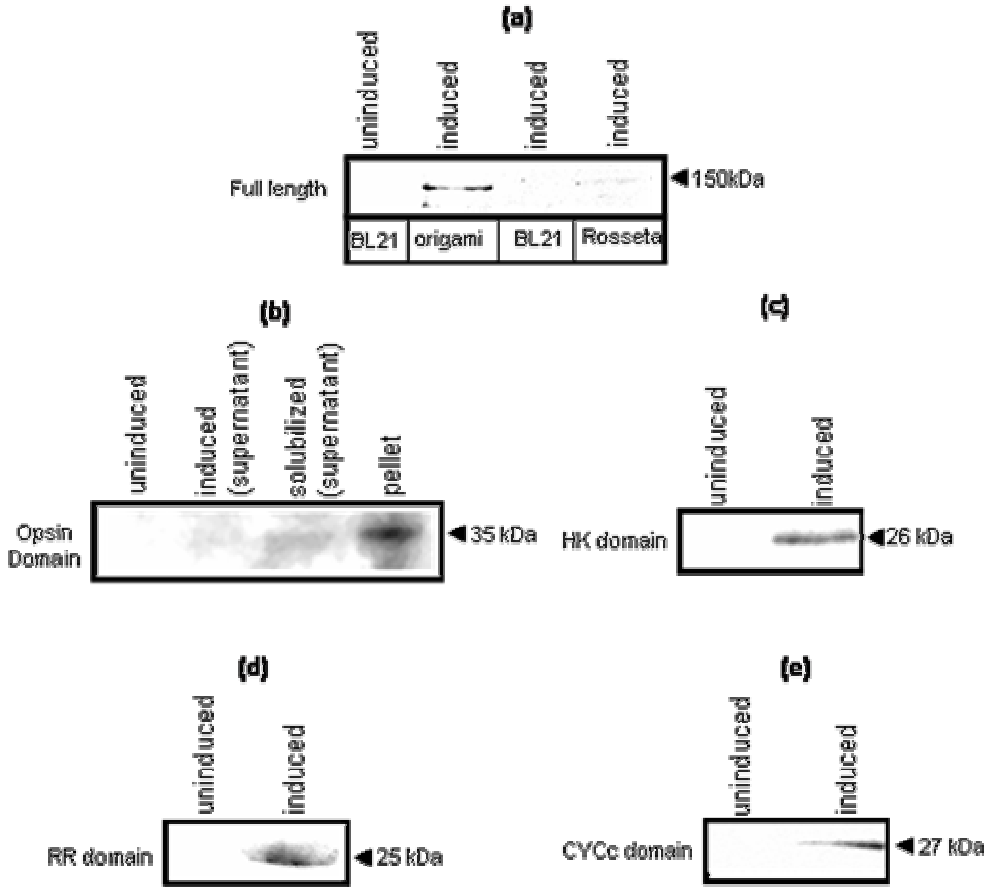

Figure 24. Heterologous expression of the full-length of Cop-5 gene and its various domains in *E.coli*. (a) The full-length *cop-5* gene was expressed in different cell strains of *E.coli* (Origami, BL-21 DE3λ and Rosseta cells). 25µg of total cell lysate of induced and uninduced cultures were resolved on an SDS-PAGE and expression was monitered by westernblotting using ant-His-tag antibody. (b) opsin domain was expressed in *E.coli* and solubilization studies were carried out. Expression and solubilization of the expressed protein was monitered by westernblotting using anti-His-tag antibody. (c-e) Expression of Histidine Kinase, Response Regulator and Cyclase domain was monitered by western blotting using ant-His tag antibodiy. The expressed protein band is shown by arrowhead.

Western blotting analysis showed that each domain was expressed in *E. coli* (Fig. 24 c-e). Since *E.coli* was not suitable for expressing functional Cop-5 protein, another expression system, namely HEK-293, was selected which would enable us to monitor functionality of the heterologous protein within the cell using calcium imaging and fluorescence microscopy.

3.3.6. Transient Expression of Cop-5 in HEK-293

Mammalian cells offer several advantages for expression of recombinant proteins. In most cases, eukaryotic proteins expressed in mammalian cells are functional because transcription, translation and posttranslational modifications are similar among eukaryotes. Expression and functional characterization of a rhodopsin protein has already been established in mammalian cells like HEK-293 (Shukla and Sullivan, 1999; Sullivan et al., 2000; Sullivan and Shukla, 1999). Moreover, our previous studies have shown HEK-293 cells to be suitable for functional expression of Channelopsin-2 (Nagel et al., 2002). It is also known that cAMP/cGMP-gated channel of bovine origin, expressed functionally in HEK-293 and was characterized by calcium imaging and electrophysiological method. Therefore, expression of the *cop-5* gene was tried in HEK-293 expression system for functional characterization by calcium imaging methods.

3.3.6.1. Expression Constructs for HEK-293 Cells

Cop-5 full-length gene (4275 bp) was cloned into the pcDNA3.1 expression vector where the *cop-5* gene was under the control of the immediate early cytomegalovirus (CMV) promoter and enhancer. The vector also contained a selectable marker *(Neo*) governed by a relatively weak promoter. *Eco*R1 and *Xho*I restriction sites were introduced at 5´ and 3´ of the *cop-5* gene by PCR, respectively. The *Eco*R1 and *Xho*I containing gene fragment was cloned into the pcDNA3.1 vector (Fig. 25a). *Xho*I restriction site was introduced both upstream and downstream of the *ecfp* gene by PCR. Enhanced cyan fluorescence (ECFP) protein encoding reporter gene was then cloned in to the C- terminus of the *cop-5* gene in Cop-5-pcDNA3.1 construct in order to produce a fusion protein (Fig.25b).

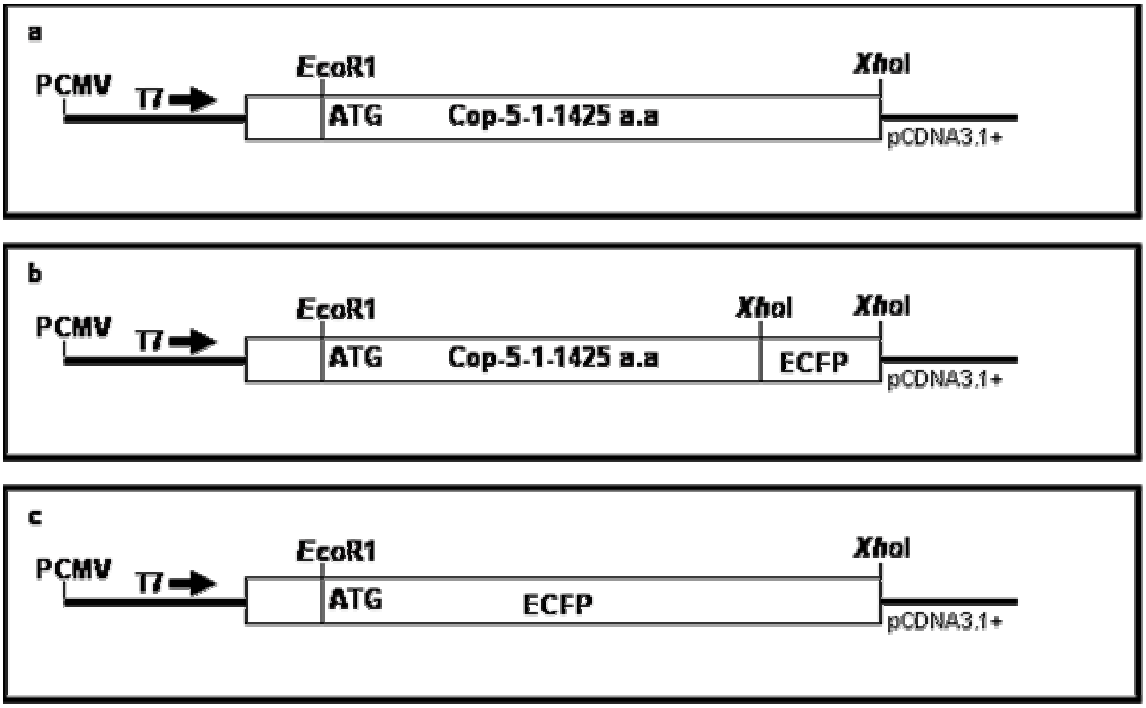

Figure 25. Cop-5 gene constructs with pCDNA3.1 for heterologous expression in Flp-TM/TS-HEK-293 cells. (a) Cop-5 full-length gene was cloned into *Eco*R1 and *Xho*I restriction sites of pcDNA 3.1 vector under ´CMV´ promoter to produce Cop-5 full-length protein. (b) ECFP reporter gene was introduced by an *Xho*I containing linker in to the Cop-5-pcDNA 3.1 construct. (c) ECFP gene was cloned into pcDNA3.1 plasmid in *Eco*R1 and *Xho*I restriction sites to be used as a positive control.

3.3.6.2. Transfection and Expression of Cop-5 in HEK-293 cells

The HEK-293-Flp-Tm (cAMP-gated ion channel) and HEK-293-Flp-TS (cGMP-gated ion channel) stable cell lines were selected for expression of Cop-5 construct in order to evaluate the proposed functional activity of this protein. These stable cell lines were expressing cAMP and cGMP gated ion channel, respectively that were able to show gating mechanism upon binding with cAMP/cGMP transducing molecule. The above-mentioned stable lines were transfected with DNA encoding Chlamyopsin-5 gene (Cop-5-pcDNA3.1 construct) using lipofectamine mediated transfection method. ECFP-pcDNA3.1 construct was used as a positive control (Fig.26c) which enabled us to calculate the transfection efficiency using fluorescence microscopic technique. It was observed that 45-50% of the cells were transfected and able to express the ECFP protein. However, it was also seen that the efficiency with Cop-5-ECFP construct was lower (25-30%) than the positive control.

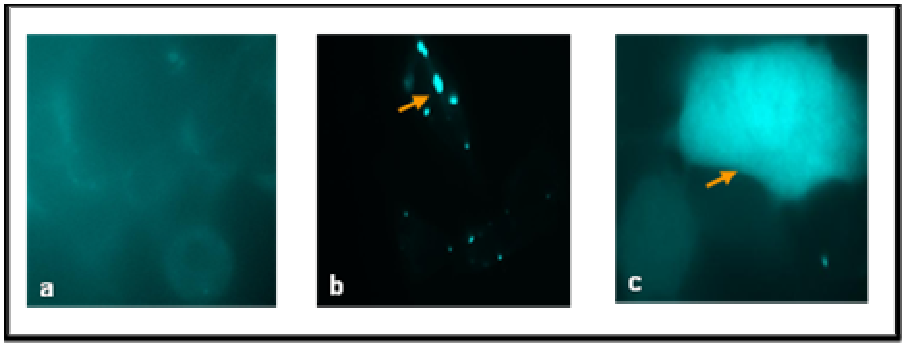

Figure 26. Expressions of Cop-5 and Cop-5-ECFP in HEK-293 cells. (a) Cop-5 expression in HEK-293 cells (shows autoflourescence). (b) Cop-5-ECFP transfected cells expressing fusion protein. (c) ECFP expression in HEK-293 cell. Orange arrow denotes the heterologously expressed protein in the HEK cells for all experiment.

3.3.6.3. Calcium Imaging of Cop-5 Expressing HEK-293 Cells

Cyclic nucleotide gated ion channels (CNG channels) selects cations over anions, discriminate poorly among monovalent cations, and are permeable to divalent cations. Therefore, in physiological ionic solutions, both monovalent and divalent cations permeate the channel and each ion species carries only a fraction of the total current. A photometric method was used to determine the Ca^{++} flux by calcium sensitive dye (Fluo-4) in HEK cells co-expressing CNG (cAMP/cGMP-gated channel) and Cop-5 protein. It was speculated that functional expression of Cop-5 would be able to hydrolyze cAMP/cGMP that will bind to the CNG channel and lead to the opening of cation channel that will result in a Ca^{++} influx. Fluo-4 loaded cells would bind calcium and it will be measured by photometric method. Cop-5 expressing cells HEK-293 cells were used to monitor the autoflourescence of expressed Cop-5 protein as a control (Fig.26a). Expressed Cop-5-ECFP was observed by epifluorescence microscopy and it was found that the expressed fusion protein localized into the organelles of the HEK-293 cells and not in the plasma membrane (Fig.26b). However, fluorescence emission intensity changes were not observed upon application of repeated blue light (480nm) pulses for activation of expressed Cop-5 in Flp-TM and TS-HEK-293 cells to measure Ca^{++} flux with photomultiplier using photon counting instrumentation (Frings et al., 2000). It was speculated that mislocalization of the expressed Cop-5 might have hampered its functional activity.

4. Discussion

4.1. Channelopsin-1 is an archaeal type opsin of *C. reinhardtii* functioning as a light- gated ion channel

In the 1970s and early 1980s, four archaeal-type rhodopsins were discovered in the cytoplasmic membrane of the archaeon *H. salinarium* (Spudich et al., 2000): the light-driven proton pumps bacteriorhodopsin (BR) and halorhodopsin; and the phototaxis receptors sensory rhodopsin I and II (SRI and SRII). Completion of the genome projects of a number of organisms has revealed the presence of archaeal rhodopsin homologues in other domains of life, namely Eubacteria and Eukaryotes (Gartner and Losi, 2003). Organisms containing these homologues inhabit very diverse environments, which include a broad range of microbial life, like proteobacteria, cyanobacteria, fungi, and algae.

The findings of Hegemann *et al* (Hegemann et al., 2001) provides the first information about an archaeal-type rhodopsin in which the seven-helix retinal binding structure is a domain of a much larger protein. Multiple sequence alignments of Chop-1 with established archaeal type opsin sequences suggested that the residues surrounding the chromophore in archaeal-type opsins are conserved. It was also found that the bacteriorhodopsin's Schiff base proton donor (D^{96} of BR) was not conserved in Chop-1 protein sequence. In Chop-1, the seven transmembrane helices (*Appendix*; A1.1) are present in the N-terminus region. Furthermore, bioinformatic analysis strongly suggested that the first hydrophobic segment in the N-terminus of Chop-1 contained the leader peptide sequence. In addition, the topology with seven transmembrane segments and the presence of a hypothetical retinal-binding site suggests that this protein might be a type-1 opsin. It is well known that replacement of M^{145} in BR produces substantial spectral shifts and this residue was implicated in spectral tuning of BR. The homologue of this residue in Chop-1 protein is G^{226} (Ihara et al., 1994). It would be interesting to know the importance of this particular amino acid for spectral tuning. The predicted proton pathway of Chop-1 was depicted based on homology to the BR, protonation and deprotonation state of Chop-1 was assumed to be dependent on pH since there are many pH-dependent processes occurring in BR that are linked to the protonation states (pKa values) of different residues, which modulate the function of BR. For example, protonation (pH 2.0) of the counterion

D^{85} in the ground state causes a red shift of the spectrum, called purple to blue transition (Lóránd et al., 1999).

The newly identified Chop-1 from *C.reinhardtii* provides an example of evolution fusing the seven-helix microbial rhodopsin motif with an extended C-terminus, presumably for photosignal transduction from the photoreceptor domain (Ridge, 2002). Predictions of phosphorylation sites of Chop-1 protein showed the presence of serine and threonine (S and T) residues in the C-terminus region. These residues might serve as potential phosphorylation targets of cellular kinases (*Appendix*; A1.3). It is tempting to speculate that the modular nature of the transducer regions allow them to function in an analogous fashion to that of components involved in visual transduction in animals. Here, light stimulated rhodopsin (metarhodopsin) activates the G-protein to initiate a series of downstream events that culminate in the closure of membrane bound cGMP channel. Termination of the cascade is partly accomplished by phosphorylation of S and T residues in rhodopsins´s C-terminus (Lagnado, 2002). However, the function of the extended C-terminus (311-723 aa) of Chop-1 is not yet clear.

The availability of the BR protein crystal structure of *H. salinarium* has opened new vistas for virtual structure prediction of new archaeal- type opsin, by using this BR structure as a template for homology modeling. The specific arrangement of the seven TM helices stabilized by a series of intra-molecular interactions mediated by several backbone and side-chain atoms seems to be conserved among the archaeal- type opsins. The success of homology modeling is determined to a high extent by the degree of sequence homology between the target and the template structures. In particular, clear structural similarity exists for highly homologous proteins with sequence identity >30% (Yang and Honig, 2000a; Yang and Honig, 2000b) while a lower sequence homology reflects divergence in the protein structures (Kalra et al., 1992). Notably, homology between the 7TM helices of Chop-1 and BR is only 23%. The homology of Chop-1 to BR and other known microbial opsins might appear small, but most amino acids that define the retinal binding pocket and the H^+-conducting ion channel are conserved. Homology modeling suggests that the folding of the N-terminal domains of the polypeptides is similar to that of haloarchaeal rhodopsins. Further studies are necessary for elucidating the structure-function relationship of this new Chop-1 rhodopsin subfamily with remarkably unique features and relation to other light-gated ion channel proteins like Vop-2 and Aop. From the structure and sequence comparisons, it was speculated that Chop-1 might function as a proton transporter in an active or passive way (Hegemann et al., 2001). Moreover, a large proton

current has been recorded from *C. reinhardtii* eyespot at acidic pH and it is not unlikely that Chop1 could be the responsible photoreceptor for photobehavioural responses (Ehlenbeck et al., 2002).

When Chop-1 was heterologously expressed in *E.coli*, it was observed that a tight control to prevent the leaky expression of protein during expansion of the bacterial cultures was crucial for the consistency of the protein production. The codon optimized *chop-1* gene has been expressed in *E.coli* while native gene was not expressed under the same experimental condition. The binding of retinal to expressed Chop-1-S apoprotein could not be observed. The refolding studies were not carried out since protein yield was very low. The expression of Chop-1-SS in *P. pastoris* was achieved as mentioned in literature for Nop-1 expression (Brown et al., 2001). In the case of Chop-1 expression, it was observed that the expressed protein did not show binding to all-*trans* retinal whereas for Nop-1 a functional expression was shown by Brown *et al*. Sineshchekov and colleagues have also reported expression of non-functional Chop-1 in *P. pastoris* (Sineshchekov et al., 2002) in an independent study.

Functional expression and light-gated ion channel activity of Chop-1 in *Xenopus* oocytes has included a new paradigm for functional diversity of the archaeal type opsins (Nagel et al., 2002). The dependence of photocurrent direction on the applied potential suggests that the reconstituted Channelrhodopsin-1 (ChR1) mediates a light-induced passive ion conductance. The light-gated ion channel activity showed selectivity and permeability for proton (H^+) over the other monovalent cations. The observed dependence of V_{rev} on pH_o implies that the ChR1 mediated light-activated conductance is passive and highly selective for proton. Outward photocurrents could be observed at extracellular pH or low intracellular pH. The action spectrum of Chop-1 in oocytes showed a peak at 500nm which closely resembles the one observed for the action spectrum of the photoreceptor current, phototaxis and photophobic responses in *C. reinhardtii* (Nagel et al., 2002). The pH dependent photocurrent, I_{P2}, recorded from intact (Ehlenbeck et al., 2002) *C. reinhardtii* was found to dominate the stationary current in continuous light at low pHo. It was speculated that I_{P2} might be carried by ChR1. During the BR photocycle, a proton is transferred from the Schiff base to D^{85} (corresponding to E^{162} in Chop1) and released to the surface by way of R^{82}, E^{194}, and E^{204}. The corresponding residues in Chop1 are R^{161}, E^{274}, and S^{284}. The key amino acid for the reprotonation of the retinal Schiff base in BR is D^{96} (Butt et al., 1989; Henderson et al., 1990). The corresponding amino acid in Chop1 is H^{173}, which was exchanged with two different amino acids (D or R). The substitution $H^{173} \rightarrow D$

resulted in a complete loss of light-gated conductance, whereas H173R was still functional (Nagel et al., 2002). These results indicate that H^{173} does not function as a proton donor of a deprotonated Schiff base. Therefore, it was suggested that in ChR1 the retinal Schiff base is not deprotonated during the photocycle (Nagel et al., 2002). It is conceivable that isomerization of retinal or a conformational change, tightly coupled to gating the ChR1 proton channel. ChR1 showed ion channel activity that opens in response to absorption of light, i.e., a combined photoreceptor and ion channel. It is not unlikely that such directly light-sensitive ion channels are widely distributed in other phototactic microalgae, as well as in gametes and zoospores of macro algae, or even in fungi (Bieszke et al., 1999). It is worthwhile to mention that a partial gene sequence has been identified in *V. carteri* genome database, which encodes a homologue of Chop-1. It was termed as Volvoxopsins-2 (Vop-2), which showed very high (75%) homology to the Chop-1 (*Appendix*; A2.5). It was also observed from the sequence alignment between Channelopsins and putative Vop-2 that Vop-2 showed higher homology to Chop-1 than to Chop-2. Therefore, it is interesting to determine the physiological function of this putative *vop-2* gene in *V. carteri* (*Appendix*; A2.5). The ability of ChR1 to mediate a large light-switched H^+ conductance in Oocytes holds promises for the use of ChR1 as a tool for measuring and/or manipulating electrical and proton gradients across the cell membrane, simply by illumination. It is known from electrophysiological and biochemical data that photoreceptors for phototaxis and photophobic responses must be enriched in the eyespot region of *C. reinhardtii*. Recently, it was shown by the indirect immunofluorescence analysis that Chop-1 is localized near the eyespot area of *C. reinhardtii* (Suzuki et al., 2003). Chop-1 and Chop-2 were localized in total membrane fractions, and Chop-1 expression dominated in the high light grown culture (Nagel et al., 2003). It was also observed that Chop-1 is mainly expressed in vegetative and gamete cells. Sineshchekov and colleagues have generated transformants in which the ratio of Chop1 and its homolog Chop2 was changed by an antisense approach (Sineshchekov et al., 2002). Sineshchekov *et al* have found that photocurrents of ChR1 deprived cells at high flash intensities were reduced, the authors concluded that ChR1 mediates the high-intensity response (Sineshchekov et al., 2002). Our results for ChR1 from *Xenopus* oocytes and *in vivo* expression characteristic (light dependent expression) support that both Channelrhodopsins control photophobic responses with different spectral sensitivity. However, gene knockout mutant are needed to understand clear physiological function of both proteins.

4.2. A second archaeal-type opsin, Channelopsin-2, of *C.reinhardtii* also functions as a light-gated cation channel

The sequence identity between Chop-2 and other archaeal- type opsins is not high, even within the 7TM domain; homology of Chop-2 to BR is only 22%. However, most amino acids that define the retinal binding site and the H^+-conducting ion network of archaeal type opsins are conserved in the Chop-2 sequence (Nagel et al., 2003). Multiple sequence alignments performed with established archaeal type opsins and Chop-2 suggests the positions of the seven transmembrane helices in the N-terminal region of Chop-2 sequence. These seven transmembrane segments are involved to form the internal pocket for the binding of all-*trans* retinal in archaeal-type opsin. The sequence alignment analysis revealed that opsin domain of Chop-2 is surrounded by more hydrophilic amino acid residues than BR; it could probably alter the hydrogen-bonding network in the opsin domain and thereby altering the pore size.

Sequence homology also showed that the first proton transfer in the photocycle from the retinal Schiff base to D^{85} is the most critical in BR, which is E^{123} residue in the Chop-2. This is a significant difference because mutagenic replacement of D^{85} in BR with T is sufficient to convert it into light activated Cl^- pump (Sasaki et al., 1995). The breaking of the hydrogen bond between D^{85} and T^{89}, was proposed to increase the pKa of D^{85} and make it the proton acceptor (Royant et al., 2000). According to the rules of coupling, the release of the proton at a pH higher than its pKa will raise, in turn, the pKa of D^{85}. This will shift the protonation equilibrium toward more complete deprotonation of the Schiff base (Zimanyi et al., 1992). The pKa of D^{85} is expected to rise very strongly upon proton release. One could expect similar event between the E^{123} and T^{127} for Chop-2 in a pH dependent manner within the photocycle. Sequence alignment revealed that the carboxylate proton donor specific to the light-activated proton pump (D^{96} in BR), which is a noncarboxylate residue in known archaeal type opsin, is replaced with H^{134} residue in Chop-2. Transfer of proton from D^{96} to the retinal Schiff base requires that the pKa of D^{96} be lowered from above 11 in the nonilluminated state to not higher than the pKa of the Schiff base, which is about 8 (Brown and Lanyi, 1996). It is known from the characterization of Chop-1 mutant (H^{173}) that this residue is not involved in the reprotonation (Nagel et al., 2002). Therefore, it might be speculated that H^{134} of the Chop-2

would not be responsible for the reprotonation of Schiff base during its photocycle. Four residues in bacteriorhodopsin are involved in proton release (E^{194} and E^{204} near the extracellular surface) and in proton uptake (T^{46} and D^{96} near the cytoplasmic surface) are substituted non-conservatively in sensory rhodopsin (Spudich et al., 2000). Two of the four are conserved in Chop-2, except for E^{194} and D^{96}, which are S^{284} and H^{134} residue in Chop-2 sequence respectively. Sequence alignment and predicted secondary structure of Chop-2 have suggested that the folding of the N-terminal opsin domains of the Chop-2 polypeptides is similar to that of haloarchaeal rhodopsins (*Appendix*; A2.1). The Chop-2 sequence showed very high homology (75%) to Chop-1 but there is no indication of the presence of 2TMH helices at the extended C-terminus of Chop-2. However, the extend C-terminal of both proteins have not shown significant homology to other known protein sequences in NCBI database, and the functional importance of this region remains unknown. The C-terminus region of the Chop-2 protein contains several S/T residues, which are predicted to be phosphorylation sites (*Appendix*; A2.4), which might have an implication in the physiological function of Chop-2 in *C. reinhardtii*.

Overexpression of foreign genes in *E coli* at low temperature improves the solubility and stability of the expressed protein (Qing et al., 2004), as the folding of recombinant proteins is favored at low temperature and degradation is less under these conditions (Baneyx, 1999). Taking these findings into the consideration, expression of Chop-2 was carried out at a lowered temperature of 18°C for 12-16hrs. Eventhough the protein was produced it was still not functional. The expression characteristics of Chop-2 in *E. coli* were very similar to that of Chop-1. However, *X. laevis* expression system was successful for functional expression of both the channelopsin proteins (Nagel et al., 2002; Nagel et al., 2003).

The involvement of ChR2 in the generation of photocurrents in *C. reinhardtii* was shown in a recent study by Sineshchekov *et al.* (Sineshchekov et al., 2002). They named this rhodopsin CSRB (*Chlamydomonas* Sensory Rhodopsin B), as its molecular function was revealed indirectly by suppression of endogenous expression, and postulated, in analogy to the archaeal sensory rhodopsins, that it is coupling to a transducer. The expression of Chop-2 was tried in *X. laevis* oocytes in the hope to get functional expression, which would then enable the characterization of the protein using two-electrode voltage clamp method. This study addressed the question of what the molecular function of the second microbial-type retinal protein (rhodopsin), ChR2, from the alga *C. reinhardtii* might be. From the large photocurrents with Chop-2 expressing *Xenopus* oocytes (Nagel et al., 2003)

cells, it can be concluded that ChR2 from *C. reinhardtii* is functionally expressed in *Xenopus* oocytes. These experiments leave little doubt that Chop2 binds all-*trans* retinal to form ChR2 and that ChR2 is a rhodopsin, which undergoes a photocycle with a cation-conducting photocycle intermediate or, in other words, an ion channel with an intrinsic light sensor. The channel has a low selectivity among cations but it is not a non-specific ion channel because it does not conduct anions. From the range of conducted cations it may be concluded that the narrowest pore size or selectivity filter of the channel (Hille, 2001) is wider than that of a voltage-activated Na^+ channel but probably slightly smaller than that of the nicotinic acetylcholine receptor, because tetra-ethyl ammonium$^+$, Mg^{++}, and Zn^{++} were not conducted.

ChR1 and ChR2 form a 7-TM motif, which is well known in other microbial type rhodopsins and G protein-coupled receptors, but a new feature for ion channels. Most ion channels are formed by polymers of subunits or are large proteins with internal repeats (Hille, 2001). A well-known exception is the cystic fibrosis transmembrane conductance regulator, where a single 12-transmembrane protein forms a chloride channel (Chen et al., 2001). However, formation of a cation channel pore by a 7-TM protein was unknown until now. The light-gated proton channel activity of Chop1 was studied in the *Xenopus* oocytes (Nagel et al., 2002). It was established for the light-driven ion pump (BR) that the actively transported proton moves along a hydrogen-bonded network, which is formed by a monomeric of BR. For ChR2 it was proposed that 7-TM helices form a cation channel that must be wide (~6 Å in diameter) to be permeable to methylated ammonium cations. In analogy to other rhodopsins, it was suggested that the channel is opened by a conformational change of the protein, after a light-induced isomerization of *all-trans* retinal. However, there is no indication that ChR1 and/or ChR2 are coupled to any signal acceptor protein, like a G protein, or to a transducer like the archaeal sensory rhodopsins (SRI and SRII) to their respective transducers. This notion is corroborated by the finding that the electrical properties of ChR1 and ChR2 are independent of the large hydrophilic C-terminus region of the protein. In *C. reinhardtii*, evidence exists for two separate light-activated conductances for H^+ and Ca^{++} but the rise times of the Ca^{++} current and the H^+ current are indistinguishable (Ehlenbeck et al. 2001). Therefore, it was impossible to decide whether both currents are directly light-gated or which of the two currents triggers the other. On the basis of the experiments described for expressed ChR1 (Nagel et al., 2002) and ChR2 (Nagel et al., 2003), it was proposed that the high-light photoreceptor current of *C. reinhardtii* is triggered by ChR1 and/or ChR2. The local depolarization or the

H^+ influx is then most likely activating a secondary Ca^{2+} conductance, also confined to the eyespot region. This secondary photoreceptor conductance decays faster than the primary current but its molecular origin still has to be identified (Ehlenbeck et al., 2002). ChR2 may be a sensory photoreceptor that is preferentially used when the cells are exposed to dim light for longer times (several hours). From the fact that ChR2 triggers much larger photocurrents than ChR1 it is immediately obvious that the observed degradation of ChR2 at higher light intensities will protect cells from the detrimental effects of continuously inward flowing cations, especially protons and calcium.

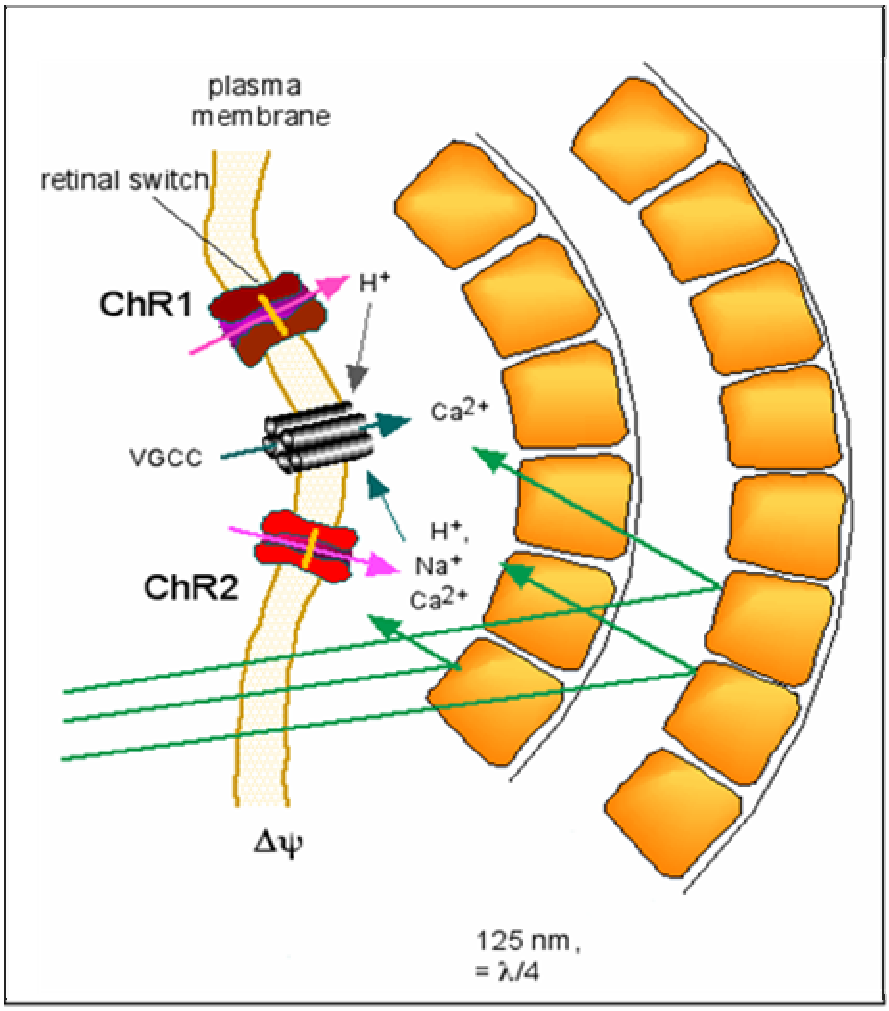

Figure 27. The proposed function of an eyespot in *C.reinhardtii* under consideration of Channelrhodopsin-1 (ChR1), Channelrhodopsin-2 (ChR2) and a voltage or H^+-gated Ca^{++} ion channel (VGCC). The voltage change, ΔΨ, is transmitted along the membrane and sensed by VGCCs in the flagellar membrane. This figure has been taken from a published paper (Kateriya et al., 2004).

This study revealed an important function for a microbial-type rhodopsin, a directly light-switched cation channel, and demonstrated the likelihood of a mechanism in light signal transduction as it may be used in *C. reinhardtii*. Function of the ChR1 and 2 has been taken in account to propose the function of the eyespot with context of secondary photoreceptor (Ca^{++}) conductance of the *C. reinhardtii*, which is depicted in a diagram (Fig.27).

Immediately after ChR1 was identified as a light-gated ion channel, it was suggested that channelrhodopsins might be used for the modulation of membrane potential and cytoplasmic pH of other eukaryotic cells than *C. reinhardtii* (Nagel et al., 2002). Similar application becomes more obvious for ChR2 with its large light-gated permeability to mono and divalent cations. It was shown that expression of ChR2 in oocytes or mammalian cells (Nagel et al., 2003) may be used as a powerful tool to increase cytoplasmic Ca^{++} concentration or to depolarize the cell membrane, simply by illumination.

4.3. Opsin coupled two-component system in *C. reinhardtii*

It was speculated on the basis of the Chop-1 and Chop-2 activity in the *Xenopus* oocytes that both proteins might be responsible for photophobic response with different spectral sensitivity in *C. reinhardtii* (Nagel et al., 2002; Nagel et al., 2003). It was then an open question which rhodopsin triggers phototaxis in *C. reinhardtii*. It was also reported that retinal synthesis itself is under the control of opsin-based photoreceptor in *C. reinhardtii* (Foster et al., 1988). Therefore, it was interesting to identify and isolate new opsin sequence from *C. reinhardtii*. Recently, three more potential putative opsin sequences have been identified from *C. reinhardtii* genome database (Kateriya et al., 2004). Very interestingly, all three newly identified Chlamyopsin (Cop-5, 6 and 7) sequences were coupled to a transducer (HK) domain. The opsin domains of the Chlamyopsin sequences were more closely related to the sensory rhodopsin from *H. salinarium* than to BR or Channelopsins. The dendogram analysis revealed that Cop-5 and 7 were closer to haloarchaeal and eubacterial opsins than to fungal opsins, which was previously known as the only archaeal-type opsin protein in eukaryotes.

One residue of known functional importance in light-activated transporters and sensors is the lysine (K) that form a protonated Schiff base linkage with retinal (Spudich et al., 2000). This important lysine residue (K^{274}) is conserved in the opsin domain of Cop-5. It is known that N^{105} of pSRII is interacting with the chromophore during photoisomerization process; interestingly this residue is replaced with D^{172} in Cop-5. Sequence alignment revealed that an important amino acid for spectral tuning in pSRII (i.e. R^{72}) is also conserved in Cop-5 (*Appendix*; A3.3). Y^{199} and charged residues of pharaonis phoborhodopsin (pSRII) are important for the interaction with its transducer (Yuki et al., 2002). It was observed in sequence alignment of Cop-5 and pSRII that this Y^{199} is replaced in Cop-5 with a hydrophobic amino acid residue, A^{268}. It was predicted that positive charges of pSRII (K^{157}, R^{162}, and R^{164}), interact with negative charges of the transducer (Royant et al., 2001), these residue are R^{226}, $V^{231}$and R^{233} in the opsin domain of Cop-5. It is interesting to note that the positively charged R^{162} is replaced with a hydrophobic residue ($V^{155)}$ in Cop-5 (*Appendix*; A3.3). This particular amino acid change might also influence on the interaction of Cop-5 opsin domain to its transducer (HK).

Interestingly, it is known that archaebacterial photoreceptors mediate phototaxis by regulating cell motility through two-component signaling cascades (Oprian, 2003). Homologs of this sensory pathway occur in all three kingdoms of life, most notably in enteric bacteria in which the chemotaxis has been extensively studied. In the photoreception of *H. Salinarium*, the receptors (SRII and I), which belong to the family of microbial type rhodopsins, are not directly fused to the transducer domain (Klare et al., 2004). However, it is bound to cognate transducer molecules (halobacterial transducer of rhodopsin, HtrII and I). In Cop-5, a unique arrangement of modular domains (Opsin, HK, H-ATPase, RR and CYCc) is seen within a single ORF of gene sequence, where opsin domain is coupled to the classical two-component system and with cyclase domain (Kateriya et al., 2004).

The structure of the NpSRII/NpHtrII complex reveals the transmembrane interaction domain between receptor and transducer. The main interactions in the complex are van der Waals contacts, predominantly at TM1-helix of the transducer and helix G of opsin domain, TM2-helix of transducer and helix F of opsin domain. Notably, only four hydrogen bonds are formed Y^{199} NpSRII to N^{74}NpHtrII in TM-1, T^{189}NpSRII to S^{62}NpHtrII in TM-2 and T^{189} NpSRII to E^{43}NpHtrII in TM-1.

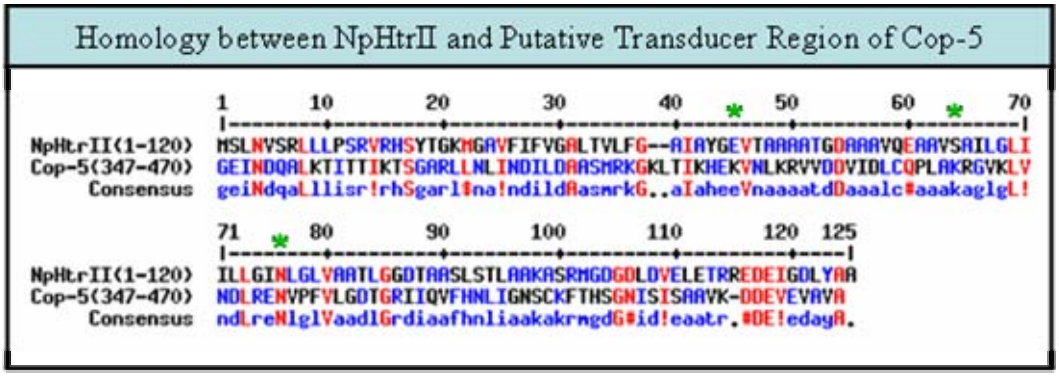

Figure 28. Sequence alignment of putative transducer domain of Cop-5 and transducer domain of NpHtrII: Important amino acid residues for interaction to opsin domain are denoted with green asterisks. Identical and homologous amino acid residues are shown in red coloure. Blue and black amino acids residues represent the stretches that are not conserved among species.

The importance of Y^{199} has already been described in the previous section. The amino acid residues for the interaction to the transducer in opsin domain of Cop-5 are replaced with A^{268} and D^{258} in the helices G and F. The putative transducer domain of the Cop-5 shows

conservation of N^{74} of NpHtrII and two other amino acid residues (E^{43} and S^{62}) are replaced by positively charged lysine (K; Fig.28). It is tempting to speculate that in Cop-5 helices F and G might show interaction with the putative transducer domain with the help of van der wall interactions as it was shown for NpSRII:NpHtrII complex (Klare et al., 2004).

The H box of the histidine kinase is also conserved in the transducer domain (HK) of Cop-5, which is not the case with prototype (NpHtrII) protein. Moreover, sequence alignment of histidine kinase domain with known PhoQ histidine kinase of *E. coli* (Marina et al., 2001) revealed that the classical N, F, G1, G2, and the recently defined G3 boxes are present within Cop-5 protein sequence (*Appendix;* A3.4). The sequence alignment of the RR domain with CheY domain of *E.coli* also shows presence of a motif (conserved D) for accepting phosphate group from HK domain (*Appendix;* A3.5), which is an example of typical two-component signaling system for chemotaxis and phototaxis. Cop-5 is unique among all known photoreceptor for phototaxis in different organism because sensor (opsin) is coupled with two-component system and with cyclase domain at the extended C-terminus. However, it is known that the cyclase plays an important role in the context of phototaxis (Ng et al., 2003; Noegel, 2004; Ntefidou et al., 2003). Two conserved residues (N and R) are thought to be involved in catalysis of cyclase (*Appendix*; A3.6). These cyclases have also important roles in a diverse range of cellular processes.

Blue light regulated adenylate cyclase activity has been reported in the *E. gracilis*, where it plays an essential role in phototaxis (Ntefidou et al., 2003; Watanabe and Suzuki, 2002). The homology based 3D modeling of modular domain suggests that secondary structure and folds for catalytic site for each modular domain are conserved in Cop-5 sequence. Based on sequence homology, predicted secondary structures and homology based 3D models of modular domains, respectively, it is proposed that the opsin domain will be able to perceive the light signal and transducer the signal, activate the two-component system and finally regulate cyclase activity of the protein.

Functional expression of both full-length and opsin domain of Cop-5 could not be obtained in *E.coli* as the expressed proteins failed to bind retinal. Flp-TM/TS-HEK-293 cells would have been a good system to study the functional activity of the expressed protein, however Cop-5 upon expression in these cells was found to be mislocalized to the organelles. Light regulated and two-component mediated cyclase activity of Cop-5 could not be observed upto now.

At present, there is no indication yet under which physiological conditions these rhodopsins with linked enzyme activity (Enzymerhodopsins) are expressed. The only hint of such a large protein being expressed is the presence of one partial Cop-5 cDNA clone that appeared in the *C. reinhardtii* EST database. If all three genes are expressed either simultaneously or under certain physiological conditions, the number of opsin-related proteins in *C. reinhardtii* expands to seven. It is the only model organism yet which posses both (Type 1 and 2) opsin proteins. The speculation that one of these new rhodopsins might contributes to phototaxis seems to be justified. However, other functions like control of retinal biosynthesis or developmental process in *C. reinhardtii* should also be taken into account (Foster et al., 1988).

The finding that rhodopsin is used for phototaxis in archaea, eubacteria, green algae and fungal zoospores might support the speculation that rhodopsin evolved from archaea via eukaryotic flagellates up to animal rhodopsins. The fact that microbial type rhodopsins (type1), no matter whether they occur in archaea or green algae, have very little homology to the animal type rhodopsin (type 2) might point out to an independent evolution. Therefore, it is conceivable that animal rhodopsins have developed from other rhodopsin related proteins that originally were not sensing light (chemoreceptor and others). Chlamyopsin and 2 might fall into this category (Kateriya et al., 2004).

5. Future Prospective

It was quite surprising to note that the newly identified Type-1 opsins of *C.reinhardtii* functions as light-gated ion channels because these opsins show homology to BR, which is a light activated proton pump (Nagel et al., 2002; Nagel et al., 2003). It would be an interesting and challenging task to decipher the molecular basis of the light-gated proton channel activity. What are the responsible amino acids in the protein for ion channel activity? Can we convert a light-activated proton pump into a channel using site directed mutagenesis? What would be the photocycle of the Channelopsins? These and many other questions involving the spectroscopy and photochemistry of the pigments would be answered if one had an expression system providing sufficient amount of the functional Channelopsins. The findings of the Hegemann *et al* and Suzuki *et al* with the predicted 3D models of Chop-1 suggested that opsin domain have very similar structural fold to that of prototype BR, with slight outward projection of helix B of Chop-1 (Hegemann et al., 2001; Suzuki et al., 2003). However, the activity of Chop-1 is different from that of BR. It is tempting to speculate that the experimental 3D structure might be different from BR, at least in the region of proton-conducting path/pore. Therefore, it is an urgent need to study structure-function relationship of Channelopsins in detail. It would be a fascinating task to map out the Chop-2 protein regions for ion selectivity and permeability filters because it shows permeability for both monovalent and divalent cations (Nagel et al., 2003). Since both proteins seems to be responsible mainly for photophobic responses with different spectral sensitivities and might influence phototaxis activity indirectly as shown by experiments in *X. laevis* oocytes (Kateriya et al., 2004; Nagel et al., 2002; Nagel et al., 2003). It would be interesting to elucidate the physiological functions of these channelopsins in *C. reinhardtii* using the gene knockout mutants. Moreover, it is also needed to isolate and characterize the homologues of the Channelopsins from other organisms (e.g. *V. carteri*) where the photoreceptor currents are much slower than in *C. reinhardtii* (Braun and Hegemann, 1999). This putative Vop-2 might have a different function/ion selectivity and permeability than the known Channelopsins. Interestingly, I have identified a partial gene sequence in the genome of *V. carteri* (Vop-2), which showed high (75%) homology to the opsin domain of the Channelopsins (*Appendix*; A2.5). The characterization of this new Volvoxopsin-2 would be of help to identify the general mechanism of the functioning of Channelopsins in different organisms. It is worthwhile to

mention that a partial opsin-like sequence has been found in the NCBI database, which originated from the *Acetabularia*. The homology analysis of this partial opsin like sequence to the BR and Channelopsins revealed that Acetabulariaopsin (Aop) is closer to the BR than that of Chop-1 (*Appendix*; A1.4). Therefore, it might be functioning, as light-activated proton pump. It was shown with ^{3}H-retnal labeling experiments that *D. salina* possess the presence of at least two retinal binding proteins, which was not surprising since the phototaxis and photophobic responses exhibits rhodopsin action spectra with different maxima (Hegemann et al., 2001; Wayne et al., 1991). However, there is no information available about their protein sequences. It would be interesting to isolate these genes for characterization and comparison with known Channelopsins and other opsins.

It is also required to understand the precise mechanism by which the ion fluxes generated with Channelopsins by the light signal modulate the flagellar function in *C.reinhardtii*. Is there any intermediate protein molecule, which also takes part in the photobehavioural responses of *C.reinhardtii*? Another intriguing question that has to be answered is if ChR 1 and 2 are responsible for the photophobic responses, and which opsin is triggering phototaxis?

Recently, the identification of opsin like proteins (Cop-5, 6 and 7) from the *C.reinhardtii* genome database provided a clue to assign photoreceptors for phototaxis. It is important to note that Cop-5 opsin domain is coupled to the classical two-component system and with cyclase domain. It is proposed that *cop-5* might have light regulated cyclase activity upon expression and the involvement of cAMP/cGMP-gated ion channel in phototaxis, in this aspect it is similar to the *E. gracilis* (Ntefidou et al., 2003). Furthermore, it has also been shown that the cell polarization, F-actin organization, and phototaxis were altered in a *Dictyostelium* with Cyclase-associated protein (CAP) knockout mutant (Noegel, 2004). Recently, another report has shown that the positive phototaxis of *Synechocystis sp*. strain PCC6803 was controlled by the red light photoreceptor (TaxD1), while the negative phototaxis was mediated by one or more yet unidentified blue light photoreceptors (Ng et al., 2003). Therefore, to understand the underlying functions of Cop-5 it is needed to get functional expression of the protein in any expression system, which would help to elucidate the proposed function of this protein. Moreover, it might include a new paradigm for the diversity of the phototaxis receptors in different organisms. It is worthwhile to mention that I have also found an opsin like sequence (Vop-3) in *V. carteri* genome database, which showed homology to the Cop-5 (*Appendix*; A3.7). It is required to

characterize function of Cop-5 (and their homologs from different organisms) and compare their functional activity in the respective organisms.

It was proposed that the photopigment for induction of retinal synthesis in *C. reinhardtii* is a rhodopsin. Moreover, the time lag analysis for induction of retinal synthesis and preliminary experiments with transcription or translation inhibitors suggested that alterations in gene expression could be involved in the induction process (Foster et al., 1988). It is interesting to note that the three new Chlamyopsin genes (Cop-5, 6 and 7) are coupled to the classical two-component system , which is known to regulate the expression of various stress response genes in bacteria (Stock et al., 1990) therefore, it would be interesting to assign the function of these Chlamyopsins in the context of retinal bio-synthesis.

In conclusion, to decipher the possible interaction between these novel opsins, their mutual control and regulation and their signaling, which might induce a manifold physiological responses, remains the most challenging and fascinating task for a photobiologist.

6. Materials and Methods

6.1. Methods

6.1.1.1. Culturing of *C. reinhardtii* in Liquid Medium

C. reinhardtii was streaked on TAP agar plate and grown for 5-7 days under autotrophic condition (0.5W/m^2) at 25°C. A single colony was inoculated into 25ml TAP (7.5mM NH_4Cl, 0.4 mM $MgSO_4$, 0.34 mM $CaCl_2$, 0.54 mM K_2HPO_4, 0.46 mM KH_2PO_4, 15 mM CH_3COONa, 20 mM Tris/Cl, 0.1% trace element, pH 7.0), medium and grown for three days at 25°C with shaking at 125 rpm. Large-scale liquid cultures were grown by inoculating the media with $1/20^{th}$ volume of the pre-grown culture. Phototrophic cultures were bubbled with CO_2 (5% in Air) for maximum growth.

6.1.1.2. Synchronization of *C. reinhardtii* cw 806 Culture

The *C. reinhardtii cw*806 cells were grown as described above. Synchronization was achieved by the alternation of light and dark period during growth (12:12). Cells were harvested at different time points and used for protein analysis.

6.1.1.3. *C.reinhardtii* Gametogenesis

For gametogenesis, liquid cultures of vegetative cells were centrifuged at 2,000 *g* for 5 minutes and resuspended in nitrogen minimal medium (NMM; 0.81mM $MgSO_4$, 0.1mM $CaCl_2$, 6.2mM KH_2PO_4, 6.8mM KH_2PO_4) at a density of 1×10^7 cells per ml. These cells were either incubated for 16 hrs in the light to generate gametes or in the dark to generate pre-gametes (Huang et al., 2003). Gametes were also obtained from pre-gametes by exposing them to blue light (460_{nm}; 30 µmol·m^{-2}·s^{-1}).

6.1.2. *E. coli* Culture

E.coli strain DH5α was streaked on LB-agar plate (1% (w/v) Bacto-Tryptone, 0.5% (w/v) Yeast Extract, 1% (w/v) NaCl) and grown overnight at 37°C. A single colony was inoculated into 25 ml. LB medium and grown overnight at 37°C with shaking at 180 rpm.

6.1.2.1. Preparation of *E. coli* Competent (DH5 α) or (BL-21) Cells

The pre-culture was inoculated from the Glycerol stock of competent cells into 50 ml of SOB (2% (w/v) Bacto-Tryptone, 0.5% (w/v) Yeast Extract, 0.05% (w/v) NaCl, 10 mM $MgCl_2$ and 2.5mM KCl) in 250ml flask and incubated at 37°C overnight with shaking at 180 rpm. A main culture of 200ml SOB was inoculated with 1ml of the pre-culture and was grown at 37°C with shaking for 2-3 hrs at 180 rpm. When the culture attained an OD_{567nm}= 0.3-0.4; cells were centrifuged at 2400rpm for 7 min at 4°C in falcon tubes, and the supernatant was discarded. Cells were resuspended in 15ml TfbI (30 mM CH_3COOK pH5.8, 50 mM $MnCl_2$, 100 mM KCl, 15% (v/v) Glycerol) solution and incubated on ice for 10 min (DH5α)/30 min (BL-21). Cells were collected by centrifugation with 2000rpm at 4°C for 5 minutes. The cell pellet was then resuspended in 2ml in TfbII (10 mM MOPS/NaOH, pH 7.0, 75 mM $CaCl_2$, 10 mM KCl, 15% (v/v) Glycerol) solution very gently and stored at -80°C in aliquots of 110µl.

6.1.2.2. Transformation of *E. coli* competent cells

Three to five nanogram of plasmid DNA or 3-5 µg quantity of ligation mixture was added to 50µl of competent cells, mixed well by gentle tapping and incubated on ice of 25 minutes. Heat shock was given for 60-90 seconds according to cell strains at 42°C. It was then incubated on ice for 2-3 minutes and 450µl SOC medium was added. This transformation mix was allowed to recover for 1 hour at 37°C. Cell culture was centrifuged at 5000rpm for 1 minute at RT and 400µl of the supernatant was removed. Cells were resuspended by gentle tipping and 50µl of resuspended culture was plated on an LB-agar plate with appropriate antibiotics. The plates were incubated at 37°C for 12-16 hrs until the colonies were apparent.

6.1.2.3. Storage of *E. coli* cells

E.coli cells were grown as described above and 800µl of overnight grown culture was supplemented with sterile glycerol to a final concentration of 20 (V/V). Cell suspension was snap frozen in liquid nitrogen and samples were stored at -80°C.

6.1.3. *P. pastoris* Culture

The stab culture of *P. pastoris* (GS115) was streaked out on an YPD plate and incubated for 5-7 days at 30°C. Once colonies were apparent on the plates, a single colony was picked and inoculated in appropriate medium for further experimentations.

6.1.3.1. Preparation of *P. pastoris* competent cells

Cells were grown in 50ml YPD medium at 30°C overnight. 500µl of overnight grown culture was re-inoculated into 500ml fresh YPD medium in 2L flask. It was again grown overnight until an OD_{600} = 1.3 to 1.5 was attained. Cells were harvested by centrifugation at 3500rpm for 5 minutes at 4°C. The pellet was resuspended in 500ml of ice-cold and sterilized water. Re-suspended cells were again centrifuged at 3500rpm for 5 minutes at 4°C. Cell pellet was then resuspended into 250ml of ice-cold sterilized water. Cells were centrifuged as described before and the resultant cell pellet was resuspended in 20ml of ice-cold 1M sorbitol. Cells were washed by centrifugation and resuspended into 1ml of ice-cold 1M sorbitol. These competent cells were used for transformation of Chop-1SS construct using electroporation.

6.1.3.2. Transformation and expression Chop-1SS in *P. pastoris* (GS115)

Chop-1-SS-pPIC9K construct was linerized using *Pme*I and purified by DNA gel extract method. 5-10µg of linearized DNA was mixed with 80µl of electro-competent cells (GS115). Cells were mixed and transferred into a 0.2 cm electroporation cuvette. Electroporation was performed with an electroporator using parameters 1.5 kV, 25 µF, and 186 Ω. 500µl of ice-cold 1M sorbitol was added and cells were incubated at 30°C for 1-2 hrs. Cells were centrifuged at 1500g for 5 minutes at 4°C. 300µl supernatant was removed and rest cells were plated on YPDS-agar plates. Plates were incubated for 2-7 days at 30°C. 20-30 colonies were picked and re-plated on Zeocine containing plates. Positive transformants were screened by colony PCR. Three positive clones were inoculated in BMGY medium and induction was carried out using 5% methanol. Expression of recombinant protein was monitored by western blotting using anti-Chop-1 antibody (see below).

6.1.3.3. Storage of the *P. pastoris* cells

A single colony was inoculated in YPD medium and incubated at 30°C for 2-3 days. This culture was re-inoculated into fresh YPD medium and grown overnight at 30°C. Cells were harvested by centrifugation; the pellet was resuspended in YPD medium and supplemented with 15% of Glycerol (V/V). Cells were snap frozen in liquid nitrogen and stored at -80°C.

6.1.4. Isolation and Purification of Nucleic Acids

6.1.4.1. Isolation of Genomic DNA from *C. reinhardtii*

Cells were grown under optimal light conditions 0.5W/m^2 at 18^{o}C and harvested by centrifugation (3500rpm for 5 min.) at 4°C. The pellet was frozen on mortar with liquid nitrogen and ground into powder. This material was used for isolation of genomic DNA using the DNeasy kit according to manufacturer's instruction (DNeasy®Plant; Qiagen).

6.1.4.2. Isolation of RNA from *C. reinhardtii*

Cells were grown under different light conditions (High, Low and Dark Light intensity) at 18^{o}C and harvested at exponential phase of growth by centrifugation (2500 rpm for 5 min) at RT. The cell pellet was then resuspended in 450µl RLT solution (RNeasy®Kit), 4.5µl β-Mercaptoethanol was added and frozen in liquid nitrogen. Frozen samples were thawed at RT and RNA was isolated according manufacturer's instructions (RNeasy®Kit).

6.1.4.3. Screening of cDNA Libraries

Four different *in vivo* excised and cloned λ ZAP-cDNA libraries were provided by Irina Szinova. These libraries were used as a template for screening of the different Chlamyopsin genes using gene specific primers.

6.1.4.4. Screening of BAC clone Libraries

BAC clones were streaked on to LB plates with appropriate antibiotics (Chloramphinicol) and grown at 37ºC overnight. A single colony was picked and resuspended in 5µl of sterilized water, it was heat denatured at 95ºC for 5 minutes. 1µl of supernatant was used as the template from each BAC clone to perform genomic PCR using *chlamyopsin* gene specific primers, respectively.

6.1.4.5. Isolation of Plasmid-DNA from *E. coli*

A single colony was picked from the plate of transformants and inoculated into 3ml 2YT medium (1.6% (w/v) Bacto-Tryptone, 1% (w/v) Yeast Extract, 0.5% (w/v) NaCl) with appropriate antibiotic and grown overnight at 37°C with shaking at 180 rpm. Cells were harvested by centrifugation at 5000 rpm for 5 minutes at RT. Plasmid DNA was isolated using Nucleospin®Plasmid Kit (Macherey Nagel) according to manufacture's instructions. The concentration of DNA was determined by UV spectroscopy at 260nm. A ratio between A260 and A280 with a value of 1.8 was used as a criterion for pure preparation of DNA.

The quality of the DNA was also ascertained by electrophoresing 0.5-1.0µg of the DNA on a 1% agarose gel followed by visualization using UV transilluminator. The plasmid-DNA was stored at -20°C.

6.1.4.6. Agarose gel Electrophoresis of DNA

Routinely 1-X TAE (40mM Tris –Acetic Acid, 1mM EDTA pH8.0) buffer was used for electrophoresis. Ethidium Bromide was added to a final concentration of 0.5µg per ml in the gel prior to casting. For most of the purposes 1-1.5%, agarose gels were used. Samples were loaded on the gel after mixing with 6-X loading dye (50% Glycerol, 7.5mM EDTA, 0.4% Xylenxyanol, and 0.4% Bromophenol Blue). Electrophoresis was carried out at a constant voltage of 80-120V for 45-130 minutes.

6.1.4.7. Isolation and Purification of DNA from Agrose gel

Restriction digested DNA as well as DNA obtained by PCR amplification was analyzed by electrophoresis on 1-2% agarose gel. The required DNA fragment was excised from the gel. Isolation and purification of PCR products/ DNA fragment from the excised piece was performed with Nucleospin® Extract Kit according to manufacture's instructions (Macherey Nagel).

6.1.4.8. Synthesis of Codon Adapted Opsin Domain of Chop-1 and Cop-5 Genes

The synthesis of Chop-1 gene was done by Entelechon GmbH, Regensburg, Germany. The synthesis of Cop-5 gene was done by M. Fuhrmann at KFZ department, Biopark, Regensburg.

6.1.4.9. Sequencing of DNA

Automated DNA sequencing was done at the sequencing facility of MWG-Biotech GmbH, Germany and Entelechon GmbH, Germany.

6.1.4.10. Digestion of DNA by Restriction Enzymes

Restriction digestion was carried out in the appropriate buffer according to manufacturer's instruction. For most purposes, 1-5 µg DNA was digested with 1-20 U of restriction enzyme in a volume of 10-50 µl of 1X reaction buffer. The digested DNA was subjected to electrophoresis for purification, analysis and interpretation.

6.1.4.11. Dephosphorylation of the Vector DNA

Dephosphorylation was carried out directly following plasmid linearization. Calf Intestine Alkaline phosphatase was added to the digestion mixture at a concentration of 1U/pmol linearized vector DNA. After 45-60 minutes incubation at 37°C, CIP was heat inactivated at 65°C for 10 minutes.

6.1.4.12. Ligation of DNA-Fragment into Vector DNA

Routinely, the vector DNA and insert were restriction digested with appropriate enzymes, purified and quantified. The insert DNA was employed at a molar excess of 2-5 folds relative to the linearized and dephosphorylated vector (100-200ng) DNA. The vector DNA and insert mixture was made up to a volume of 10-15µl with 1X ligation reaction buffer and 2-5 units of T4 DNA ligase. Ligation reaction was carried out for two hours at room temperature/overnight at 16°C.

6.1.4.13. Polymerase Chain Reaction

Polymerase Chain Reaction was carried out in 50µl volume with the following ingredient (Saiki et al., 1988).

10x PCR Buffer	5µl
10x dNTP Mixture (2mM)	5µl
25µM Sense Primer	1µl
25µM Anti-sense Primer	1µl
Template-DNA (10ng)	1µl
Taq-DNA-Polymerase	1U
Water	Up to 50µl

Cycling conditions were as follows:

1. 95°C for 3-5 minutes	Denaturation
2. 93°C for 45 seconds	Denaturation
3. 56-70°C for 30 seconds	Annealing
4. 72°C for 1min/1kb	Extension
Step 2-4 30 Cycles	
72°C for 7 minutes	Final extension.

6.1.4.14. Colony-PCR for Screening of Positive Clones

E. coli transformants were picked and resuspended in 5µl of H_2O in a PCR tube, heated for 5 min at 95°C and centrifuged briefly. The PCR reaction was setup and performed as mentioned above with 1µl of supernatant as the template. PCR products were analyzed on 1% agrose gel.

6.1.5. Protein Chemistry Methods

6.1.5.1. Heterologous Expression of Proteins in *E.coli*

Competent cells were transformed with appropriate expression constructs. Positive clones were screened by colony PCR. Single positive colony was picked and inoculated in to 10ml of LB containing appropriate antibiotic. The culture was grown at 37°C with constant shaking at 180 rpm for 12-16 hours. The culture was expanded to a larger culture of one liter with one $1/20^{th}$ volume of pre- culture. Cells were allowed to grow at 37°C with shaking at 180 rpm until an OD_{600}= 0.6 was attained. The culture was then chilled at 4°C for 30 minutes prior to induction with 0.3mM IPTG. Induction was carried out for 12-16 hrs at 30°C. Cells were then harvested by centrifugation at 5000 rpm for 15 minutes at 4 °C. Pellet was resuspended in MOPS-EDTA buffer. The cell suspension was sonicated for 15 pulses at 0°C to avoid heat denaturation of the protein. It was then centrifuged at 12500 rpm for 45 minutes at 4 °C. The supernatant was collected and used for the protein estimation using BCA test. Twenty-five microgram of the total protein was resolved on 10-12% SDS-PAGE gel. Expression of recombinant protein was checked by western blotting using anti-His (Novagen)/protein specific antibodies (Chop-1 and Chop-2).

6.1.5.2. Expression of Cop-5 in *E.coli* using BL-21 (C41) Expression strain

The *cop-5-S* ET21a+ construct were transformed into the BL-21 (C41) cells using electroporation (1.5 KV, 800 Ω and 125µF) method. Transformants were screened by colony PCR. One positive clone was inoculated into 10 ml LB medium to grow a pre-culture for expression of Cop-5-S protein. It was then re-inoculated into fresh medium to grow until $OD_{578\lambda}$ =0.6 attained. Thereafter, the culture was induced with 1.0 mM IPTG at 37°C for 2.5 hrs, and induced cells were harvested by centrifugation at 4500 rpm for 10 minutes at 4°C. The pellet was resuspended in buffer (150mM Nacl, 25mM NaiP, and 2mM EDTA, pH 8.0). It was then sonified for five pulses with an interval for 30 seconds at maximum output without fine tip; samples were on the ice for all time. Ultracentrifugation

was carried out at 40,000 rpm for 30 minutes at 4ºC for and the obtained pellet was homogenized with homogenizer potter in buffer (300mM NaCl, 50mM Na-P buffer, 2% Dodecyl Maltose, pH 8.0). Solubilization of expressed Cop-5 was carried out overnight at 4ºC on slow shaking platform. Solubilized protein samples were centrifuged at 45000 rpm for 1hrs at 4ºC. The supernatant of each sample was collected and samples were used for SDS-PAGE following by immunoblotting.

6.1.5.3. Preparation of Membrane Fraction of *E. coli*

The total membrane fractions from *E.coli* were prepared by Lysozyme/EDTA treatment followed by osmotic lyses and further centrifugation at 35000 rpm for 90 min at 4 °C (Osborn et. al., 1972). The supernatant of each fraction was collected and total protein content of this sample was measured using BCA test. 25µg of the total protein was resolved on the SDS-gel. The obtained fractions were analyzed for expression of recombinant protein by immunoblotting using anti His-tag (Novagen)/ protein specific antibodies.

6.1.6. Gene Constructs for Expression of Chlamyopsins

All plasmid construct of Chlamyopsin genes were cloned by PCR based sub-cloning method. Different variants of Chlamyopsin genes were amplified by PCR and restriction sites at the upstream and downstream of the gene were introduced using gene specific primers (Table-6), which were containing recognition sequence for respective restriction enzyme(s). These gene fragment and vector were digested with appropriate restriction enzymes. Restricted digested vector and gene fragment were separated on 1-1.5% agrose gel. Gene fragment and vector were purified by using DNA extract kit. Purified gene fragment and vector were ligated by using ligation reaction. Ligation mixture was transformed into the *E.coli* DH5α cells and transformants were screened for positive clones by colony PCR. Three plasmids were isolated from the positive clones for each construct and all construct were checked by automated DNA sequencing.

Table 4.

Constructs	Template	Primers (Table.6)	Vector
Chop-1-S	Chop-1 Synthetic	Chop-1-S-FW+Rev	pMALc2
Chop-1-SS (E.coli)	cDNA Clone	Chop-1N-FW+Rev	Chop-1S-pMALc2
Chop-1-SS (*P.pastoris*)	Chop-1SS-pMALc2	Chop-1SS-FW+Rev	pPIC9K
Chop-2	cDNA Clone	Chop-2-Fw+Rev	pET21a(+)
Chop-1-C	cDNA Clone	Chop-1-C- FW+Rev	pET21a(+)&pMALc2
Chop-2-C	cDNA Clone	Chop-2-C- FW+Rev	pET21a(+)&pMALc2
Cop-5-S	Cop-5 Synthetic	Cop-5-S-FW+Rev	pET21a(+)
Cop-5-HK	Cop-5-FL	Cop-5-HK-Fw+Rev	pET21a(+)
Cop-5-RR	Cop-5-FL	Cop-5-RR-Fw+Rev	pET21a(+)
Cop-5-Cyc	Cop-5-FL	Cop-5-Cyc-Fw+Rev	pET21a(+)
Cop-5-FL	Cop-5-FL Semi-synthetic	Cop-5-FL-Fw+Rev	pET21a(+)
Cop-5-FL-HEK	Cop-5-FL Semi-synthetic	Cop-5-FL-FW and Cop-5-FL-Rev-HEK	pCDNA3.1(+)
ECFP	ECP-Plasmid	ECFP-FW+Rev	pCDNA3.1(+)
Cop-5-FL-ECFP	ECP-Plasmid	ECFP-FW+Rev	Cop-5-FL-pCDNA3.1 (+)

6.1.6.1. Expression of Chlamyopsins in *E.coli*

Table 5. Gene constructs and different experimental conditions for expression

Construct	Expression strain	Medium	Cold shock	Amount of IPTG	Induction period /°C
Chop-1-S	BL-21 DE3λ *pLys*	LB		0.6 mM	16hrs/ 18°C
Chop-1-SS	BL-21 DE3λ *pLys*	LB		0.6 mM	16hrs/ 18°C
Chop-2	BL-21DE3 λ	TB	0.5hrs/ 0°C	0.6 mM	2.5 hrs/37°C
Chop-1-C	BL-21DE3 λ	LB		1.0 mM	2.5 hrs/37°C
Chop-2-C	BL-21DE3 λ	LB		1.0 mM	2.5 hrs/37°C
Cop-5-S	C41	LB		1.0 mM	2.5 hrs/37°C
Cop-5-HK	BL-21DE3 λ	TB	0.5hrs/ 0°C	0.6 mM	16hrs/ 18°C
Cop-5-RR	BL-21DE3 λ	TB	0.5hrs/ 0°C	0.6 mM	16hrs/ 18°C
Cop-5-Cyc	BL-21DE3 λ	TB	0.5hrs/ 0°C	0.6 mM	16hrs/ 18°C
Cop-5-FL	Origami/Rosetta	TB	0.5hrs/ 0°C	0.6 mM	16hrs/ 18°C

6.1.6.2. Protein Estimation by BCA Method

The protein content of the samples were determined with Bicinchoninic Acid (BCA) reagent (Pierce, Rockford, Ill, USA) using Bovine Serum Albumin (BSA) as standard, according to manufacture's instructions.

6.1.6.3. Precipitation of Proteins by TCA

An equal volume of 20% TCA (Trichloroacetic Acid) was added to the protein samples. The TCA-protein mixture was incubating on ice for 30 minutes and centrifuged for 15 min at 4°C. The supernatant was removed carefully and 300 µl of cold acetone was added. The sample was then centrifuged for 5 min at 4°C. The supernatant was discarded and the pellet was dried and resuspended in SDS-PAGE loading buffer.

6.1.6.4. Sodium Dodecyl Sulphate-Poly-Acrylamide Gel Electrophoresis (SDS-PAGE)

Protein separation by SDS-PAGE was used to determine the relative abundance and purity of major proteins in a sample and their approximate molecular weights. Protein samples were heated in sample buffer containing 10mM 2-β-mercaptoethanol and 10% SDS at 95°C for 5 minutes or 45°C for 30 min. From each sample, 25µg of the total protein was loaded onto each lane and resolved on SDS-PAGE at a constant current of 30 mA.

6.1.6.5. Staining of Protein Gel

The SDS-PAG was immersed in staining solution (0.2% Coomassie Brilliant Blue dye in 45:45:10 % Methanol: Water: Acetic Acid), sealed in a plastic box and left overnight on a shaker with agitation at (RT) or for 2 to 3 hours at 37°C. It was then removed from the staining solution and placed in destaining solution (25% Methanol, 65% H_2O, and 10% Acetic Acid mixture) with agitation for a few hours until the bands on the gel were clearly visible.

6.1.6.6. Western Blotting for Protein Detection

Protein samples were resolved on the SDS-PAG as described previously. Semi-dry blotting system (Bio-Rad) was used for the transfer of proteins onto a nitrocellulose membrane (Hybond-Amersham). Protein transfer was performed at $2mA/cm^2$ for 45 Min. The completion of protein transfer on the membrane was confirmed using red ponceau dye or pre-stained standard protein marker. The protein bound membrane was washed twice with PBS and once using PBS-Tween 0.05% (V/V) buffer to remove un-bound protein from the

membrane, and each was carried out with, shaking 50-100 rpm for 10 minutes at RT. Blocking was performed using 7% (W/V) milk powder in PBS-tween for 1 hour at RT or overnight at 4°C. Washed membrane was incubated with appropriate concentration of primary antibody (1:1000 for anti-His-tag; 1: 2000 for anti-Chop1 and 1:2000 for anti-Chop-2) in 7% (W/V) milk containing PBS-tween buffer for 1 hour at RT or overnight at 4°C. The membrane was then washed 3 times with 10ml PBST with gentle shaking at RT. This membrane was incubated with appropriate concentration of secondary antibodies in 7% (W/V) milk containing PBS-tween buffer at RT for 1-2 hrs. The membrane was then washed to remove un-bound secondary antibody. It was then immersed in the detection buffer, which had appropriate concentration (1:2000 for anti-IgG Mouse and 1:10000 for anti-IgG Rabbit) of the BCIP and NTB for colorimetric detection of the immunoblots. The detection of His-tagged fusion expressed protein was done by immuno-enzymatic method as described in manual. In the case of protein specific antibody, working dilutions were determined empirically for 1° and 2° antibodies.

6.1.7. Detection of Channelopsin Proteins from *C. reinhardtii*

C. reinhardtii cell (strain 806) was grown in TAP medium under different light conditions (high, low and dark) and harvested after 3 days. Cells were disrupted by sonication; the total membrane fraction was collected by using centrifugation at 30,000rpm for 40minutes at 4°C. Total protein content of each membrane fraction was quantified using BCA test. 25µg of total protein sample was mixed with 2X loading dye and heated at 45°C for 30 minutes. Membrane proteins fractions were resolved on SDS-PAGE, and Chop1 and Chop2 were detected by protein blotting using anti-Chop-1 and anti-Chop-2 antibodies at a dilution of 1: 2000 and the secondary antibody at a dilution of 1:5000.

6.1.8. Transient Expression of Cop-5 in HEK-293

The *Cop-5* encoding full-length gene and *cop-5-ecfp* fusion encoding genes were cloned into the vector pcDNA3.1 for expression in Flp-TS/TM-HEK-293 cells. The general procedure for transfection and expression into HEK-293 were taken from the supplier's instruction manual (Invitrogen). Regeneration of the expressed recombinant protein with retinal was adapted from the Shukla *et al* (Shukla and Sullivan, 1999).

6.1.9. Flow Chart for Bioinformatic Analysis of the Chlamyopsins

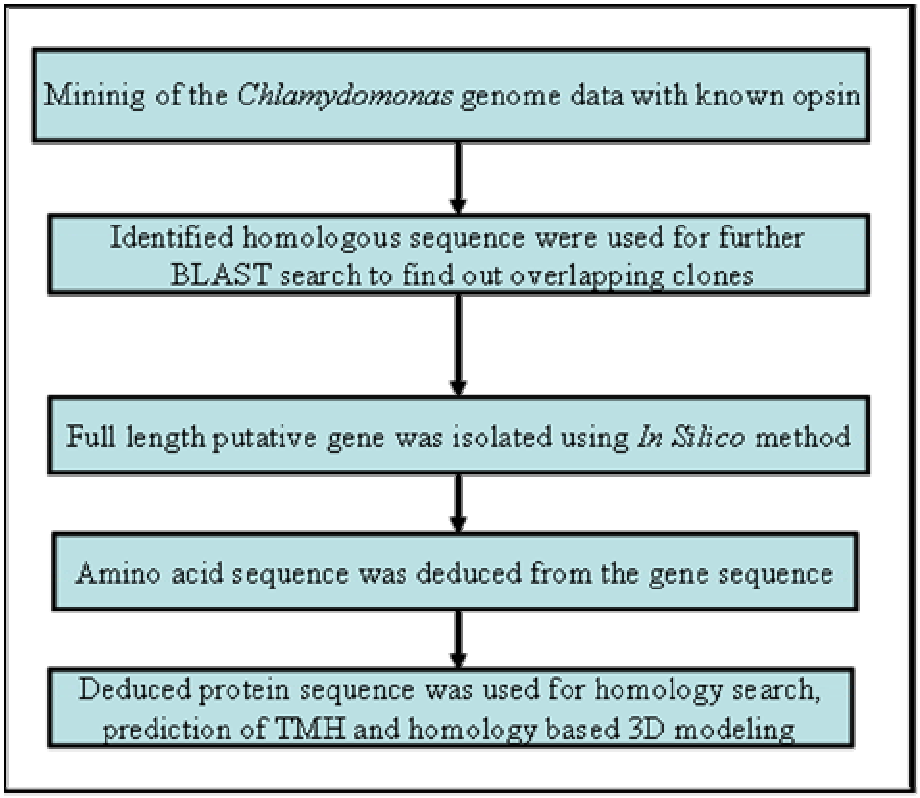

6.2. Materials

6.2.1. Cell Strains

Cells	Marker/ Phenotype	References/Source
C. reinhardtii cc-124^{-} strain	Wild type	Duke University, USA
C. reinhardtii cc-125^{+}	Wild type	Duke University, USA
C. reinhardtii cw-2	Cell wall deficient	Duke University, USA
C. reinhardtii cw-806		Smyth, Syracuse, USA
E. coli C41 (DE3λ) and C43		Engelhardt
E. coli DH10B		(Grodberg and Dunn, 1988)
E. coli DH5α		(Hanahan, 1983)
E. coli BL-21(DE3λ)		Novagen
E. coli BL-21(DE3λ)pLys		Invitrogen
HEK-293-Flp-TM/TS		Research Centre, Julich
P. pastoris GS115	(his4,Mut2)	Invitrogen
X. laevis		Nagel
Origami (DE3)		Novagen
Rosetta		Novagen

6.2.2. Vectors

Vectors	Selection Marker	Source
pArg 7.8	amp	Fuhrmann
pBluescript KS^{-}	Amp and lacZ	Stratagen
pcDNA3.1	amp	Invitrogen
pET21a (+)	amp	Novagen
pET35b	kan	Novagen
pECFP	kan	Kaup (Julich)
pPIC9K	amp	Invitrogen
pGEMHE	amp	Hedrich
pGEM-HE-Rg	amp	Schieries
pMALc2	amp	Schieries
pUC18	amp	Hildebrandt

6.2.3. EST and BAC clones

EST/BAC Clones	Source	Identified Gene
EST AV641459	Kasauza EST Project, Japan	Channelopsin-1
EST AV643095	Kasauza EST Project, Japan	Channelopsin-2
EST AV394119	Kasauza EST Project, Japan	Chlamyopsin-5
BAC-17m1 and17m15	CGUI, USA	Chlamyopsin-4
BAC-24p13	CGUI, USA	Chlamyopsin-5

6.2.4. Computer Programs used for the Analysis of Chlamyopsins

Program	Web Link	References
Multalin	www.prodes.toulouse.inra.fr/multalin/multalin.html	(Corpet, 1988)
CDART	www.ncbi.nlm.nih.gov	(Geer et al., 2002)
Sequence Inversion	www.entelechon.com	
X3M-3D Modeling	www.cbs.dtu.dk/service/CPHmodels/	
PDB Files Viewer	www.ncbi.nlm.nih.gov	
RasMol	www.openrasmol.org	
SMART	http://smart.embl-heidelberg.de/	(Schultz et al., 2000)
Codon Usage	http://gcua.schoedl.de/	
GeneScan	http://genes.mit.edu/GENSCAN.html	(Burge and Karlin, 1998)
NetPhos	http://www.cbs.dtu.dk/services/NetPhos/	(Blom et al., 1999)
SignalP	http://www.cbs.dtu.dk/services/SignalP/	(Bendtsen et al., 2004)
TM-pred	http://www.ch.embnet.org/software/TMPRED_form.html	

6.2.5. Chemicals, Enzymes and Kits

6.2.5.1. Chemicals

Agar	Amresco
Agarose	BD-USA
Ampicillin	Sigma
Bacto-peptone	Difco
Bacto-Trypton	Difco
Bacto-Yeast-Extract	Difco
BCA	Pierce
Coomassie Blue	Serva
DEPC	Sigma
dATP,dTTP,dCTP &dGTP	MBI-Fermentas
Ethidium bromide	Sigma
Formamide	Sigma
Glassware	Braun
IPTG	Roth
β-Mercaptoethanol	Roth
NBT	Sigma
Ni^{++}-NTA-Agarose	Qiagen
Nitrocellulose	Schleicher & Schuel
Phenol	Roth
Ponceau S	Sigma
Rotiphoreses Gel 40	Roth
TEMED	Bio-Rad
Tween20R	Sigma
X-Gal	Sigma
X-Phosphate (BCIP)	Sigma

All other chemicals were purchased from the Merck Company.

6.2.5.2. Enzymes and Proteins

BSA	Sigma
CIP	MBI-Fermentas
DNA-Polymerase	MBI-Fermentas
DyNAzymeTM	Finzymes
Pfu-DNA-Polymerase	Promega
T4-DNA-Ligase	MBI-Fermentas
Taq-Polymerase	Schiereis/Self Made
Vent Polymerase	NEB
Restriction Enzymes	NEB & MBI-Fermentas

6.2.5.3. Kits

TOPO-TA-Cloning Kit	Invitrogen
Echo-Expression Kit	Invitrogen
RT-PCR Kit	Boehringer Mannheim
RNeasy Kit	Qiagen
DNA/Plasmid Isolation Kit	Macherey&Nagel
DNeasy® Plant Kit	Qiagen

6.2.6. Instruments

Analytic Weighting Machine	Mettler
Autoclave	LSL, H+H Lab Techinque
Centrifuge	Dupont (Sorvall) Beckmann
Circulating Water bath	New Brunswick Scientific
Culture Flask	Nalgene
Drying Chamber	Heraeus
Flow through Centrifuge	Wesfalia Separator
Fine Balance	Sartorius
Gel Apparatus	Self-prepared
Gel Drier	Bio-Rad
Gel Document System	Infors

Gradient Mixture	Self Prepared
Heating Block	Grant
Fermentor	Bioengineering
Magnetic Stirrer	Heidolph
Membrane Hybond N+	Amersham
Parr-bomb	Ashcroft
PCR-Cycler	Stratagene
pH-Meter	Knick, MTW
Pipetten	Gilson
Pure Water	Millipore
Blotting Apparatus	Bio-Rad
Spectrophotometer	Beckmann
Table Centrifuge	Eppendorf
Ultrasonicator	Branson
Videoprinter	Mitsubishi
Vortexor	Heidolph
Water Bath	Lauda

6.2.7. Antibodies

6.2.7.1. Primary Antibody

Anti-His-tag	Novagen

6.2.7.2. Secondary Antibodies

Anti-rabbit IgG HRP-conjugated	Chemicon (Working dilution 1: 10,000)
Anti-mous IgG HRP-conjugated	Novagen (Working dilution 1: 2000)

6.2.8. Solutions and Buffers

2x Lysis Buffer for *Chlamydomonas*
2% CTAB
100 mM Tris/Cl, pH 8.0
1.4 M NaCl
20 mM EDTA
0.2% b-Mercaptoethanol

De-staining Buffer (Immunoblot)
100 mM NaCl
100 mM Tris/Cl pH 9.5

Runing Buffer
10 mM MOPS/ NaOH pH 6.8
1mM EDTA

Blocking Buffer (Immunoblots)
150 mM NaCl
16 mM Na_2HPO_4
1.8 mM NaH_2PO_4
0.05% Tween 20
7% Milk Powder

Blotting Buffer (Immunoblot)
2.5 mM Na-Phosphate pH 6.5
0.1% SDS

PBS (Phosphate Buffered Saline)
150 mM NaCl
16 mM Na_2HPO_4
1.8 mM NaH_2PO_4

10x Probe Buffer for Agarose Gel
20% Ficoll 400
0, 1 M EDTA pH 8.0
0.25% Bromphenol Blue

Buffer A (Ni^{2+} -Chromatography)
6M Guanidium Hydrochloride
0.1 M NaH_2PO_4
10 mM Tris/Cl, pH 8.0

Buffer B (Ni^{2+} -Chromatography)
8M Urea
0.1 M NaH_2PO_4
10 mM Tris/Cl, pH 7.2

Buffer C (Ni^{2+} -Chromatography)
8 M Urea
0.1 M NaH_2PO_4
10 mM Tris/Cl, pH 6.3

Buffer D (Ni^{2+} -Chromatography)
8 M Urea
0.1M NaH_2PO_4
10 mM Tris/Cl, pH 5.0

Following chemicals were dissolved in one liter to prepare trace element solution.

22g $ZnSO_4 7H_2O$

11.4g H_3BO_3

5.06g $MnCl_2 4H_2O$

4.99g $FeSO_4 7H_2O$

1.61g $CoCl_2 6H_2O$

1.57g $CuSO_4 5H_2O$

1.1g $(NH_4)_6 Mo_7O_{24} 2H_2O$

50g EDTA

TfbI

30 mM KAc/HAc, pH5.8

50 mM $MnCl_2$

100 mM KCl

15% (v/v) Glycerol
Sterilized by Filter

TfbII

10 mM MOPS/NaOH, pH 7.0

75 mM $CaCl_2$

10 mM KCl

15% (v/v) Glyceriol
Sterilized by Filter

6.2.9. Oligonucleotides

Table 6.

Oligonucleotide	Sequence
Chop-1-S-Fw	AAAGGATCC ATGTCCCGTC GTCCATGG
Chop-1-S-Rev	TTTAAGCTT A TACAAAAGAA TATGTT
Chop-1-N-FW	TTT AAGCTT GGCGACATCCGCAAGAAG
Chop-1-N-Rev	TTT AAGCTT GGCC TCGGCGTCGC CGTT
Chop-1-SS-FW	TTTGAATTCATGTCCCGTCGTCCATGG
Chop-1-SS-Rev	TTTCCTAGGGCCGCCGGCTGCAGCGTT
Chop-1-C-Fw	AAAGAATTCATGCACGAGCACA TCCTGCTG
Chop-1-C-Rev	TTT AAGCTT CTCGCC CAGCTCGTTC TT
Chop-2-Fw	AAAGAATTC ATGGATTATG GAGGCGCC
Chop-2-Rev	TTT AAGCTT G TCGCGCATGA CCAGGAA
Chop-2-C-Fw	AAAGAATTC CATATCCTCATCCACGGC
Chop-2-C-Rev	TTT AAGCTT ATTCTGCAGCATCTCCGC
Cop-5-S-Fw	AAAGAATTCATGCCAGCCA CTAGTCGT
Cop-5-S-Rev	TTT AAGCTT TCTATTGCC TTCTTCGAC
Cop-5-HK-Fw	AAAGAATTCATGATCAAGACCTCGGGCGCA
Cop-5-HK-Rev	TTTAAGCTTCCAGCATCTTGTCCGTGAACG
Cop-5-RR-Fw	AAAGAATTCATGAAGGGCGCCCTGAAG
Cop-RR-Rev	TTTAAGCTT CAGCACGCGCTCCGGCC
Cop-5-Cyc-Fw	AAA GAA TTCATG ATC GCG GGC GCC ATA
Cop-5-Cyc-Rev	TTTAAGCTTCTT GCT CCA ACG GCT GGT
Cop-5-FL-Fw	AAAGAATTCATGCCAGCCA CTAGTCGT
Cop-5-FL-Rev	TTT AAGCTT CATGAACAGCGCCTG CGC
ECFP-FW	TTTGAATTCCTCGAGATGGTGAGCAAGGGGAG GAG
ECFP-Rev	AAACTCGAGCTTGTACAGCTCGTCCATGCC
Cop-5-FL-RevHEK	TTT CTCGAG CATGAACAGCGCCTG CGC

The introduced restriction sites in the sense and antisense primers are highlighted in blue and red respectively.

7. Appendix

7.1. Bioinformatic Analysis of Channelopsin-1

7.1.1. Prediction of Putative TMH for Chop-1 Protein Sequence

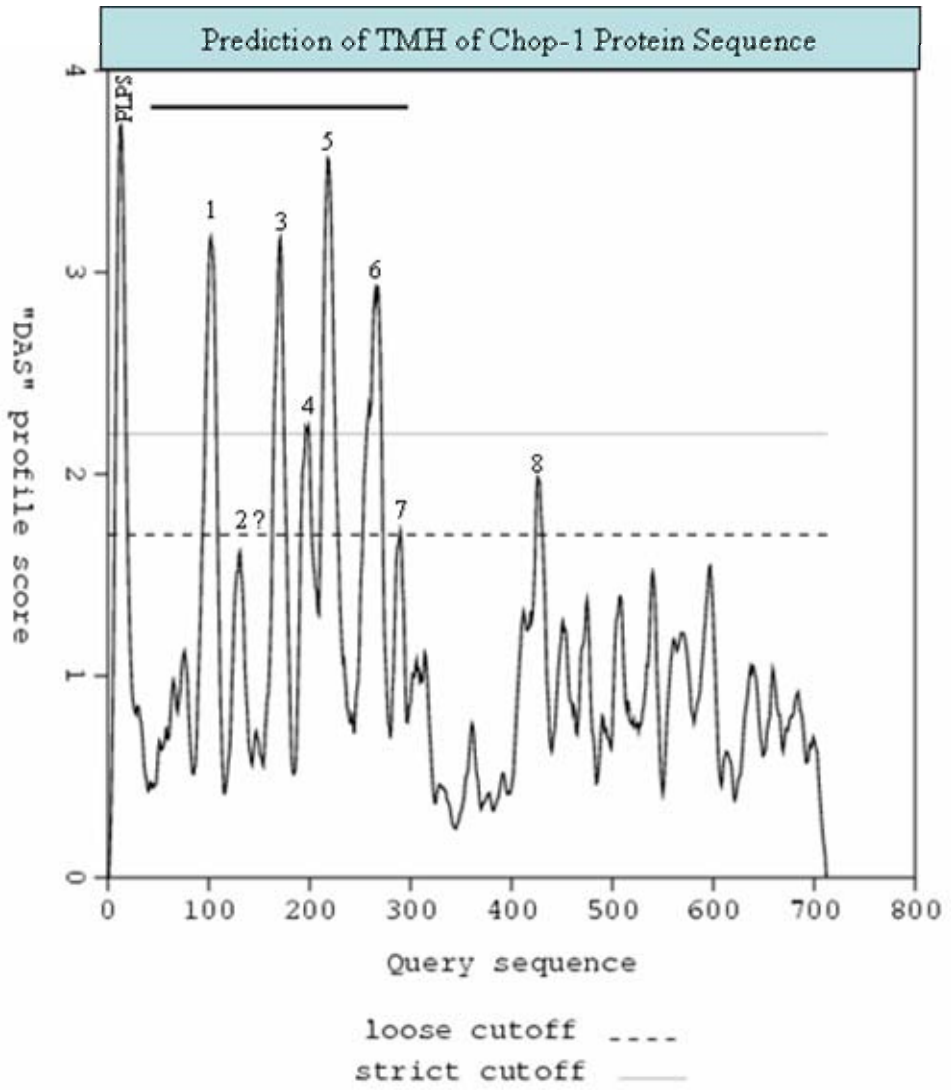

A1.1. Prediction of putative TMH of Chop-1 using hydropathy plot analysis. The location of amino acid residues of Chop-1 is plotted on the X-axis, whereas Y-axis numbers represent calculated score for the predicted TMH region in protein sequence based on hydrophobicity scale of amino acid residues. Peaks are denoting the score of predicted TMH (Y-axis), and corresponding amino acids location in the query sequence (X-axis). Opsin domain of Chop-1 is marked with a black bar at the N-terminus and putative TMH of opsin domain are indicated in numbers. First peak of TMH at N-terminus is the PLPS (Putative Leader Peptide Sequence).

7.1.2. Prediction of Leader Peptide Sequence in Chop-1

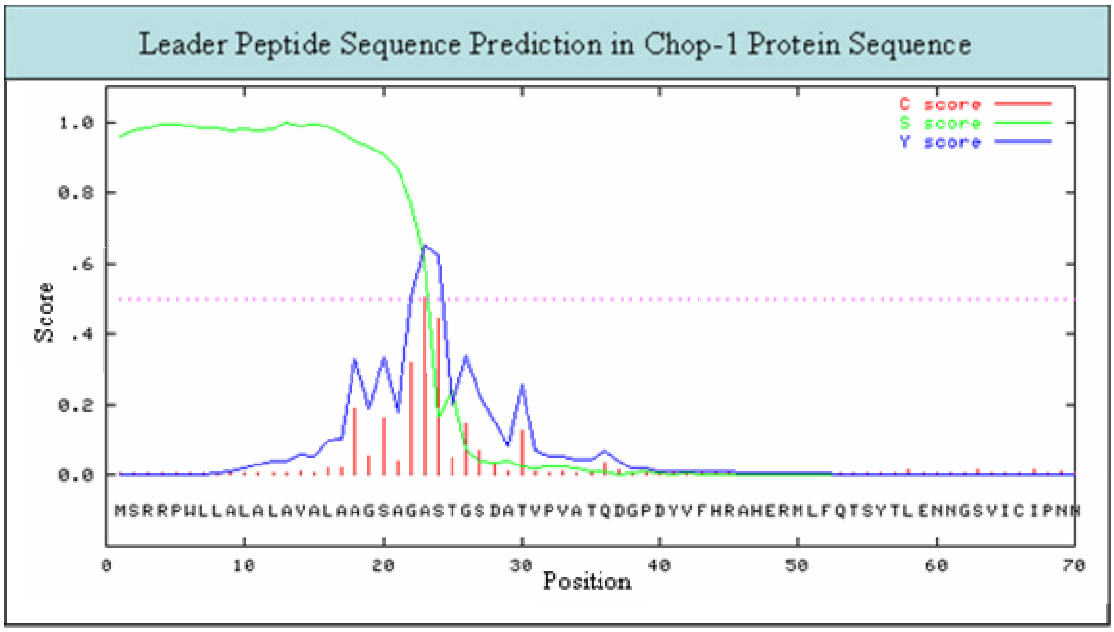

A1.2. Prediction of leader peptide sequence for Chop-1. The location of amino acid residues of Chop-1 plotted on the X-axis and Y-axis number represent calculated score of the potential cleavage site in predicted leader peptide sequence. The *C*-score is an estimation of the probability of the position of amino acids as belonging to the signal peptide or not. *S*-score is an estimation of the probability of the signal peptide in protein sequence. *Y*-score is the geometric average value of the C-score and smoothed derivative of S-score. Calculated score is derived from the stretch of hydrophobic amino acid residues at the N-terminus of the protein. SignalP analysis predicted potential cleavage site at the 23th amino acid residue at N-terminus of the Chop-1 protein sequence.

7.1.3. Prediction of Putative Phosphorylation Sites in Chop-1

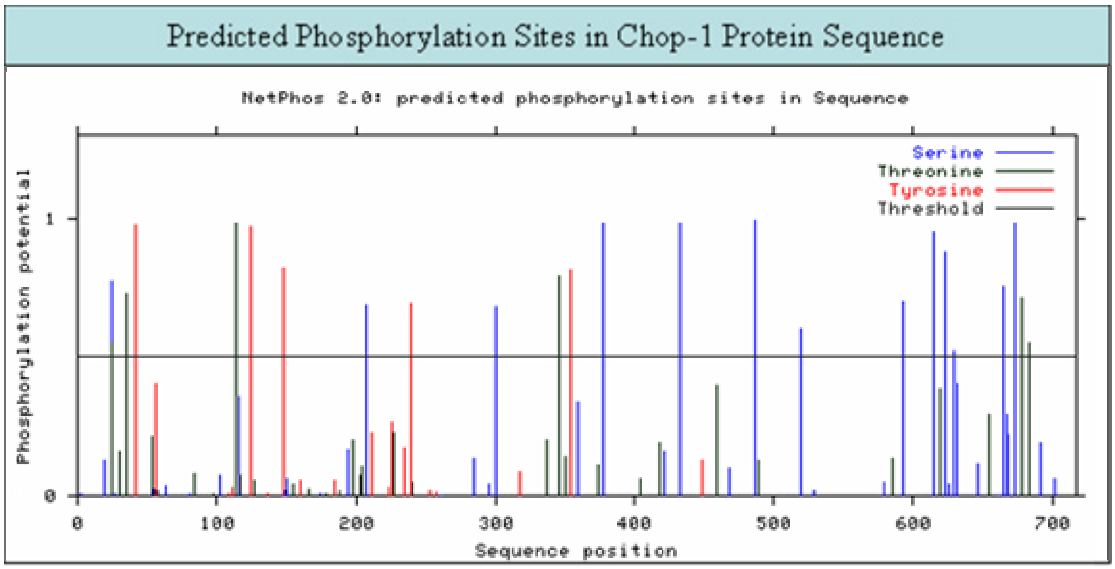

A1.3. Analysis of putative phosphorylation pattern of the Chop-1 protein sequence. The location of amino acid residues of Chop-1 is plotted on the X-axis and predicted score of the potential phosphorylation of a residue in the protein sequence is plotted on Y-axis. C-terminus of the Chop-1 protein has a number of putative phosphorylation sites.

7.1.4. Homology of Acetabularia Opsin (Aop) to Channelopsins

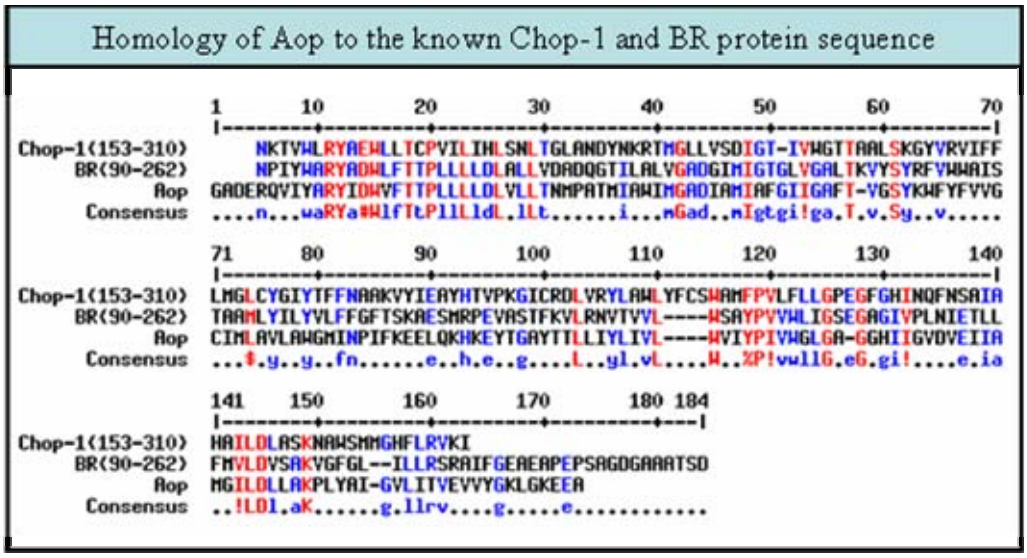

A1.4. Sequence alignment of putative Acetabularia opsin (Aop) with Channelopsins (Chop-1 and 2). Identical and homologous amino acid residues in both proteins are shown in red colure. Retinal binding motif showed presence of conserved lysine (K) amino acid residue for Schiff-base linkage in the putative helix G of the Aop. Putative Aop protein sequence is seems to be more homologues to the BR than Channelopsins.

7.2. Bioinformatic Analysis of Channelopsin-2

7.2.1. Prediction of Putative TMH for Chop-2 Protein Sequence

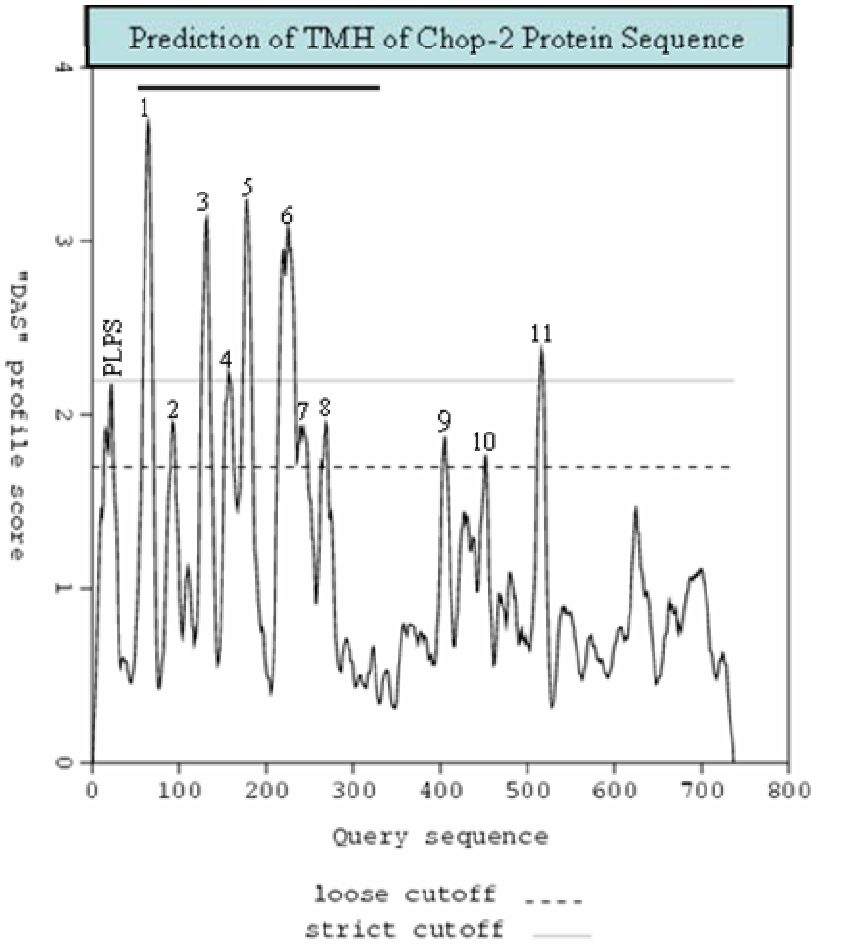

A2.1. Prediction of putative TMH of Chop-2 using hydropathy plot analysis. The location of amino acid residues of Chop-2 is plotted on the X-axis, whereas Y-axis numbers represent calculated score for the predicted TMH region in protein sequence based on hydrophobicity scale of amino acid residues. Peaks are denoting the score of predicted TMH (Y-axis), and corresponding amino acids location in the query sequence (X-axis). Opsin domain of Chop-2 is marked with a black bar at the N-terminus and putative TMH of opsin domain are indicated in numbers. First peak of TMH at N-terminus is the PLPS (Putative Leader Peptide Sequence).

7.2.2. Prediction of Leader Peptide Sequence in Chop-2

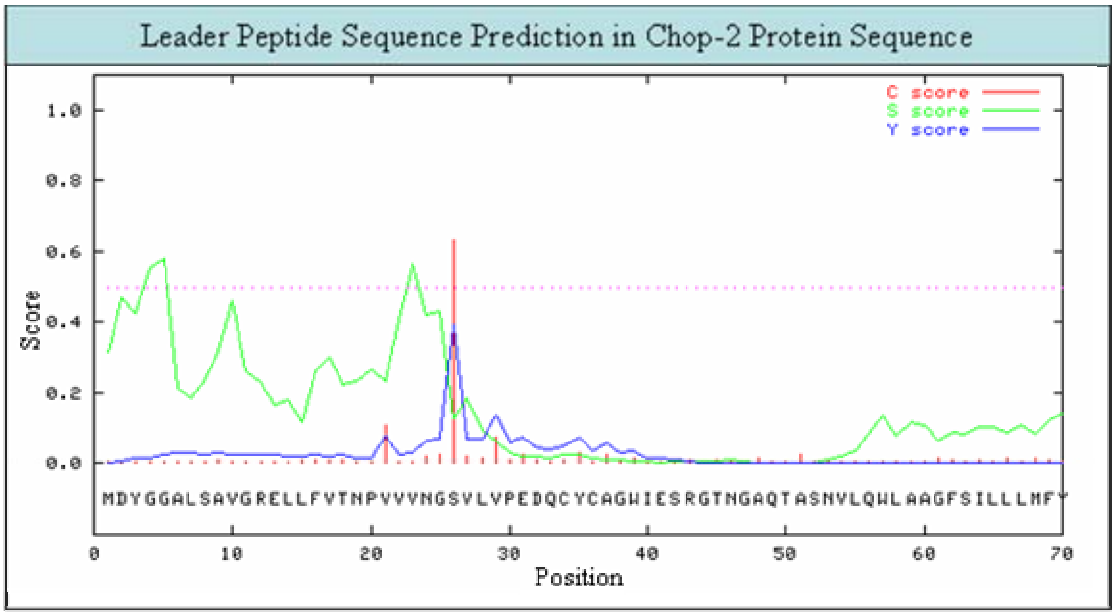

A2.2. Prediction of leader peptide sequence for Chop-2. The location of amino acid residues of Chop-2 plotted on the X-axis and Y-axis number represent calculated score of the potential cleavage site in predicted leader peptide sequence. The *C*-score is an estimation of the probability of the position of amino acids as belonging to the signal peptide or not. *S*-score is an estimation of the probability of the signal peptide in protein sequence. Y-score is the geometric average value of the C-score and smoothed derivative of S-score. Calculated score is derived from the stretch of hydrophobic amino acid residues at the N-terminus of the protein. SignalP analysis predicted potential cleavage site at the 26th amino acid residue at N-terminus of the Chop-2 protein sequence.

7.2.3. CDART Analysis of Chop-2 for Identification of Domain

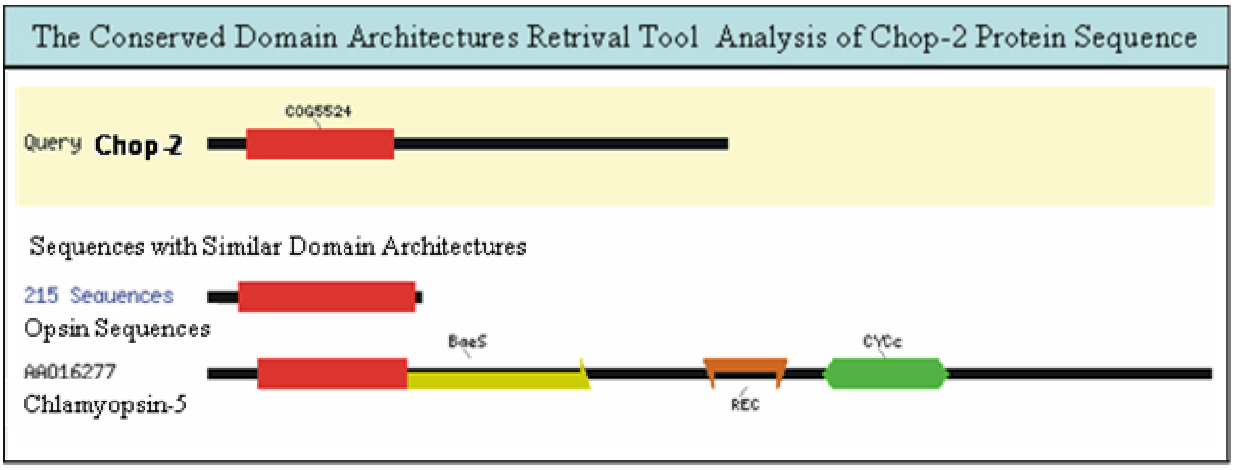

A2.3. Analysis of Chop-2 protein sequence with CDART. Bacteriorhodopsin like domain was found at N-terminus (1-300 a.a) of the Chop-2 protein sequence. This analysis has recognized more than 215 opsin sequences in the NCBI database, which had similar domain architecture (opsin) like one within query protein sequence. Chlamyopsin-5 sequence has appeared as a unique sequence. Homologues of the C-terminus of Chop-2 were not found in the database.

7.2.4. Identification of Putative Phosphorylation Sites for Chop-2

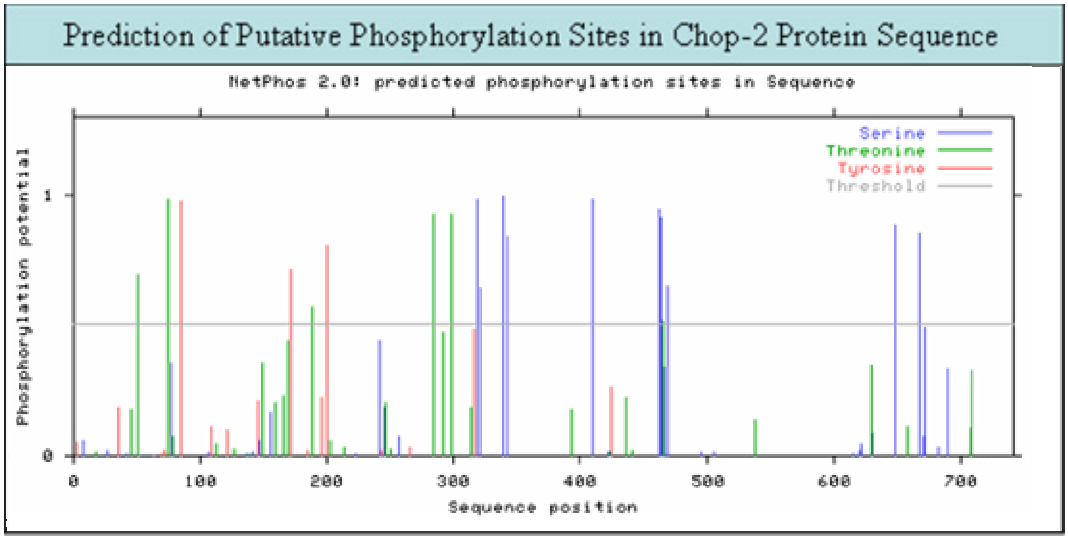

A2.4. Prediction of putative phosphorylation sites in the Chop-2 protein. The location of amino acid residues of Chop-2 is plotted on the X-axis and predicted score for the potential phosphorylation of a particular residue in the protein sequence is plotted on Y-axis. Chop-2 shows patch of putative phosphorylation sites (mainly serine) just after the opsin domain at the C-terminus.

7.2.5. Homology between Channelopsins and Putative Vop-2

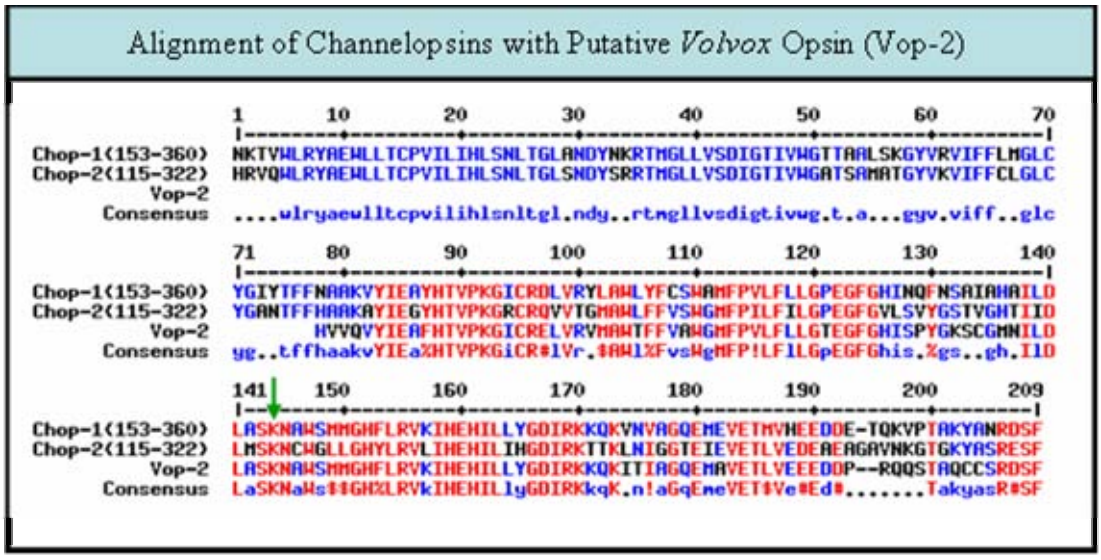

A2.5. Sequence alignment of putative Volvoxopsin (Vop-2) with Channelopsins (Chop-1 and 2). Identical and homologous amino acid residues in both proteins are shown in red colure. Retinal binding motif showed presence of conserved lysine (K) amino acid residue for Schiff-base linkage in the putative helix G of the Vop-2. Putative Vop-2 protein sequence is seems to be more homologues to the Chop-1 than Chop-2 protein.

7.3. Bioinformatic Analysis of Chlamyopsin-5

7.3.1. Prediction of Putative TMH for Cop-5 Protein Sequence

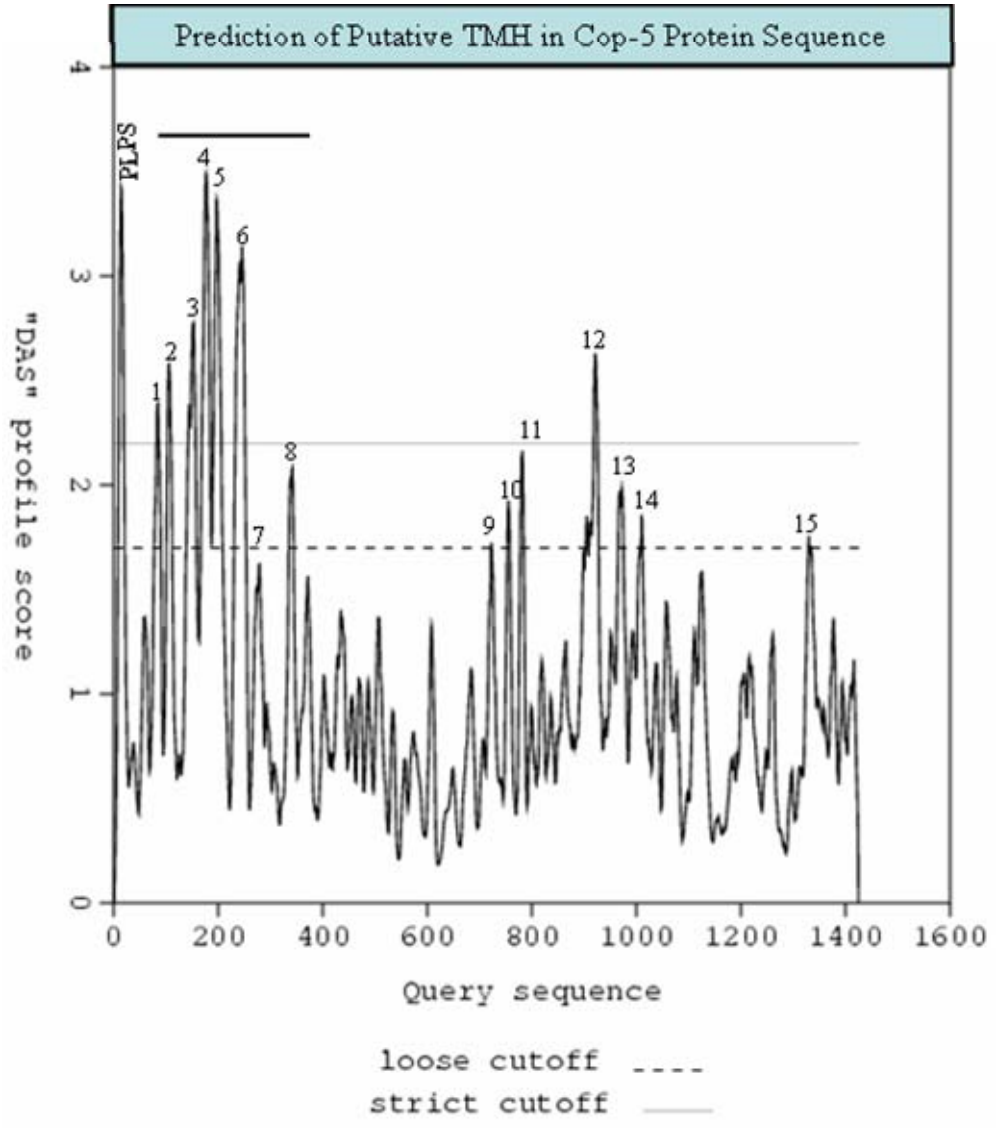

A3.1. Prediction of putative TMH of Cop-5 using hydropathy plot analysis. The location of amino acid residues of Cop-5 is plotted on the X-axis, whereas Y-axis numbers represent calculated score for the predicted TMH region in protein sequence based on hydrophobicity scale of amino acid residues. Peaks are denoting the score of predicted TMH (Y-axis), and corresponding amino acids location in the query sequence (X-axis). Opsin domain of Cop-5 is marked with a black bar at the N-terminus and putative TMH of opsin domain are indicated in numbers. First peak of TMH at N-terminus is the PLPS (Putative Leader Peptide Sequence).

7.3.2. Prediction of Leader Peptide Sequence in Putative Cop-5

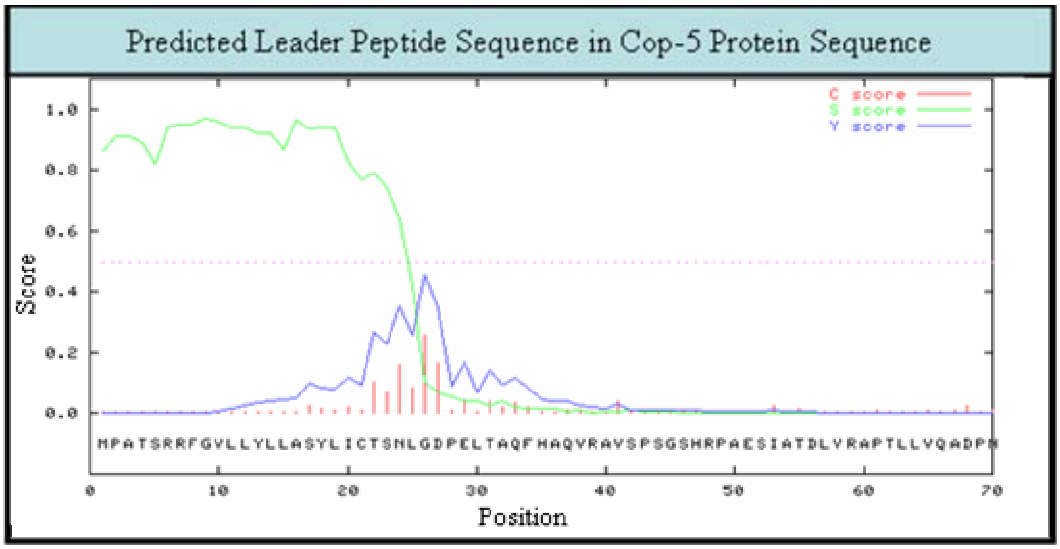

A3.2 Prediction of leader peptide sequence for Cop-5. The location of amino acid residues of Cop-5 plotted on the X-axis and Y-axis number represent calculated score of the potential cleavage site in predicted leader peptide sequence. The *C*-score is an estimation of the probability of the position of amino acids as belonging to the signal peptide or not. *S*-score is an estimation of the probability of the signal peptide in protein sequence. Y-score is the geometric average value of the C-score and smoothed derivative of S-score. Calculated score is derived from the stretch of hydrophobic amino acid residues at the N-terminus of the protein. SignalP analysis predicted potential cleavage site at the 23th amino acid residue at N-terminus of the Cop-5 protein sequence.

7.3.2.1. Homology between pSRII and Opsin Domain of Cop-5

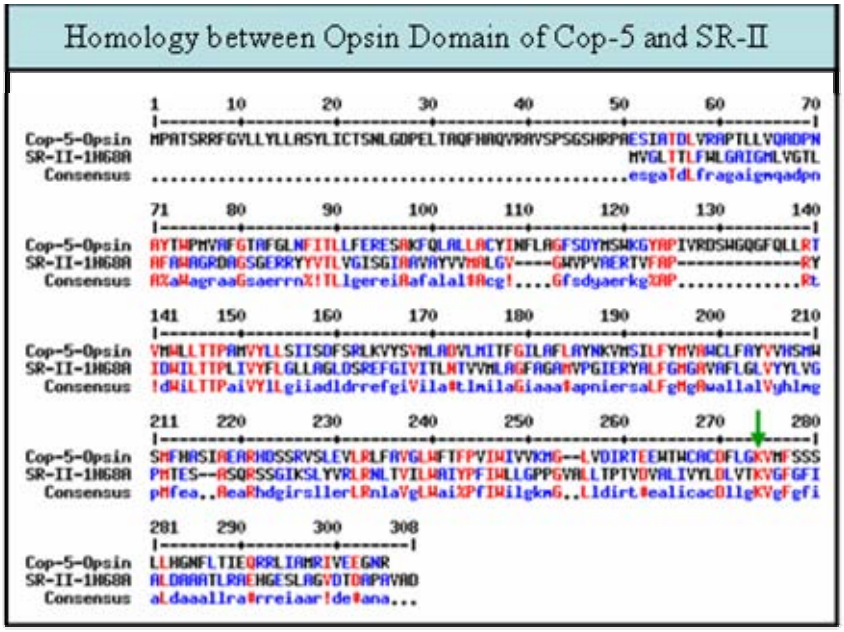

A3.3. Sequence alignment of pSRII and Cop-5. Identical and homologous amino acid residues in both proteins are shown in red colure. Retinal binding motif showed presence of conserved lysine (K) amino acid residue for Schiff-base linkage in the putative helix G of the Cop-5. Different amino acid in both sequence are seen in black and blue.

7.3.2.2. Homology between Cop-5 HK Domain and HK Domain of *E.coli*

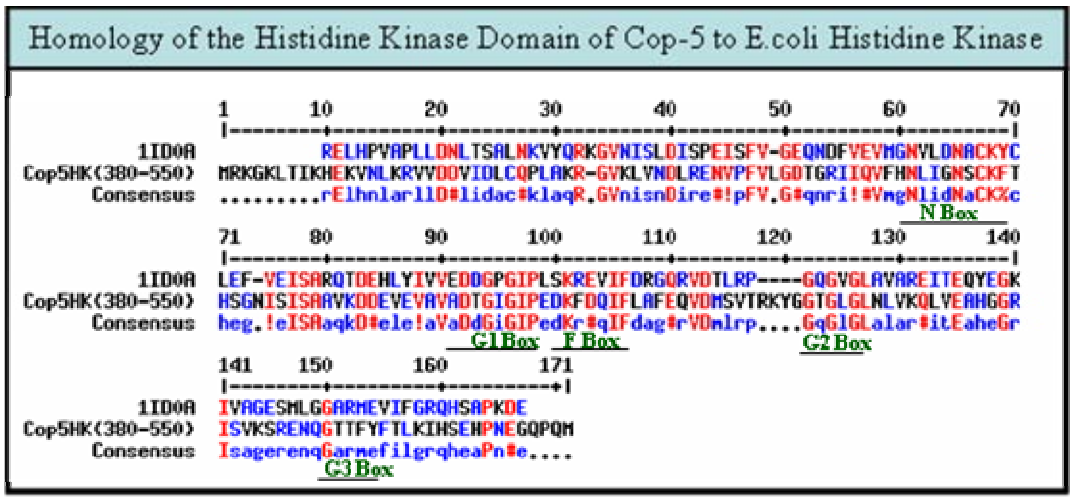

A3.4. Sequence alignment of HK domain of Cop-5 with HK domain of *E.coli.* Identical and homologous amino acids in both proteins are marked in red colure. Different amino acid residues between the both proteins are denoted in black or blue colour. Catalytically important boxes (N, G1, G2 and G3) are denoted by black bars. H box is presented in this sequence alignment.

7.3.2.3. Homology between Cop-5 RR Domain and *E.coli* RR Domain

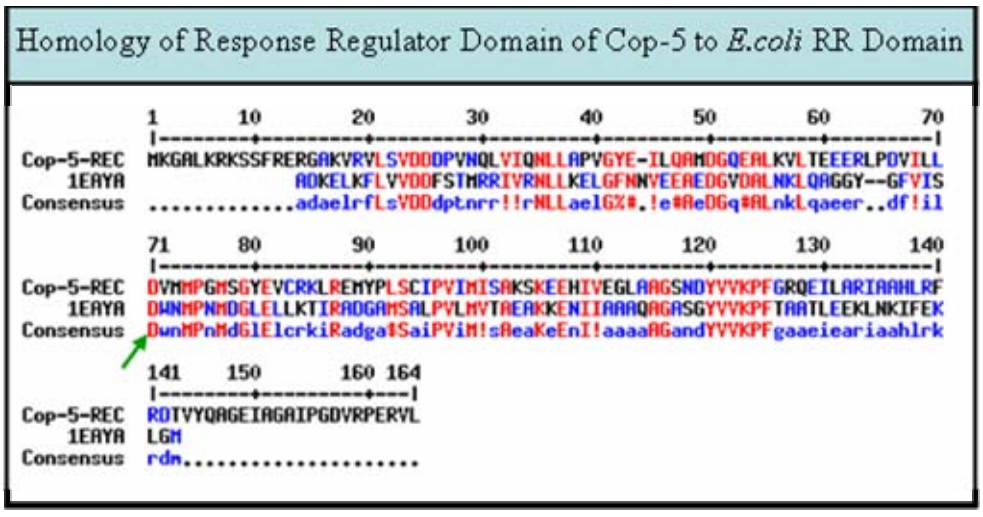

A3.5. Sequence alignment of RR domain of Cop-5 and RR domain of *E.coli*. Conserved aspartic (D) amino acid residue of the phosphate acceptor motif is marked with green coloured arrow. Identical and homologous amino acid residues are shown in red colour. Blue and black coloured amino acids residues represent the stretches that are not conserved among species.

7.3.2.4. Homology between Cop-5 Cyclase and Cyclase of *T. brucei*

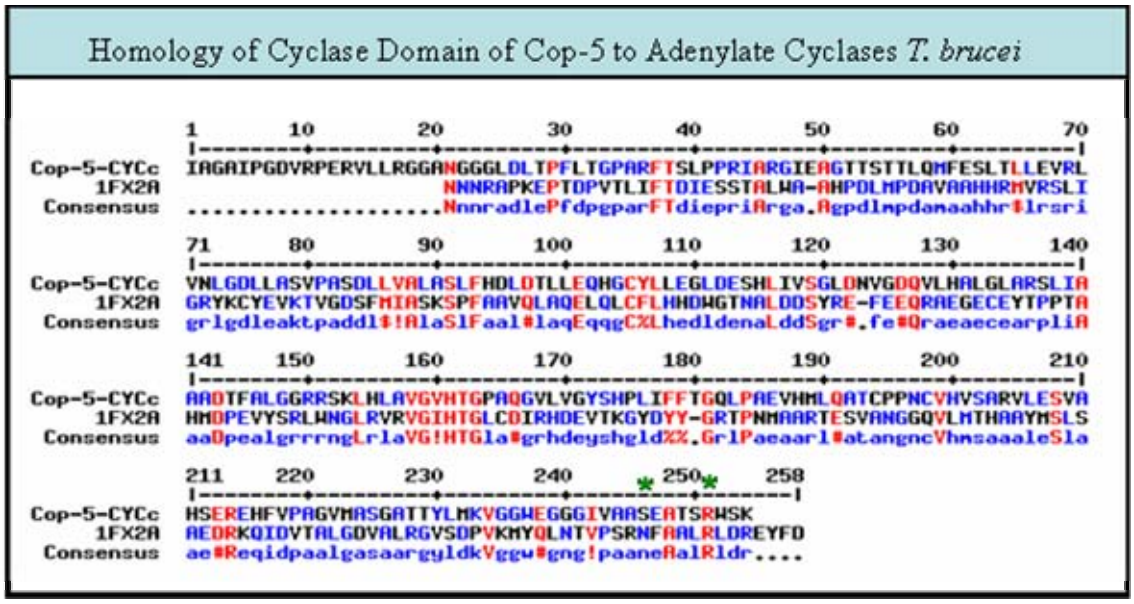

A3.5. Multiple sequence alignment of Cyclase domain of Cop-5 with Cyclase domain of *T.brucei.* All Identical and homologous amino acid residue are shown in red colour. Different amino acid residues between the both proteins are denoted in black or blue colour. Green colour asterisked residues know to be involved in the catalysis of cyclase domain of *T.brucei.*

7.3.2.5. Homology between Opsin Domain of Cop-5 and Putative Vop-3

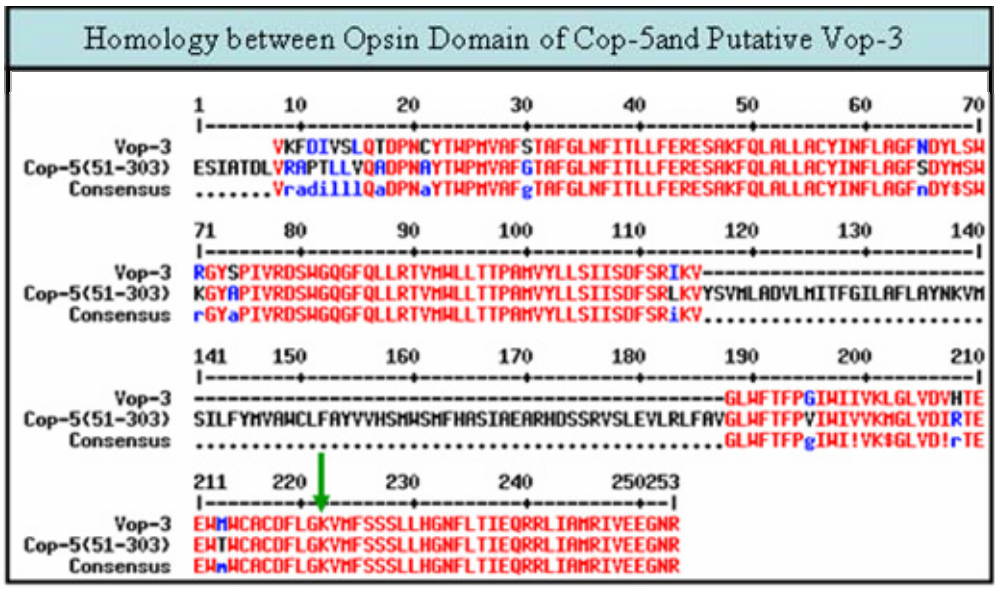

A3.6. Sequence alignment between opsin domains of Cop-5 (50-180 a.a) and opsin domain of Vop-3. All Identical and homologous amino acid residues among the species are shown in red colour. Different amino acid residues between the both proteins are denoted in black or blue colour. Retinal binding motif showed presence of conserved lysine (K) amino acid residue for Schiff-base linkage in the putative helix G of the Vop-3.

8. References

Akashi, H. (1994). Synonymous codon usage in *Drosophila melanogaster*: natural selection and translational accuracy. Genetics *136*, 927-935.

Amann, E. (1985). Plasmid vectors for the regulated, high level expression of eukaryotic genes in *Escherichia coli*. Dev Biol Stand *59*, 11-22.

Baneyx, F. (1999). Recombinant protein expression in *Escherichia coli*. Curr Opin Biotechnol *10*, 411-421.

Baylor, D. (1996). How photons start vision. Proc Natl Acad Sci U S A *93*, 560-565.

Beckmann, M., and Hegemann, P. (1991). In vitro identification of rhodopsin in the green alga *Chlamydomonas*. Biochemistry *30*, 3692-3697.

Beja, O., Aravind, L., Koonin, E. V., Suzuki, M. T., Hadd, A., Nguyen, L. P., Jovanovich, S. B., Gates, C. M., Feldman, R. A., Spudich, J. L., *et al.* (2000). Bacterial rhodopsin: evidence for a new type of phototrophy in the sea. Science *289*, 1902-1906.

Bendtsen, J. D., Henrik, N., Heijne, G. V., and and Brunak, S. (2004). Improved prediction of signal peptides: SignalP 3.0. J Mol Biol *340*, 783-795.

Berman, H. M., Westbrook, J., Feng, Z., Gilliland, G., Bhat, T. N., Weissig, H., Shindyalov, I. N., and Bourne, P. E. (2000). The Protein Data Bank. Nucleic Acids Res *28*, 235-242.

Bieszke, J. A., Spudich, E. N., Scott, K. L., Borkovich, K. A., and Spudich, J. L. (1999). A eukaryotic protein, NOP-1, binds retinal to form an archaeal rhodopsin-like photochemically reactive pigment. Biochemistry *38*, 14138-14145.

Blom, N., Gammeltoft, S., and and Brunak, S. (1999). Sequence- and structure-based prediction of eukaryotic protein phosphorylation sites.
Journal of Molecular Biology *294*, 1351-1362.

Braun, F. J., and Hegemann, P. (1999). Two light-activated conductances in the eye of the green alga *Volvox carteri*. Biophys J *76*, 1668-1678.

Brown, L. S., Dioumaev, A. K., Lanyi, J. K., Spudich, E. N., and Spudich, J. L. (2001). Photochemical reaction cycle and proton transfers in Neurospora rhodopsin. J Biol Chem *276*, 32495-32505.

Brown, L. S., and Lanyi, J. K. (1996). Determinationof the transiently lowered pK of the retinal Schiff base during the photocycle of bacteriorhodopsin. Proc Natl Acad Sci USA *93*, 1731–1734.

Burge, C. B., and Karlin, S. (1998). Finding the genes in genomic DNA. Curr Opin Struct Biol *8*, 346-354.

Burns, M., and Baylor, D. (2001). Activation, deactivation, and adaptation in vertebrate photoreceptor cells. Annu Rev Neurosci *24*, 779-805.

Butt, H. J., Fendler, K., Bamberg, E., Tittor, J., and Oesterhelt, D. (1989). Aspartic acids 96 and 85 play a central role in the function of bacteriorhodopsin as a proton pump. Embo J *8*, 1657-1663.

Calenberg, M., Brohnsonn, U., Zedlacher, M., and Kreimer, G. (1998). Light- and Ca2+-modulated heterotrimeric GTPases in the eyespot apparatus of a flagellate green alga. The Plant Cell *10*, 91-103.

Chen, G. Q., and Gouaux, J. E. (1996). Overexpression of bacterio-opsin in *Escherichia coli* as a water-soluble fusion to maltose binding protein: efficient regeneration of the fusion protein and selective cleavage with trypsin. Protein Sci *5*, 456-467.

Chen, J. H., Chang, X. B., Aleksandrov, A.A and, and Riordan, J. R. (2001). CFTR is a monomer: biochemical and functional evidence. J Membr Biol *188*, 55-71.

Christophe, C., Martin Jambon. , Gilbert Deléage and Christophe Geourjon (2001). Geno3D: automatic comparative molecular modelling of protein. Bioinformatics *18*, 213-214.

Corpet, F. (1988). Multiple sequence alignment with hierarchical clustering. Nucleic Acids Res *16*, 10881-10890.

Dieckmann, C. L. (2003). Eyespot placement and assembly in the green alga *Chlamydomonas*. Bioessays *25*, 410-416.

Ebnet, E., Fischer, M., Deininger, W., and Hegemann, P. (1999). Volvoxrhodopsin, a light-regulated sensory photoreceptor of the spheroidal green alga *Volvox carteri*. Plant Cell *11*, 1473-1484.

Ehlenbeck, S., Gradmann, D., Braun, F. J., and Hegemann, P. (2002). Evidence for a light-induced H(+) conductance in the eye of the green alga *Chlamydomonas reinhardtii*. Biophys J *82*, 740-751.

Fain, G., Matthews, H., Cornwall, M., and Koutalos, Y. (2001). Adaptation in vertebrate photoreceptors. Physiol Rev *81*, 117-151.

Feng Gai, K. C., Hasson, J., Cooper McDonald, and Anfinrud, P. A. (1998). Chemical Dynamics in Proteins: The Photoisomerization of Retinal in Bacteriorhodopsin. Science *279*, 1886-1891.

Foster, K., and Smyth, R. (1980). Light Antennas in phototactic algae. Microbiol Rev *44*, 572-630.

Foster, K. W., Saranak, J., Patel, N., Zarilli, G., Okabe, M., Kline, T., and Nakanishi, K. (1984). A rhodopsin is the functional photoreceptor for phototaxis in the unicellular eukaryote *Chlamydomonas*. Nature *311*, 756-759.

Foster, K. W., Saranak, J., and Zarrilli, G. (1988). Autoregulation of rhodopsin synthesis in *Chlamydomonas reinhardtii*. Proc Natl Acad Sci U S A *85*, 6379-6383.

Frings, S., Hackos, D. H., Dzeja, C., Ohyama, T., Hagen, V., Kaupp, U. B., and Korenbrot, J. I. (2000). Determination of fractional calcium ion current in cyclic nucleotide-gated channels. Methods Enzymol *315*, 797-817.

Fuhrmann, M., Deininger, W., Kateriya, S., and Hegemann, P. (2003). Rhodopsin-related proteins, Cop1, Cop2 and Chop1, in *Chlamydomonas reinhardtii*. (Cambridge, UK, Royal Society of Chemistry).

Fuhrmann, M., Deininger, W., Kateriya, S., and Hegemann, P. (2003). Rhodopsin-related proteins, Cop1, Cop2 and Chop1, in *Chlamydomonas reinhardtii*. (Cambridge, UK, Royal Society of Chemistry).

Fuhrmann, M., Stahlberg, A., Govorunova, E., Rank, S., and Hegemann, P. (2001). The abundant retinal protein of the *Chlamydomonas* eye is not the photoreceptor for phototaxis and photophobic responses. J Cell Sci *114*, 3857-3863.

Gärtner, W. (2000). Invertebrate visual pigments., Vol 3 (Amsterdam, Elsevier).

Gartner, W., and Losi, A. (2003). Crossing the borders: archaeal rhodopsins go bacterial. Trends Microbiol *11*, 405-407.

Geer, L. Y., Domrachev, M., Lipman, D. J., and Bryant, S. H. (2002). CDART: protein homology by domain architecture. Genome Res *12*, 1619-1623.

Gierasch, L. (1989). Signal sequences. Biochemistry *28*, 923-930.

Grodberg, J., and Dunn, J. J. (1988). ompT encodes the *Escherichia coli* outer membrane protease that cleaves T7 RNA polymerase during purification. J Bacteriol *170*, 1245-1253.

Hanahan, D. (1983). Studies on transformation of *Escherichia coli* with plasmids. J Mol Biol *166*, 557-580.

Hardie, R. (2001). Phototransduction in *Drosophila melanogaster*. J Exp Biol *204*, 3403-3409.

Hardie, R., and Raghu, P. (2001). Visual transduction in *Drosophila*. Nature *413*, 186-193.

Harz, H., and Hegemann, P. (1991). Rhodopsin-regulated calcium current *Chlamydomonas*. Nature *351*, 489.

Hegemann, P. (1997). Vision in microalgae. Planta *203*, 265-274.

Hegemann, P., Fuhrmann, M., and Kateriya, S. (2001). Algal sensory photoreceptors. J Phycol *37*, 668-676.

Hegemann, P., and Harz, H. (1998). How microalgae see the light, Vol 56 (Cambridge, University press).

Henderson, R., Baldwin, J. M., Ceska, T. A., Zemlin, F., Beckmann, E., and Downing, K. H. (1990). Model for the structure of bacteriorhodopsin based on high-resolution electron cryo-microscopy. J Mol Biol *213*, 899-929.

Hille, B. (2001). Ion Channels of Excitable Membranes (Sunderland, MA).

Hisatomi, O., and Tokunaga, F. (2002). Molecular evolution of proteins involved in vertebrate phototransduction. Comp Biochem Physiol B Biochem Mol Biol *133*, 509-522.

Hohenfeld, I. P., Wegener, A. A., and Engelhard, M. (1999). Purification of histidine tagged bacteriorhodopsin, pharaonis halorhodopsin and pharaonis sensory rhodopsin II functionally expressed in *Escherichia coli*. FEBS Lett *442*, 198-202.

Holland, E. M., Braun, F. J., Nonnengasser, C., Harz, H., and Hegemann, P. (1996). The nature of rhodopsin-triggered photocurrents in *Chlamydomonas*. I. Kinetics and influence of divalent ions. Biophys J *70*, 924-931.

Holland, E. M., Harz, H., Uhl, R., and Hegemann, P. (1997). Control of phobic behavioral responses by rhodopsin-induced photocurrents in *Chlamydomonas*. Biophys J *73*, 1395-1401.

Ihara, K., Amemiya, T., and Miyashita, Y. a. M., Y. (1994). Met-145 is a
key residue in the dark adaptation of bacteriorhodopsin homologs,. Biophys J *67*, 1187-1191.

Ihara, K., Umemura, T., Katagiri, I., Kitajima-Ihara, T., Sugiyama, Y., Kimura, Y., and Mukohata, Y. (1999). Evolution of the archaeal rhodopsins: evolution rate changes by gene duplication and functional differentiation. J Mol Biol *285*, 163-174.

Jung, K. H., Trivedi, V.D., and Spudich, J.L (2003). Demonstration of a sensory rhodopsin in eubacteria. Mol Microbiology *47*,, 1513 -1522.

Kalra, S. P., Fuentes, M., Fournier, A., Parker, S. L., and Crowley, W. R. (1992). Involvement of the Y-1 receptor subtype in the regulation of luteinizing hormone secretion by neuropeptide Y in rats. Endocrinology *130*, 3323-3330.

Kane, J. F. (1995). Effects of rare codon clusters on high-level expression of heterologous proteins in *Escherichia coli*. Curr Opin Biotechnol *6*, 494-500.

Karnik, S. S., Nassal, M., Doi, T., Jay, E., Sgaramella, V., and Khorana, H. G. (1987). Structure-function studies on bacteriorhodopsin. II. Improved expression of the bacterio-opsin gene in *Escherichia coli*. J Biol Chem *262*, 9255-9263.

Kateriya, S., Nagel, G., Bamberg, E., and Hegemann, P. (2004). "Vision" in single-celled algae. News Physiol Sci *19*, 133-137.

Kimura, Y., Vassylyev, D. G., Miyazawa, A., Kidera, A., Matsushima, M., Mitsuoka, K., Murata, K., Hirai, T., and Fujiyoshi, Y. (1997). Surface of bacteriorhodopsin revealed by high-resolution electron crystallography. Nature *389*, 206-211.

Klare, J. P., Gordeliy, V. I., Labahn, J., Büldt, G., , and Steinhoff, H. J., Engelhard, M. (2004). The archaeal sensory rhodopsin II/transducer complex:
a model for transmembrane signal transfer. 564, 219-224 (

Kolbe, M., Besir, H., Essen, L. O., and Oesterhelt, D. (2000). Structure of the light-driven chloride pump halorhodopsin at 1.8 A resolution. Science *288*, 1390-1396.

Lagnado, L. (2002). Signal Amplification: Let's Turn Down The Lights. Curr Biol *12*, 215-217.

Landau, E. M., Pebay-Peyroula, E., and Neutze, R. (2003). Structural and mechanistic insight from high resolution structures of archaeal rhodopsins. FEBS Lett *555*, 51-56.

Lanyi, J. K. (2004). Bacteriorhodopsin. Annu Rev Physiol *66*, 665-688.

Letunic, I., Goodstadt, L., Dickens, N. J., Doerks, T., Schultz, J., Mott, R., Ciccarelli, F., Copley, R. R., Ponting, C. P., and Bork, P. (2002). Recent improvements to the SMART domain-based sequence annotation resource. Nucleic Acids Res *30*, 242-244.

Liman, E., and Buck, L. (1994). A second subunit of the olfactory cyclic nucleotide-gated channel confers high sensitivity to cAMP. Neuron *13*, 611-621.

Liman, E., Tytgat, J., and Hess, P. (1992). Subunit stoichiometry of a mammalian K+ channel determined by construction of multimeric cDNAs. Neuron *9*, 861-871.

Litvin, F. F., Sineshchekov, O. A., and Sineshchekov, V. A. (1978). Photoreceptor electric potential in the phototaxis of the alga *Haematococcus pluvialis*. Nature *271*, 476-478.

Lóránd, K., Péter, G., Sándor Száraz, and Ormos, a. P. (1999). Chloride Ion Binding to Bacteriorhodopsin at Low pH: An Infrared Spectroscopic Study. Biophys J, *76*, 1951-1958.

Luecke, H., Richter, H. T., and Lanyi, J. K. (1998). Proton transfer pathways in bacteriorhodopsin at 2.3 angstrom resolution. Science *280*, 1934-1937.

Luecke, H., Schobert, B., Lanyi, J. K., Spudich, E. N., and Spudich, J. L. (2001). Crystal structure of sensory rhodopsin II at 2.4 angstroms: insights into color tuning and transducer interaction. Science *293*, 1499-1503.

Marina, A., Mott, C., Auyzenberg, A., Hendrickson, W. A., and Waldburger, C. D. (2001). Structural and mutational analysis of the PhoQ histidine kinase catalytic domain. Insight into the reaction mechanism. J Biol Chem *76*, 41182-41190.

Melkonian, M., and Robenek, H. (1980). Eyespot membranes of *Chlamydomonas reinhardii*: a freeze-fracture study. J Ultrastruct Res *72*, 90-102.

Miledi, R. (1982). A calcium-dependent transient outward current in *Xenopus laevis* oocytes. Proc R Soc Lond B Biol Sci *215*, 491-497.

Montell, C. (1999). Visual transduction in *Drosophila*. Annu Rev Cell Dev Biol *15*, 231-268.

Nagel, G., Kelety, B., Mockel, B., Buldt, G., and Bamberg, E. (1998). Voltage dependence of proton pumping by bacteriorhodopsin is regulated by the voltage-sensitive ratio of M1 to M2. Biophys J *74*, 403-412.

Nagel, G., Mockel, B., Buldt, G., and Bamberg, E. (1995). Functional expression of bacteriorhodopsin in oocytes allows direct measurement of voltage dependence of light induced H+ pumping. FEBS Lett *377*, 263-266.

Nagel, G., Ollig, D., Fuhrmann, M., Kateriya, S., Musti, A. M., Bamberg, E., and Hegemann, P. (2002). Channelrhodopsin-1: a light-gated proton channel in green algae. Science *296*, 2395-2398.

Nagel, G., Szellas, T., Huhn, W., Kateriya, S., Adeishvili, N., Berthold, P., Ollig, D., Hegemann, P., and Bamberg, E. (2003). Channelrhodopsin-2, a directly light-gated cation-selective membrane channel. Proc Natl Acad Sci U S A *100*, 13940-13945.

Nagel, G., Szellas, T., Riordan, J. R., Friedrich, T., and Hartung, K. (2001). Non-specific activation of the epithelial sodium channel by the CFTR chloride channel. EMBO Rep *2*, 249-254.

Nassal, M., Mogi, T., Karnik, S. S., and Khorana, H. G. (1987). Structure-function studies on bacteriorhodopsin. III. Total synthesis of a gene for bacterio-opsin and its expression in Escherichia coli. J Biol Chem *262*, 9264-9270.

Ng, W.-O., Grossman, A. R., and and Bhaya, D. (2003). Multiple Light Inputs Control Phototaxis in *Synechocystis sp*. Strain PCC6803. J Bacteriol *185*, 1599–1607.

Ng, W. V., Kennedy, S. P., Mahairas, G. G., Berquist, B., Pan, M., Shukla, H. D., Lasky, S. R., Baliga, N. S., Thorsson, V., Sbrogna, J., *et al.* (2000). Genome sequence of *Halobacterium species* NRC-1. Proc Natl Acad Sci U S A *97*, 12176-12181.

Noegel, A. A. B.-W., R. Sultana, H. Muller, R. Israel, L. Schleicher, M. Patel, H. and Weijer, C.J. (2004). The cyclase-associated protein CAP as regulator of cell polarity and cAMP signaling in *Dictyostelium*. Mol Biol Cell *15(*934-945.

Ntefidou, M., Iseki, M., Watanabe, M., Lebert, M., and Hader, D. P. (2003). Photoactivated adenylyl cyclase controls phototaxis in the flagellate *Euglena gracilis*. Plant Physiol *133*, 1517-1521.

Oprian, D. D. (2003). Phototaxis, chemotaxis and the missing link. Trends Biochem Sci *28*, 167-169.

Pompejus, M., Friedrich, K., Teufel, M., and Fritz, H. J. (1993). High-yield production of bacteriorhodopsin via expression of a synthetic gene in *Escherichia coli*. Eur J Biochem *211*, 27-35.

Qing, G., Ma, L. C., Khorchid, A., Swapna, G. V., Mal, T. K., Takayama, M. M., Xia, B., Phadtare, S., Ke, H., Acton, T., *et al.* (2004). Cold-shock induced high-yield protein production in *Escherichia coli*. Nat Biotechnol *22*, 877-882.

Rao, V. R., and Oprian, D. D. (1996). Activating mutations of rhodopsin and other G protein-coupled receptors. Annu Rev Biophys Biomol Struct *25*, 287-314.

Reilander, H., and Weiss, H. M. (1998). Production of G-protein-coupled receptors in yeast. Curr Opin Biotechnol *9*, 510-517.

Ridge, K. D. (2002). Algal rhodopsins: phototaxis receptors found at last. Curr Biol *12*, R588-590.

Royant, A., Edman, K., Ursby, T., Pebay-, Peyroula E., Landau E.M., and and Neutze. R (2000). Helix deformation is coupled to vectorial proton transport in the photocycle of bacteriorhodopsin. Nature *406*, 645–648.

Royant, A., P. Nollert, K., Edman, R. N., E. M. Landau., E. Pebay-Peyroula., and Navarro., a. J. (2001). X-ray structure of sensory rhodopsin II at 2.1-Å resolution. Proc Natl Acad Sci USA *98*, 10131-10136.

Rudolph, J., and Oesterhelt, D. (1995). Chemotaxis and phototaxis require a CheA histidine kinase in the archaeon *Halobacterium salinarium*. Embo J *14*, 667-673.

Ruiz-Gonzalez, M. X., and Marin, I. (2004). New insights into the evolutionary history of type 1 rhodopsins. J Mol Evol *58*, 348-358.

Saiki, R. K., Gelfand, D. H., Stoffel, S., Scharf, S. J., Higuchi, R., Horn, G. T., Mullis, K. B., and Erlich, H. A. (1988). Primer-directed enzymatic amplification of DNA with a thermostable DNA polymerase. Science *239*, 487-491.

Sakmar, T. P. (1998). Rhodopsin: a prototypical G protein-coupled receptor. Prog Nucleic Acid Res Mol Biol *59*, 1-34.

Sasaki, J., Brown, L., Chon, Y. S., Kandori, H., Maeda, A., Needleman, and R., L., J.K. (1995). Conversion of bacteriorhodopsin into a chloride ion pump. Science *269*, 73-75.

Schafer, G., Engelhard, M., and Muller, V. (1999). Bioenergetics of the Archaea. Microbiol Mol Biol Rev *63*, 570-620.

Schmies, G., Chizhov, I., and Engelhard, M. (2000). Functional expression of His-tagged sensory rhodopsin I in *Escherichia coli*. FEBS Lett *466*, 67-69.

Schmies, G., Engelhard, M., Wood, P. G., Nagel, G., and Bamberg, E. (2001). Electrophysiological characterization of specific interactions between bacterial sensory rhodopsins and their transducers. Proc Natl Acad Sci U S A *98*, 1555-1559.

Schultz, J., Copley, R. R., Doerks, T., Ponting, C. P., and Bork, P. (2000). SMART: a web-based tool for the study of genetically mobile domains. Nucleic Acids Res *28*, 231-234.

Sharp, P. M., Cowe, E., Higgins, D. G., Shields, D. C., Wolfe, K. H., and Wright, F. (1988). Codon usage patterns in *Escherichia coli*, *Bacillus subtilis*, *Saccharomyces cerevisiae*, *Schizosaccharomyces pombe*, *Drosophila melanogaster* and *Homo sapiens*; a review of the considerable within-species diversity. Nucleic Acids Res *16*, 8207-8211.

Shimono, K., Iwamoto, M., Sumi, M., and Kamo, N. (1997). Functional expression of pharaonis phoborhodopsin in *Escherichia coli*. FEBS Lett *420*, 54-56.

Shukla, P., and Sullivan, J. M. (1999). Normal and mutant rhodopsin activation measured with the early receptor current in a unicellular expression system. J Gen Physiol *114*, 609-636.

Sineshchekov, O. A., Jung, K. H., and Spudich, J. L. (2002). Two rhodopsins mediate phototaxis to low- and high-intensity light in *Chlamydomonas reinhardtii*. Proc Natl Acad Sci U S A *99*, 8689-8694.

Snutch, T. P. (1988). The use of *Xenopus* oocytes to probe synaptic communication. Trends Neurosci *11*, 250-256.

Spudich, J. L., Yang, C. S., Jung, K. H., and Spudich, E. N. (2000). Retinylidene proteins: structures and functions from archaea to humans. Annu Rev Cell Dev Biol *16*, 365-392.

Stewart, A. K., Chernova, M. N., Kunes, Y. Z., and Alper, S. L. (2001). Regulation of AE2 anion exchanger by intracellular pH: critical regions of the NH(2)-terminal cytoplasmic domain. Am J Physiol Cell Physiol *281*, C1344-1354.

Stock, J. B., Stock, A. M., and Mottonen, J. M. (1990). Signal transduction in bacteria. Nature *344*, 395-400.

Stoeckenius, W., and Lozier, R. H. (1974). Light energy conversion in *Halobacterium halobium*. J Supramol Struct *2*, 769-774.

Subramaniam, S., and Henderson, R. (2000). Molecular mechanism of vectorial proton translocation by bacteriorhodopsin. Nature *406*, 653-657.

Sullivan, J. M., Brueggemann, L., and Shukla, P. (2000). Electrical approach to study rhodopsin activation in single cells with early receptor current assay. Methods Enzymol *315*, 268-293.

Sullivan, J. M., and Shukla, P. (1999). Time-resolved rhodopsin activation currents in a unicellular expression system. Biophys J *77*, 1333-1357.

Suzuki, T., Yamasaki, K., Fujita, S., Oda, K., Iseki, M., Yoshida, K., Watanabe, M., Daiyasu, H., Toh, H., Asamizu, E., *et al.* (2003). Archaeal-type rhodopsins in *Chlamydomonas*: model structure and intracellular localization. Biochem Biophys Res Commun *301*, 711-717.

Takahashi, T., Yoshihara, K., Watanabe, M., Kubota, M., Johnson, R., Derguini, F., and Nakanishi, K. (1991). Photoisomerization of retinal at 13-ene is important for phototaxis of *Chlamydomonas reinhardtii*: simultaneous measurements of phototactic and photophobic responses. Biochem Biophys Res Commun *178*, 1273-1279.

Vasina, J. A., and Baneyx, F. (1997). Expression of aggregation-prone recombinant proteins at low temperatures: a comparative study of the *Escherichia coli* cspA and tac promoter systems. Protein Expr Purif *9*, 211-218.

Vought, B., Salcedo, E., Chadwell, L., Britt, S., Birge, R., and Knox, B. (2000). Characterization of the primary photointermediates of *Drosophila* rhodopsin. Biochemistry *39*, 14128-14137.

Watanabe, M., and Suzuki, T. (2002). Involvement of reactive oxygen stress in cadmium-induced cellular damage in *Euglena gracilis*. Comp Biochem Physiol C Toxicol Pharmacol *131*, 491-500.

Wayne, R., Kadota, A., Watanabe, M., and Furuya, M. (1991). Photomovement in *Dunaliella salina*: fluence rate-response curves and action spectra. Planta *184*, 515-524.

Xia, X. (1996). Maximizing transcription efficiency causes codon usage bias. Genetics *144*, 1309-1320.

Xia, X. (1998). How optimized is the translational machinery in *Escherichia coli*, *Salmonella typhimurium* and *Saccharomyces cerevisiae*? Genetics *149*, 37-44.

Yang, A. S., and Honig, B. (2000a). An integrated approach to the analysis and modeling of protein sequences and structures. I. Protein structural alignment and a quantitative measure for protein structural distance. J Mol Biol *301*, 665-678.

Yang, A. S., and Honig, B. (2000b). An integrated approach to the analysis and modeling of protein sequences and structures. II. On the relationship between sequence and structural similarity for proteins that are not obviously related in sequence. J Mol Biol *301*, 679-689.

Yokoyama, S. (2000). Phylogenetic analysis and experimental approaches to study color vision in vertebrates. Methods Enzymol *315*, 312-325.

Yuki, S., Masayuki, I., Kazumi, S., and, and Naoki, K. (2002). Tyr-199 and Charged Residues of pharaonis Phoborhodopsin Are Important for the Interaction with its Transducer. Biophys J, *83*, 427-432.

Zacks, D. N., Derguini, F., Nakanishi, K., and Spudich, J. L. (1993). Comparative study of phototactic and photophobic receptor chromophore properties in *Chlamydomonas reinhardtii*. Biophys J *65*, 508-518.

Zimanyi, L., V´ar´o G., Chang, M., Ni, B., Needleman, R., and Lanyi, J. K. (1992). Pathways
of proton release in the bacteriorhodopsin
photocycle. Biochemistry *31*.

Zuker, C. (1996). The biology of vision of *Drosophila*. Proc Natl Acad Sci U S A *93*, 571-576.

Bio-Data

Name:	Suneel Kumar Kateriya
Date of Birth:	30th June 1977
Birth Place:	Kannauj (U.P) India
Sex:	Male
Martial status:	Married

Educational Qualification:

Bachelor of Science (B. Sc) in Zoology, Botany and Chemistry from University of Kanpur, India.

Master of Science (M. Sc) in Biotechnology from School of Biotechnology at Banaras Hindu University, Varanasi, India.

Project Work for M. Sc Dissertation: The project work has been carried out on "Microbial Surfactants" under the supervision of Prof. Ashok Kumar at School of Biotechnology, BHU.

Duration: **One year.**

Present Research work:

Project: Microbial-Type Rhodopsins from *Chlamydomonas reinhardtii*: Identification, expression and characterization.

Research Experience:

I have also done two years research work with the project "Enhancement of refolding yield and thermal stability of Glucose oxidase by solvent Engineering". This work was carried out under the guidance of Dr. Rajiv Bhat at Centre for Biotechnology, JNU. Duration: **1998-2000.**

Fellowships and National Level Exams:

Department of Biotechnology (DBT) has provided financial support during my master degree in Biotechnology.

CSIR-JRF: I have cleared CSIR- JRF exam, while I was in the final year of my M. Sc degree.

GATE: I could qualify the GATE exam as well in 1998 with 73 percentile.

UGC-JNU-JRF: Since I have cleared JNU entrance exam for PhD program. It enabled me to get JRF from UGC as well. There I could complete my JRF tenure followed by promotion to SRF.

ICAR-NET (Plant-Biotechnology): I have appeared for an exam, which was conducted by Agricultural Scientists Recruitment Board (ASRB) ICAR, New Delhi. There I could qualify ICAR-NET for Plant Biotechnology.

I have joined an international PhD program at University of Regensburg, Germany in 2000. I was able to get DFG fellowship for completion of my graduate study. DFG is a funding agency for basic research in Germany.

Memberships:

Life membership for "Indian Biophysical Society"

Workshops/Meeting:

(I) Sequence Analysis and Molecular Modelling- India.

(II) Molecular Biology of Stress Response-India.

(III) 13th International Biophysics Congress-India.

(IV) Dissecting G-Protein-Coupled Receptors (GPCR): Structure, Function and Ligand Interaction, Germany. Jan. 24-26, 2002.

(V) The 10th International Conference on the Cell and Molecular Biology of *Chlamydomonas***,** Vancouver, Canada - June 11-16, 2002**.**

(VI) Leeds Ion Channel Workshop 2003. Leeds, U.K, London.

(VII) 11th International Conference on Retinal Proteins- (11th ICRP). June 20-24, 2004, Germany.